



Cutting Edge Conference 2025

# AT THE CROSSROADS OF THREE REALMS

15.09.2025

FACULTY OF CHEMISTRY AND  
CHEMICAL TECHNOLOGY, LJUBLJANA

[www.cutting-edge.si](http://www.cutting-edge.si)

# **BOOK OF ABSTRACTS:**

## **Cutting Edge – AT THE CROSSROAD OF THREE REALMS**

Organizator in založnik zbornika:

Fakulteta za kemijo in kemijsko tehnologijo, Univerza v Ljubljani

Kraj dogodka:

Fakulteta za kemijo in kemijsko tehnologijo, Univerza v Ljubljani

Uredniki:

Jure Jakoš, Klara Klemenčič, Ines Babnik

Oblikovanje in prelom:

Jure Jakoš, Klara Klemenčič

Organizacijski odbor:

Ines Babnik, Jure Jakoš, Klara Klemenčič

Publikacija je izšla v elektronski obliki in je dostopna na spletnem naslovu:

<http://www.cutting-edge.si/wp-content/uploads/2025/09/CE-BoA-2025.pdf>

Ljubljana, Slovenija, 2025

Kataložni zapis o publikaciji (CIP) pripravili v Narodni in univerzitetni knjižnici v Ljubljani

[COBISS.SI](#)-ID [248110083](#)

ISBN 978-961-7078-60-2 (PDF)

# Meet the Sponsors Powering Cutting Edge 2025



# AT THE CROSSROADS OF THREE REALMS

The 2025 Cutting Edge Conference took place on 15<sup>th</sup> September 2025 at the Faculty of Chemistry and Chemical Technology, University of Ljubljana. This year's theme, **At the Crossroads of Three Realms**, showcased scientific research at the intersection of academia, industry, and public institutions.

Through a rich program of lectures spanning **chemistry, biochemistry, pharmacy, materials science, and related disciplines**, the conference aimed to bring science closer to its participants while supporting them in shaping their current and future career paths.

The event welcomed **over 100 participants** from Slovenia and abroad, representing diverse fields of research. Among them, **71 researchers** presented their work within three thematic sessions: **Science Behind the Living, Materials of the Future, and Technologies for the Earth and Environment**.

For the second time in Cutting Edge's history, a special session titled **Young Minds<sup>2</sup>** was organized for **secondary school students**. A total of **32 young participants** had the opportunity to present the outcomes of their school research projects and actively engage in the conference.

The program began at 8:30 a.m. with opening remarks by prof. dr. Marko Novinec, the next Dean of the Faculty, and Ines Babnik, President of the Cutting Edge Society. The opening was followed by a series of lectures and poster presentations. The one-day conference concluded with an awards ceremony, where prizes were presented for the best poster and the best oral presentation. After the formal program, participants were invited to an afternoon networking session, offering opportunities to connect with sponsors and fellow researchers.

We would like to express our sincere gratitude to the scientific committee members: doc. dr. Jakob Kljun, Uroš Rapuš, Jernej Imperl, Tilen Zorko and Benjamin Poljanc, as well as the many students from the Faculty who contributed to the success of the event. Special thanks also go to our collaborators and sponsors, particularly the Faculty of Chemistry and Chemical Technology, University of Ljubljana, for their outstanding cooperation and unwavering support.

The Cutting Edge Organizing Committee is deeply grateful to all presenters and participants for their thought-provoking contributions. May critical thinking, a willingness to embrace diverse perspectives, and boundless curiosity continue to guide you.

We look forward to seeing you all again at the **Cutting Edge Conference 2027!**

*– Cutting Edge Organizing Team*

# CONFERENCE SCHEDULE

8:00	Registration and poster installment	
8:30	<b>Opening ceremony</b> Ines Babnik, prof. dr. Marko Novinec	
8:45	<b>LabCore</b> Where there's a will, there's a way: Start-up in the pharmaceutical and chemical industry	
9:15	<b>dr. Iva Hafner Bratkovič</b> Curiosity-driven immunology research inspires novel treatment strategies	
9:35	<b>doc. dr. Luka Ležaič</b> From bench to bedside - clinical translation of radiopharmaceuticals in first-in-human trials	
9:55	Coffee break	
10:10	<b>Jafral</b> The use of bacteriophage technology to address upcoming health & biotechnology challenges	
10:40	<b>dr. Matjaž Mazaj</b> Smart materials for a breathable future: Tackling CO <sub>2</sub> indoors	
11:00	<b>dr. Matija Uršič</b> What we learn from burning things	
11:20	<b>Lek Pharmaceuticals d.d.</b> From vision to reality: Setting up a new state of the art bioinjectables drug product production site	
11:35	Coffee break	
11:50	<b>prof. dr. Petar Djinović</b> Using light for new discoveries in catalytic reactions	
12:10	<b>assoc. prof. dr. Gabriela Kalčíková</b> The secret life of microplastics: Understanding their environmental impacts	
12:30	<b>Krka d.d.</b> From mg to kg - Development of API synthesis	
12:45	Lunch	
14:00	Elevator pitch sessions	Young Minds <sup>2</sup> (13:45–15:30)
15:00	Poster session & coffee break	
16:30	Closing remarks and award ceremony	
17:00	Afternoon mingle	

# TABLE OF CONTENTS

## AT THE CROSSROADS OF THREE REALMS

<b>1</b>	Ana Gotvajn	<b>35</b>	Maja Pristavec
<b>2</b>	Ana Šijanec	<b>36</b>	Maja Svete
<b>3</b>	Andrej Bogataj	<b>37</b>	Marcel Tušek
<b>4</b>	Azmat Ullah	<b>38</b>	Mark Loborec
<b>5</b>	Blaž Antonin	<b>39</b>	Martin Jazbec
<b>6</b>	Blaž Kozjek	<b>40</b>	Martina Potočnik
<b>7</b>	Brina Klinar	<b>41</b>	Matic Plut
<b>8</b>	Dane Jemc	<b>42</b>	Matjaž Dlouhy
<b>9</b>	Daša Čebulj	<b>43</b>	Natalija Tomažin
<b>10</b>	Domen Tomc	<b>44</b>	Neja Lesinšek
<b>11</b>	Endis Aletić	<b>45</b>	Nejc Virant
<b>12</b>	Filip Petrovič	<b>46</b>	Nina Krašovec
<b>13</b>	Helena Potočnik	<b>47</b>	Špela Žunec
<b>14</b>	Ines Babnik	<b>48</b>	Tadej Menegatti
<b>15</b>	Iza Rozman	<b>49</b>	Tadej Pirc
<b>16</b>	Jaka Janežič	<b>50</b>	Tal Čarman
<b>17</b>	Jan Hočevár	<b>51</b>	Tia Kralj
<b>18</b>	Jan Kogovšek	<b>52</b>	Tina Kosovel
<b>19</b>	Jan Očepek	<b>53</b>	Tina Logonder
<b>20</b>	Jan Vidergar	<b>54</b>	Tjaša Likeb
<b>21</b>	Jana Bregar	<b>55</b>	Tjaša Žerdoner
<b>22</b>	Jerneja Kladnik	<b>56</b>	Tonja Oman Sušnik
<b>23</b>	Jure Jakoš	<b>57</b>	Urša Košak
<b>24</b>	Jure Kovač	<b>58</b>	Veronika Plut
<b>25</b>	Karin Rot	<b>59</b>	Vinz Ymannuelle Tatad
<b>26</b>	Karolina Mulec	<b>60</b>	Vitan Šlamberger
<b>27</b>	Katja Gubič	<b>61</b>	Zala Cvitanič
<b>28</b>	Klara Klemenčič	<b>62</b>	Zala Kramar
<b>29</b>	Klara Razboršek	<b>63</b>	Zala Trbežnik
<b>30</b>	Klara Urankar	<b>64</b>	Zarja Uranjek
<b>31</b>	Klemen Klopčič	<b>65</b>	Žiga Gerdina
<b>32</b>	Liam Manevski	<b>66</b>	Žiga Močnik
<b>33</b>	Luka Jedlovčnik	<b>67</b>	

## TABLE OF CONTENTS

### YOUNG MINDS<sup>2</sup>

<b>68</b>	Aljaž Kostevc Redek, Danial Doustmohammadi, Mihajlo Krstić
<b>69</b>	Brina Zver, Klara Grantaša
<b>70</b>	Eva-Arolea Trdan
<b>71</b>	Gregor Čekada, Niko Noliml
<b>72</b>	Iva Jaklin
<b>73</b>	Jakob Ritlop
<b>74</b>	Jon Milič
<b>75</b>	Katarina Šela, Lara Marzidovšek
<b>76</b>	Lan Dular
<b>77</b>	Lara Širovnik, Petra Ouček
<b>78</b>	Luka Tomažin, Ajk Kalaba, Aljaž Maraž
<b>79</b>	Mija Kapun, Emilija Rojnik
<b>80</b>	Petra Ouček, Lani Habjanič
<b>81</b>	Tisa Lombar, Urban Perko
<b>82</b>	Urban Ocvirk
<b>83</b>	Vid Kodrič, Matic Izak, Anika Gregori Kmecl
<b>84</b>	Vinko Kosten
<b>85</b>	Živa Anderluh, Jošt Dolinar



# **ABSTRACTS**

AT THE CROSSROADS OF  
THREE REALMS



# ***Cold Plasma-activated Water (PAW): Reactive Oxygen and Nitrogen Species (RONS) Among Key Factors Contributing to PAW Antimicrobial Activity***

Ana Gotvajn<sup>\*1</sup>, Helena Prosen<sup>2</sup>, Breda Jakovac Strajn<sup>1</sup>, Štefan Pintarič<sup>1</sup>

<sup>1</sup> Veterinary Faculty, University of Ljubljana, Gerbičeva ulica 60, SI-1000 Ljubljana, Slovenija

<sup>2</sup> Faculty of Chemistry and Chemical Technology, University of Ljubljana, Večna pot 113, SI-1000 Ljubljana, Slovenija

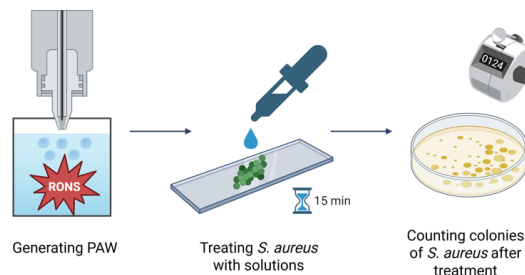
PAW is a new type of disinfectant that differs from most commonly used chemical disinfectants in that it does not contain any added chemical substances that would form degradation products of themselves after the antimicrobial effect, which could pollute the environment and pose a health risk. PAW is created when water is treated with plasma. Plasma is often defined as the fourth state of matter and is an ionised gas. When plasma interacts with water, chemical reactions take place that lead to the formation of RONS.

The RONS formed, which are known to contribute to the antimicrobial activity of PAW, can be divided into short-lived and long-lived species. The former, such as hydroxyl radicals ( $\bullet\text{OH}$ ), nitric oxide (NO) and peroxynitrite ( $\text{ONOO}^-$ ), usually have a half-life of nanoseconds to a few seconds and then tend to react and form more stable molecules. Long-lived species, such as hydrogen peroxide ( $\text{H}_2\text{O}_2$ ), ozone ( $\text{O}_3$ ), nitrite ( $\text{NO}_2^-$ ) and nitrate ( $\text{NO}_3^-$ ), have a half-life of minutes to days. Physical damage to the vital cellular structures and the induction of oxidative stress in the bacterial cell are two fundamental principles of the antimicrobial effect of RONS.

In the preliminary studies the efficacy of the antimicrobial activity of PAW generated with a plasma jet device using filtered air was tested on *Staphylococcus aureus* according to modified standard ISO 4833-1:2013. (Scheme 1, Table 1).

**Table 1:** Logarithmic reduction of *S. aureus* after 15-minute treatment with 0.1 mL of prepared solutions (\*Saline-corrected values)

Solutions	Log <sub>10</sub> reduction	Log <sub>10</sub> reduction*
NaCl (0.9%)	1.05	
PAW	<b>4.53</b>	<b>3.49</b>
PAW + NaCl (2:1)	3.83	2.78
PAW + NaCl (1:1)	3.79	2.74
PAW + NaCl (1:9)	1.98	0.93



**Scheme 1:** Visual summary of preliminary studies  
(Created in <https://BioRender.com>)

It is known that the presence of impurities can reduce the effectiveness of the disinfectants used. Therefore, future research will focus on the efficacy of the antimicrobial activity of PAW in the presence of organic matter, which is in line with chosen standards for testing the efficacy of chemical disinfectants. At the same time, we will monitor the pH, ORP and concentration of selected RONS, thus contributing to a more comprehensive understanding of the role of key factors in the antimicrobial activity of PAW. Identifying potentially newly formed compounds after disinfection in the presence of impurities will contribute to evaluating the safety of this mode of disinfection for human, animal and environmental health.

## **References:**

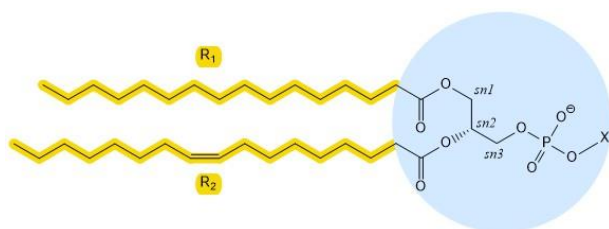
- Wong, K. S.; Chew, N. S. L.; Low, M.; Tan, M. K. Plasma-Activated Water: Physicochemical Properties, Generation Techniques, and Applications. *Processes* **2023**, *11* (7), 2213.
- Herianto, S.; Arcega, R. D.; Hou, C.-Y.; Chao, H.-R.; Lee, C.-C.; Lin, C.-M.; Mahmudiono, T.; Chen, H.-L. Chemical Decontamination of Foods Using Non-Thermal Plasma-Activated Water. *Sci. Total Environ.* **2023**, *874*, 162235.
- Wang, H.; Han, R.; Yuan, M.; Li, Y.; Yu, Z.; Cullen, P. J.; Du, Q.; Yang, Y.; Wang, J. Evaluation of Plasma-Activated Water: Efficacy, Stability, Physicochemical Properties, and Mechanism of Inactivation against *Escherichia coli*. *LWT* **2023**, *184*, 114969.

# Lecithin Analysis: Determination of Phospholipids

Ana Šijanec,<sup>1</sup> Matevž Pompe\*,<sup>1</sup>

<sup>1</sup> Faculty of Chemistry and Chemical Technology, University of Ljubljana, Večna pot 113, SI-1000 Ljubljana, Slovenia

Phospholipids (Figure 1) are amphiphilic molecules with different polar head groups and non-polar fatty acid tails that differ in length and saturation. As essential components of cell membranes, they form bilayers in all living organisms. Their unique structural properties enable applications such as natural emulsifiers and encapsulating agents in pharmaceutical, food and cosmetic formulations, where they facilitate the formation of micelles and liposomes to improve the stability, bioavailability and delivery of active ingredients<sup>1</sup>. A common natural source of phospholipids in the industry is lecithin. The performance of lecithin in different formulations is highly dependent on its phospholipid composition. Differences in head group type and fatty acid saturation affect the type of structures lecithin can form and its emulsifying behavior. Therefore, characterizing the phospholipid profile of lecithin is essential to ensure the stability and functionality of the final product<sup>2</sup>.



**Figure 1:** Phospholipid structure

The analysis of phospholipids is usually based on commercial reference standards. However, the high structural diversity of phospholipids requires numerous standards to cover all possible variants in complex mixtures such as lecithin. Given the cost, limited availability and time required for extensive comparisons, this approach is often inefficient and impractical<sup>3</sup>.

In this study, we developed and optimized a qualitative method for the determination of phospholipids

in lecithin without the use of reference standards. Reversed-phase high-performance liquid chromatography was coupled with high-resolution mass spectrometry to separate and detect the phospholipid species. Molecular ions were recorded in full scan mode and analyzed using a custom Python script that generated a list of possible phospholipid structures for each  $m/z$  value. The identification was confirmed by matching the MS/MS fragmentation patterns with the theoretical predictions.

The proposed method provides a reliable, cost-effective alternative for phospholipid profiling in complex lipid matrices and demonstrates that standard-free identification is possible using high-resolution analytical tools in combination with computational support.

## References:

1. Xie, M. Phospholipids. In *Encyclopedia of Food Chemistry*; Melton, L.; Shahidi, F., Varelis, P.; Eds.; Academic Press, **2019**, 214–217.
2. Cui, L.; Decker, E.M; Phospholipids in Foods: Prooxidants or Antioxidants? *J. Sci. Food Agric.* **2015**, 96.
3. McHowat, J.; Jones, J. H.; Creer, M. H.; Quantitation of Individual Phospholipid Molecular Species by UV Absorption Measurements. *J. Lipid Res.* **1996**, 37 (11), 2450–2460.

**Funding information:** We are grateful for the financial support from the junior research grant for Ana Šijanec and program grant P1-0153 of the Slovenian Research and Innovation Agency (ARIS). The authors also acknowledge the support of the Centre for Research Infrastructure at the University of Ljubljana, Faculty of Chemistry and Chemical Technology, which is part of the Network of Research and Infrastructural Centers UL (MRIC UL) and is financially supported by ARIS; Infrastructure program No. I0-0022.

# Role of Surface Pretreatment in Film Formation and Corrosion Protection of AZ-Series Magnesium Alloys

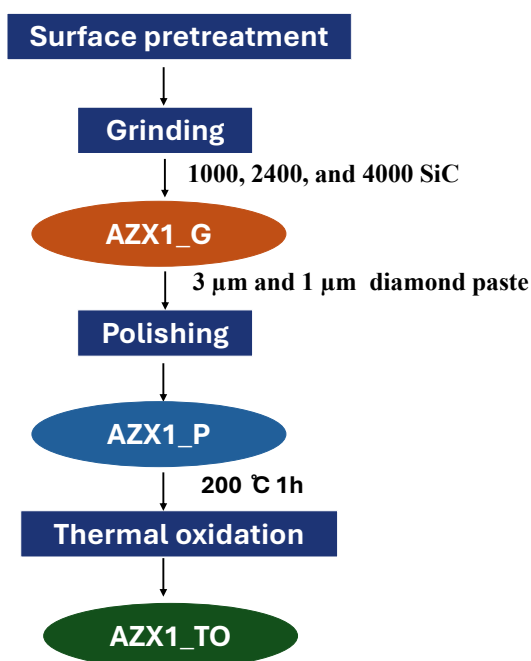
Nina Kovač,<sup>1,2</sup> Andrej Bogataj,<sup>1</sup> Ingrid Milošev,<sup>1</sup> Peter Rodič\*,<sup>1</sup>

<sup>1</sup> Department of Physical and Organic Chemistry, Jožef Stefan Institute, Jamova cesta 39, SI-1000 Ljubljana, Slovenia

<sup>2</sup> Jožef Stefan International Postgraduate School, Jamova cesta 39, SI-1000 Ljubljana, Slovenia

Lightweight and biocompatible, the AZ-series magnesium alloys, specifically, AZ31, AZ61, and AZ91, have significant potential for biomedical and structural applications.<sup>1,2</sup> However, their practical use remains limited by high corrosion susceptibility, particularly in chloride-rich environments. The corrosion behaviour of magnesium is strongly influenced by (i) its composition (content of aluminium and zinc) and (ii) the stability of its surface oxide layer. Therefore, the surface conditions are essential to enhance corrosion resistance.<sup>3</sup> This study examines the impact of mechanical surface pretreatment and thermal oxidation on the formation of oxide films and the corrosion performance of AZ31, AZ61, and AZ91 alloys.

The experimental workflow is outlined in Scheme 1. Each alloy underwent three surface pretreatments: (i) ground (e.g., AZ31\_G, AZ61\_G, AZ91\_G), (ii) ground and polished (e.g., AZ31\_P, AZ61\_P, AZ91\_P), (iii) ground, polished, and thermally oxidised at 200 °C (e.g., AZ31\_TO, AZ61\_TO, AZ91\_TO).



**Scheme 1:** Experimental workflow for AZ series magnesium alloys with varying aluminium content (X = 3, 6, 9 wt.%) and constant zinc content (1 wt.%).

The surface morphology and chemical composition were characterised using scanning electron microscopy coupled with energy-dispersive X-ray spectroscopy (SEM/EDS), both pre- and post-exposure to a corrosive medium. Potentiodynamic polarization was used to assess corrosion behaviour, and it was evaluated in 0.1 M NaCl solution.

Potentiodynamic measurements revealed a lower corrosion current density and a more positive pitting potential for the thermally oxidised sample, which was supported by an improved surface morphology after immersion. These findings highlight the critical role of surface condition in passive film formation and demonstrate that both thermal oxidation and increasing aluminium content in the alloy series (from AZ31 to AZ91) contribute to enhanced corrosion resistance in chloride environments.

Future work could focus on investigating how different surface pretreatments influence the adhesion of protective surface coatings, enabling improved performance in diverse application environments.

## References:

1. Zhang, J.; Miao, J.; Balasubramani, N.; Cho, D. H.; Avey, T.; Chang, C. Y.; Luo, A. A. Magnesium Research and Applications: Past, Present and Future. *J. Magnes. Alloys* **2023**, *11* (11), 3867–3895.
2. Zhang, T.; Wang, W.; Liu, J.; Wang, L.; Tang, Y.; Wang, K. A Review on Magnesium Alloys for Biomedical Applications. *Front. Bioeng. Biotechnol.* **2022**, *10*, 953344.
3. Feliu, S.; Llorente, I. Corrosion Product Layers on Magnesium Alloys AZ31 and AZ61: Surface Chemistry and Protective Ability. *Appl. Surf. Sci.* **2015**, *347*, 736–746.

**Funding information:** The financial support from the Slovenian Research and Innovation Agency (ARIS) research core funding No. P1-0134, P2-0393 and through the ARIS projects J2-60047.

# Photodegradation of pharmaceuticals using lignin carbon quantum dots based hybrid photocatalyst under visible light solar simulator

Azmat Ullah,<sup>1</sup> Jan Hočevar,<sup>1</sup> Boštjan Žener,<sup>1</sup> Iskra, Jernej,<sup>1</sup> Urška Lavrenčič Štangar,<sup>1</sup> Jelena Papan Djaniš\*,<sup>1,2</sup>

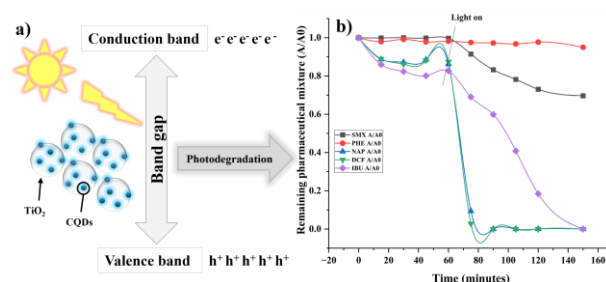
<sup>1</sup> Faculty of Chemistry and Chemical Technology, University of Ljubljana, Večna pot 113, SI-1000 Ljubljana, Slovenia

<sup>2</sup> Centre of Excellence for Photoconversion, Vinča Institute of Nuclear Sciences, National Institute of the Republic of Serbia, University of Belgrade, 11351 Belgrade, Serbia

Pharmaceuticals detected in water environments are posing a serious environmental concern for aquatic life and human beings<sup>1</sup>. Different methods are used for removal or degradation of pharmaceuticals from water including adsorption, membrane filtration, reverse osmosis and advance oxidation processes or photodegradation<sup>2</sup>. Among these methods, photodegradation is more promising because it requires only light sources to break down a range of complex pharmaceutical structures<sup>3</sup>. The photocatalysts have major problems with electron hole recombination and wide band gaps of available efficient photocatalysts. Lignin derived CQDs as a green candidate for photocatalysis are extensively explored due to their high surface area and photoluminescence properties<sup>4</sup>. These CQDs can be synergistically coupled with the other photocatalysts to lower their band gap and reduce electron hole recombination like titanium dioxide (TiO<sub>2</sub>). TiO<sub>2</sub> is used as a reference photocatalyst due to high efficiency, low cost and toxicity. But TiO<sub>2</sub> is active in UV light source due to wide band gap and electron hole recombination also affects its efficiency.

In this study, lignin based CQDs were synthesized through hydrothermal method. The synthesized CQDs were used to prepare a hybrid with TiO<sub>2</sub>. In one study, tetracycline used as a broad-spectrum antibiotic, was photodegraded with TiO<sub>2</sub> and CQDs/TiO<sub>2</sub> hybrid under visible light using solar simulator. The hybrid showed better photodegradation of tetracycline as compared with bare TiO<sub>2</sub> proving the synergistic effect of CQDs on TiO<sub>2</sub>.

After successful photodegradation of tetracycline under visible light, a five pharmaceuticals mixture was also photodegraded with bare TiO<sub>2</sub> and CQDs/TiO<sub>2</sub> hybrid as shown in **Figure 1**. The results showed that increasing the CQDs percentage in CQDs/TiO<sub>2</sub> improves its photocatalytic performance. This improved photocatalytic performance indicates the synergistic effect of CQDs on CQDs/TiO<sub>2</sub>.



**Figure 1:** a) CQDs/TiO<sub>2</sub> photocatalyst and b) photodegradation of five pharmaceuticals mixture with CQDs/TiO<sub>2</sub>

## References:

1. Asadzadeh Patehkhori H.; Fattahi M.; Khosravi-Nikou M. Synthesis and characterization of ternary chitosan–TiO<sub>2</sub>–ZnO over graphene for photocatalytic degradation of tetracycline from pharmaceutical wastewater *Sci. Rep.* **2021**, *11* (1) 1–17.
2. Jabeen A.; Salem Alsaieri N.; Katubi K. M. S.; Shakir I.; Alrowaili Z.A.; Al-Buraihi M. S.; Warsi M. F. Synthesis and characterisation of MXene based-LDH photocatalytic materials for the removal of toxic pharmaceutical effluents *M. J. Mol. Liq.* **2024**, *405*, 125066.
3. Matoh L.; Žener B.; Kovačić M.; Hušić H.; Arčon I.; Levstek M.; Lavrenčič Štangar U. Photocatalytic sol-gel/P25 TiO<sub>2</sub> coatings for water treatment: Degradation of 7 selected pharmaceuticals *Ceram. Int.* **2023**, *49* (14), 24395–24406.
4. Malitha M. D.; Molla M. T. H.; Bashar M. A.; Chandra D.; Ahsan M. S. Fabrication of reusable carbon quantum dots (CQDs) modified nanocomposite with enhanced visible light photocatalytic activity. *Sci. Rep.* **2024**, *14*, 17976.

**Funding information:** The authors acknowledge to Slovenian Research Agency (ARIS) through research core funding grants P1-0134, and P1-0418, and research project J2-50061.

# Synthesis and characterization of copper(I) complexes with chelating 2-(methylthio)pyrimidines

Blaž Antonin,<sup>1</sup> Uroš Rapuš,<sup>1</sup> Jakob Kljun\*,<sup>1</sup>

<sup>1</sup> Faculty of Chemistry and Chemical Technology, University of Ljubljana, Večna pot 113, SI-1000 Ljubljana, Slovenia

Copper(I) complexes with 2,2'-bipyridine or structurally related *N,N*-ligands have attracted significant attention due to their promising cytotoxicity useful in cancer treatment, as well as interesting optical and electrochemical properties<sup>1</sup>. As copper(I) in most cases exhibits tetrahedral geometry, stoichiometric ratio between metal and bidentate chelating ligand can be either 1:1 or 1:2. In the former case, additional co-ligands must also be present and can provide a way to improve certain properties. One of them is solubility. Nonpolar groups can increase lipophilicity and thus increase bioavailability of compound, for which phosphine ligands are often used<sup>2,3</sup>.

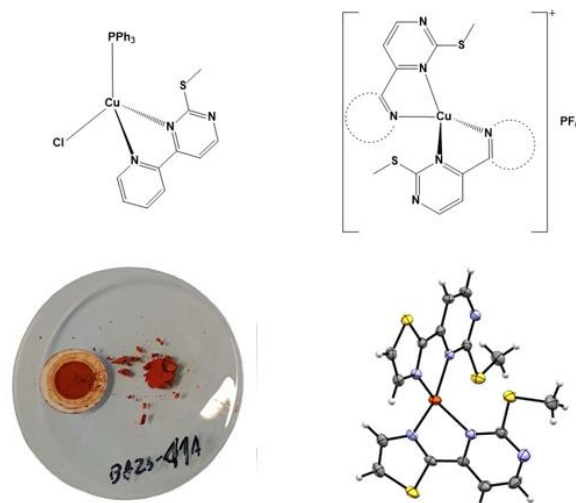
In this work, copper(I) complexes were prepared using 4-heteroaryl-2-(methylthio)pyrimidines, where heteroaryl groups were different heterocycles with nitrogen at position 2', which provides a coordination mode analogous to 2,2'-bipyridine.

Five new complexes from two sets, using six bipyridine-like ligands, were synthesized and characterized by NMR, IR and UV-VIS spectroscopy, mass spectrometry and CHN elemental analysis. Crystal structures of five of them were determined by X-ray diffraction on single crystal.

To prepare the first series of compounds, cuprous chloride was reacted with the *N,N*-ligand and triphenylphosphine in stoichiometric ratio 1:1:1. The resulting complex was prepared and characterized with one ligand, but the reaction was not as successful with other ligands. Single crystals of one additional complex were obtained but the low yield of the synthesis did not allow us a comprehensive physicochemical characterization. Synthesis of complexes with other ligands was also unsuccessfully attempted. The main issue is, except in the first case, the preferential formation of the insoluble binuclear complex of cuprous chloride and triphenylphosphine [ $\text{Cu}_2\text{Cl}_2(\text{PPh}_3)_3$ ].

In the second set of compounds ligands are bound to central ion in stoichiometric ration 2:1. This can be

achieved by using a salt with non-coordinating anion, such as  $\text{PF}_6^-$ . Crystal structures of some complexes were determined and the geometries of the complexes synthesized were shown to be deformed tetrahedral.



**Figure 1:** Schemes, picture of the product and an example of a crystal structure of prepared complex in stoichiometric ratio 1:1 (left) and 1:2 (right). Thermal ellipsoids were drawn at 50% probability level.

## References:

1. Constable, E. C.; Housecroft, C. E. The Early Years of 2,2'-Bipyridine—A Ligand in Its Own Lifetime. *Molecules* **2019**, 24 (21).
2. Alvarez, N.; Noble, C.; Torre, M. H.; Kremer, E.; Ellena, J.; Peres de Araujo, M.; Costa-Filho, A. J.; Mendes, L. F.; Kramer, M. G.; Facchin, G. Synthesis, Structural Characterization and Cytotoxic Activity against Tumor Cells of Heteroleptic Copper(I) Complexes with Aromatic Diimines and Phosphines. *Inorg. Chim. Acta.* **2017**, 466, 559–564.
3. Babgi, B. A.; Mashat, K. H.; Abdellattif, M. H.; Arshad, M. N.; Alzahrani, K. A.; Asiri, A. M.; Du, J.; Humphrey, M. G.; Hussien, M. A. Synthesis, Structures, DNA-Binding, Cytotoxicity and Molecular Docking of  $\text{CuBr}(\text{PPh}_3)(\text{Diimine})$ . *Polyhedron* **2020**, 192, 114847.



# Intensification of the Carbonization Process Using Microbubbles

Blaž Kozjek,<sup>1,2</sup> prof. dr. Igor Plazl\*,<sup>1</sup>

<sup>1</sup> Faculty of Chemistry and Chemical Technology, University of Ljubljana, Večna pot 113, SI-1000 Ljubljana, Slovenia ([igor.plazl@fkkt.uni-lj.si](mailto:igor.plazl@fkkt.uni-lj.si))

<sup>2</sup> Belinka Perkemija d.o.o. Zasavska cesta 95, SI-1231 Ljubljana – Črnuče. ([ziga.kobal@belinka.si](mailto:ziga.kobal@belinka.si))

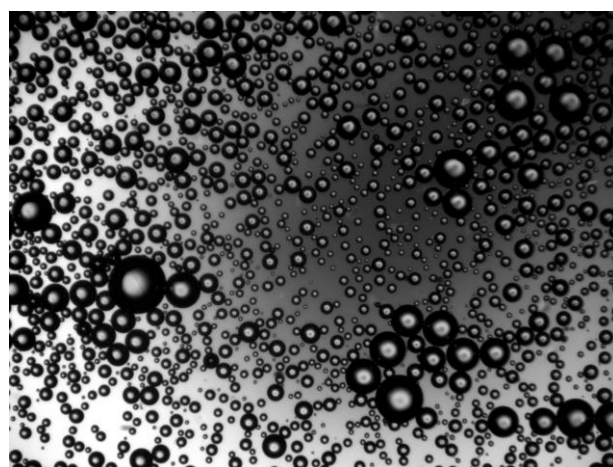
The intensification of gas–liquid contact processes plays a central role in the development of sustainable technologies for carbon capture and utilization (CCU). One promising approach is the use of microbubbles to enhance the interfacial area for gas–liquid reactions, thereby improving mass transfer efficiency and reactor performance. In this study, we investigated the formation and stability of air microbubbles in a microchannel as a simplified model for future application in CO<sub>2</sub> absorption and utilization processes.<sup>1,3</sup>

A Carmin D2 water-powered injector was used to generate a two-phase bulk mixture of air and water in a mixing chamber. Due to the internal design of the injector, air was passively drawn into the flow under a pressure of ~5 bar, forming bubbles with diameters in the range of 30–70 µm. The two-phase mixture was then fed into a polymethyl methacrylate (PMMA) microchannel with dimensions of 2 cm × 0.5 cm × 500 µm, where bubble flow characteristics were monitored under a microscope. A key part of the study was evaluating bubble stability, size distribution, residence time, and the influence of surfactant addition. Tween 20 (polyoxyethylene sorbitan monolaurate) was used in concentrations ranging from 0.1 to 3% w/w to assess its impact on bubble integrity and persistence over time.

Microbubble dynamics were recorded and analyzed using ImageJ software, where threshold-based image segmentation allowed for the quantification of maximum, minimum, and average bubble diameters, as well as the number of bubbles per frame. The residence time of bubbles was estimated from time-lapse video, and their deformation or coalescence was tracked during transit. Without surfactant, bubbles were prone to rapid merging or disappearance, particularly at higher flow rates. In contrast, with Tween 20, the system achieved a distinct, stable bubbly flow regime, and microbubbles retained their structure for extended durations—a promising observation for CO<sub>2</sub> mass transfer applications.

Although air was used as a model gas, the setup and methodology are directly transferrable to CO<sub>2</sub> systems, where the dissolution and reaction rates are even more relevant. The microreactor concept demonstrated here

provides a controllable environment to study gas–liquid interactions at the microscale and shows significant potential for integration into compact, modular CCU devices. This study lays the groundwork for further experiments using CO<sub>2</sub> under similar conditions, where enhanced gas–liquid mass transfer can be quantified using the same framework.



**Figure 1:** Visualization of air microbubbles flowing through a 0.5 cm-wide microchannel. Conditions: 1% Tween 20, 3000 µL/min total flow rate. Bubbles remain stable and evenly dispersed, with an average diameter of 46.2 µm

## References:

1. Parmar, R.; Majumder, S.K. Microbubble generation and microbubble-aided transport process intensification—A state-of-the-art report, *Chem. Eng. Process.: Process intensification*, **2013**, *64*, 79–97.
2. Upadhyay, A.; Dalvi, S. V. Microbubble Formulations: Synthesis, Stability, Modeling and Biomedical Applications, *Ultrasound Med Biol.* **2019**, *45* (2), 301–343.
3. Hong, H.; Heng, J.; Parra-Escudera, C.; Lu, J. Influence of Influent Properties on Microbubble Size in Pressurized Dissolution-Based Generation Methods. *Chem. Eng. Sci.* **2025**, *314*, 121755
4. Guha, F.; Abser, Y. Md.; Mandal, B. H.; Ji, B.; Mandal, B. J.: Recent advancements in carbon capture, utilization, and sequestration technologies. *Sustain. Chem. One World* **2025**, *7*, 100075

# Insight into the biodiversity of non-biting midges (Chironomidae) in Sečovlje Salterns through DNA barcoding

Brina Klinar,<sup>1</sup> Eva Smrekar,<sup>1</sup> Petra Tavčar Verdev,<sup>1</sup> Marko Dolinar\*,<sup>1</sup>

<sup>1</sup> Faculty of Chemistry and Chemical Technology, University of Ljubljana, Večna pot 113, SI-1000 Ljubljana, Slovenia

Sečovlje salterns have a long history of producing sea salt. Although the harvests nowadays are typically small and strongly affected by climate and seasonal weather, salt in Sečovlje is still produced using a traditional method that dates back to the 14<sup>th</sup> century<sup>1</sup>.

*Petola*, a mineralized microbial substrate, plays a vital role in traditional salt production, serving as a foundation in salt crystallization ponds. Unfortunately, *petola* is not immune to pests. Insects such as brine flies (*Ephydra*) and non-biting midges (*Chironomidae*) are known to infest *petola* with their larvae, leading to degradation of *petola* and, consequently, a reduction in both the quantity and quality of the harvested salt<sup>2</sup>.

In a previous study, the identity of the non-biting midges found in the Sečovlje salterns could not be determined beyond the family level<sup>1,2</sup>. In this study, an effort was made to determine the genus of the specimens through DNA barcoding.

A total of 13 specimens, comprising insects of both sexes, were selected for analysis. After the isolation of genomic DNA, a specific region of the cytochrome oxidase I gene (COI) was amplified using PCR. This region is widely used as a barcode for species identification in animals. The resulting DNA fragment was inserted into the pJET vector, which was then cloned in *Escherichia coli*. After the plasmid isolation, the inserts were sequenced, and the obtained sequences were analyzed using NCBI BLAST and BOLD databases. Genetic distances between the sequences were calculated with MEGA software.

All of the sequences we obtained showed a high percentage of similarity to a reference sequence assigned to members of the genus *Chironomus* (Table 1). In all cases, the identity was higher than 98%, which allowed us to conclude that all the specimens indeed belong to the genus *Chironomus*. Additionally, three sequences exhibited strong similarity to the reference sequence of *Chironomus salinarius*. Genetic distances between all of the obtained sequences were within the range of normal interspecific distances for the genus *Chironomus*, suggesting that all analyzed specimens could belong to *Chironomus salinarius*.

The results indicate that the non-biting midges infesting *petola* in the Sečovlje salterns likely belong to the genus *Chironomus* (Table 1). Given that this species is known to inhabit environments with higher salinity<sup>3</sup>, it is plausible that all of the analyzed specimens belong to *Chironomus salinarius*. However, the data do not allow us to conclude with complete certainty that all midges in the Sečovlje salterns belong to this species.

**Table 2:** Sequence analysis using BLAST and BOLD databases. The sex of the specimens, determined based on insects morphology, is indicated in the second column. The results of the BLAST search are presented in the third column. The fourth column shows the percentage of identity between the query sequence and the BLAST barcode match. The results of the BOLD search are presented in the fifth column. The sixth column shows the percentage of identity between the query sequence and the BOLD barcode match.

SPECIMEN	SEX	BLAST MATCH	IDENTITY	BOLD MATCH	IDENTITY
O1	F	<i>Chironomus sp.</i>	99,70%	<i>Chironomus sp.</i>	99,70%
O2	M	<i>Chironomus sp.</i>	99,70%	<i>Chironomus sp.</i>	99,70%
O3	M	<i>Chironomus sp.</i>	99,39%	<i>Chironomus sp.</i>	99,39%
O4	M	<i>Chironomus sp.</i>	99,55%	<i>Chironomus sp.</i>	99,55%
O5	M	<i>Chironomus sp.</i>	99,70%	<i>Chironomus sp.</i>	99,70%
O6	F	<i>Chironomus salinarius</i>	98,94%	<i>Chironomus salinarius</i>	99,09%
O7	M	<i>Chironomus salinarius</i>	99,10%	<i>Chironomus salinarius</i>	99,10%
O8	F	<i>Chironomus salinarius</i>	98,79%	<i>Chironomus salinarius</i>	98,94%
O9	F	<i>Chironomus sp.</i>	99,85%	<i>Chironomus sp.</i>	99,85%
O10	F	<i>Chironomus sp.</i>	99,39%	<i>Chironomus sp.</i>	99,39%
O11	M	<i>Chironomus sp.</i>	99,70%	<i>Chironomus sp.</i>	99,70%
O12	M	<i>Chironomus sp.</i>	99,70%	<i>Chironomus sp.</i>	99,70%
O13	M	<i>Chironomus sp.</i>	99,85%	<i>Chironomus sp.</i>	99,85%

## References:

- Jelenovec U.; Juteršek M.; Mraz J.; Štrancar V.; Tomažič M.; Uzar A.; Vogrinec L.; Glavaš N.; Klun K.; Dolinar M. Mikroorganizmi petole in solinskega blata iz Sečovljskih solin. *Bilten Fakultete za kemijo in Kemijsko tehnologijo Univerze v Ljubljani*, Ljubljana, 2022, <http://web.fkkt.uni-lj.si/biokemija/petola18.pdf> (accessed on 16.7.2025)
- Juteršek, M.; Dolinar, M. Chironomid larvae destroy cultivated microbial mat in protected Adriatic salterns. *Aquat. Conserv.: Mar. Freshw. Ecosyst.* **2021**, *31* (10), 2987–2994.
- Cartier, V.; Claret, C.; Garnier, R.; Franquet, E. How salinity affects life cycle of a brackish water species, *Chironomus salinarius* Kieffer (Diptera: Chironomidae). *J. Exp. Mar. Biol. Ecol.* **2011**, *405* (1–2), 93–98.

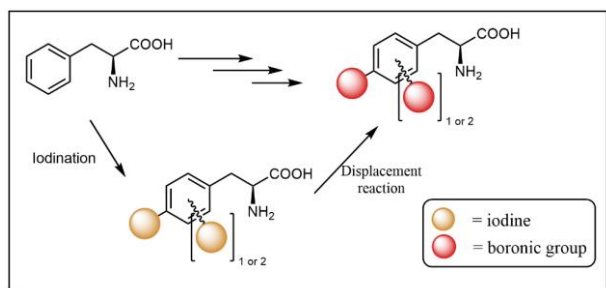
# Towards novel delivery agents for boron neutron capture therapy:

Dane Jemc,<sup>1</sup> Nejc Šerčer,<sup>1</sup> Filip Angelevski,<sup>1</sup> Martin Gazvoda\*,<sup>1</sup>

<sup>1</sup> Faculty of Chemistry and Chemical Technology, University of Ljubljana, Večna pot 113, SI-1000 Ljubljana, Slovenia, ([martin.gazvoda@fkkt.uni-lj.si](mailto:martin.gazvoda@fkkt.uni-lj.si))

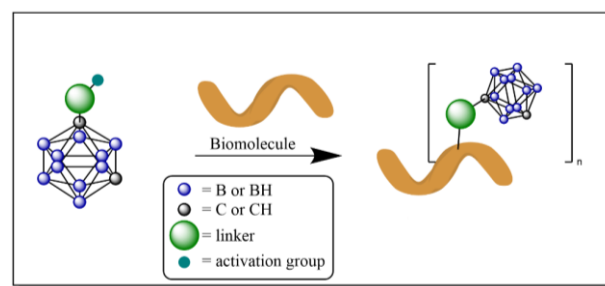
Boron neutron capture therapy (BNCT) is a binary cancer treatment based on the  $^{10}\text{B}(n, \alpha)^7\text{Li}$  nuclear reaction. Non-toxic boron-10 and non-ionizing thermal neutron beam have no therapeutic effect individually, but together they produce high-energy alpha particles and lithium ions that travel only slightly less than a cell's diameter, thus allowing for highly selective energy deposition and targeted tumor destruction.<sup>1</sup> Currently, sodium mercapto-undecahydro-*closo*-dodecaborate (BSH) and *L*-4-(dihydroxyboryl)phenylalanine (BPA) are the primary boron delivery agents used in clinical BNCT applications. These however suffer from non-ideal tumor uptake and retention.<sup>2</sup> Boronated amino acids are interesting, since the tumor uptake is usually high; on the other hand, the boron load is generally low.<sup>3</sup> Incorporation of *closo*-carborane constituents into biomolecules such as peptides and antibodies is an attractive alternative for greater boron delivery; however, problems with lipophilicity and protein aggregation arise when boron load is too high.<sup>4</sup>

Borylation of small molecules can be achieved through halogenation of aromatic systems followed by transition-metal-catalyzed or organometallic substitution reactions. Using this general strategy, we envisioned the synthesis of a polyborylated phenylalanine derivative as an analogue of BPA. The iodination step was successfully completed, while the subsequent introduction of boronyl groups has proven more challenging. Several reaction systems, including Miyaura and Grignard conditions, have been explored, and the overall synthesis is currently undergoing further optimization.



**Figure 1:** Synthetic principle for development of high boron load molecules with borylation.

In addition, bioconjugation reagents based on *closo*-1,7-dicarbadoecaborane (*m*-carborane) are being developed. The reactivity necessary for conjugation with biomolecules can be reached by functionalizing the carborane cage with a suitable activating groups. There is potential for further tuning of reagent properties by introduction of substituents at the non-functionalized carbon. Synthesised reagents will be tested for conjugation with selected biomolecular targets.



**Figure 2:** Synthetic principle for development of high boron load biomolecules containing carboranes.

## References:

1. Valliant, J. F.; Guenther, K. J.; King, A. S.; Morel, P.; Schaffer, P.; Sagbein, O. O.; Stephanson, K. A. The medicinal chemistry of carboranes. *Coord. Chem. Rev.* **2002**, *232*, 173–230.
2. Scholz, M.; Hey-Hawkin, E. Carboranes as Pharmacophores: Properties, Synthesis, and Application Strategies. *Chem. Rev.* **2011**, *111*, 7035–7062.
3. Hu, K.; Yang, Z.; Zhang, L.; Xie, L.; Wang, L.; Xu, H.; Josephson, L.; Liang, S. H.; Zhang, M.-R. Boron agents for neutron capture therapy. *Coord. Chem. Rev.* **2019**, *405*, 213139.
4. Gruzdev, D. A., Levit, G. L., Krasnov, V. P., Charushin, V. N. Carborane-containing amino acids and peptides: Synthesis, properties and applications. *Coord. Chem. Rev.* **2021**, *433*, 213753.

**Funding information:** Slovenian Research Agency (ARIS) grant J1-6000



# Esterification of PEG derivate with succinic anhydride

Daša Čebulj,<sup>1</sup> Matic Rogan,<sup>1</sup> Jerneja Kladnik,<sup>1</sup> Damijana Urankar,<sup>1</sup> Janez Košmrlj\*,<sup>1</sup>

<sup>1</sup> Faculty of Chemistry and Chemical Technology, University of Ljubljana, Večna pot 113, SI-1000 Ljubljana, Slovenia

Succinic anhydride (**Scheme 1, 2**) is a cyclic anhydride derived from succinic acid. It is industrially produced by catalytic hydrogenation of maleic anhydride. It plays an important role in organic chemistry as it easily reacts with nucleophiles and participates in reactions such as hydration, amidation and esterification. Succinic anhydride is of great importance in various industrial processes, serving as a precursor in the production of surfactants, cosmetics, pharmaceuticals, and pigments<sup>1,2</sup>.

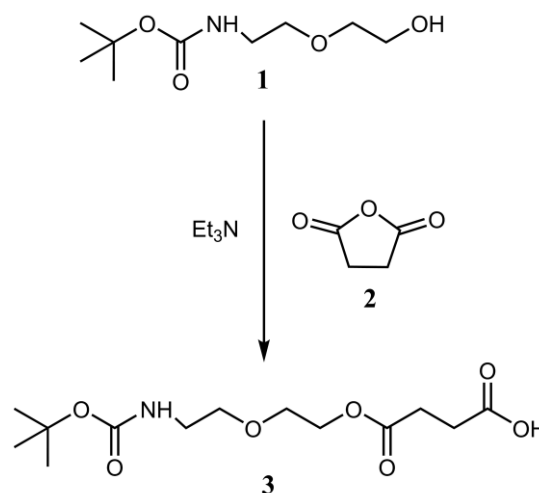
Esterification with succinic anhydride is a promising approach in polymer and materials science. For example, Leszczyńska et al.<sup>3</sup> showed that surface modification of cellulose nanocrystals with succinic anhydride produces thermally stable succinylated cellulose nanocrystals that may be used as reinforcing agents in polymer composites.

Additionally, Cai et al.<sup>4</sup> prepared a polyethylene glycol (PEG) prepolymer by reacting PEG with succinic anhydride, followed by coupling with a prepolymer of bi(o-carboxyphenyl)adipate and salicylic acid (SA). The functionalized PEG polymer showed desirable properties as a drug delivery system, such as high SA loading efficiency and slow release rate of SA in gastrointestinal conditions.

In this work, we explored the esterification of succinic anhydride (**2**) with a PEG-derived alcohol, *tert*-butyl(2-(2-hydroxyethoxy)ethyl)carbamate (**1**), to prepare an ester (**3**) with potential applications in materials science. The reaction scheme is shown in **Scheme 1**. Triethylamine served both as a base and a solvent for this reaction. The reaction mixture was stirred overnight at room temperature. Afterwards, it was extracted with dichloromethane, and the organic layer was washed with 1 M hydrochloric acid and distilled water. The organic phase was dried over anhydrous sodium sulfate, and excess solvent was removed under reduced pressure using a rotary evaporator. In this way, the pure 2,2-dimethyl-4,12-dioxo-3,8,11-trioxa-5-azapentadecan-15-oic acid (**3**) was isolated. Its structure and purity were confirmed by <sup>1</sup>H and <sup>13</sup>C NMR spectroscopy, IR spectrometry, as well as Electrospray Ionization High-Resolution Mass Spectrometry.

The successful synthesis and characterization of 2,2-dimethyl-4,12-dioxo-3,8,11-trioxa-5-azapentadecan-15-

oic acid (**3**) demonstrate that this approach is suitable for esterification of PEG-derived alcohols with succinic anhydride. The obtained compound shows potential for further applications in materials chemistry.



**Scheme 1:** Esterification of PEG-derived alcohol (**1**) with succinic anhydride (**2**).

## References:

1. Worberg, A. Succinic Acid and Succinic Anhydride. In *Kirk-Othmer Encyclopedia of Chemical Technology*; John Wiley & Sons, Ltd, 2025; pp 1–20.
2. *Succinic Anhydride - an overview | ScienceDirect Topics*. <https://www.sciencedirect.com/nukweb.nuk.uni-lj.si/topics/medicine-and-dentistry/succinic-anhydride> (accessed 2025-07-18).
3. Leszczyńska, A.; Radzik, P.; Szefer, E.; Mičušík, M.; Omastová, M.; Pielichowski, K. Surface Modification of Cellulose Nanocrystals with Succinic Anhydride. *Polymers* **2019**, *11* (5), 866.
4. Cai, Q.; Zhu, K. J.; Zhang, J. Salicylic Acid and PEG-Contained Polyanhydrides: Synthesis, Characterization, and In Vitro Salicylic Acid Release. *Drug Deliv.* **2005**, *12* (2), 97–102.

**Funding information:** The study was supported by the Slovenian Research and Innovation Agency (ARIS; Research Core Funding grant P1-0230).

# Improving Repeatability of Gas Diffusion Electrode Measurements for Alkaline Water Electrolysis

Domen Tomc<sup>1,2</sup>, Katja Jeraj<sup>1,2</sup>, Miha Hotko<sup>1,3</sup>, Nejc Hodnik<sup>\*1,3</sup>

<sup>1</sup> Department of Materials Chemistry, National Institute of Chemistry, Hajdrihova ulica 19, SI-1000 Ljubljana, Slovenia

<sup>2</sup> Faculty of Chemistry and Chemical Technology, University of Ljubljana, Večna pot 113, SI-1000 Ljubljana, Slovenia

<sup>3</sup> University of Nova Gorica, SI-5000 Nova Gorica, Slovenia

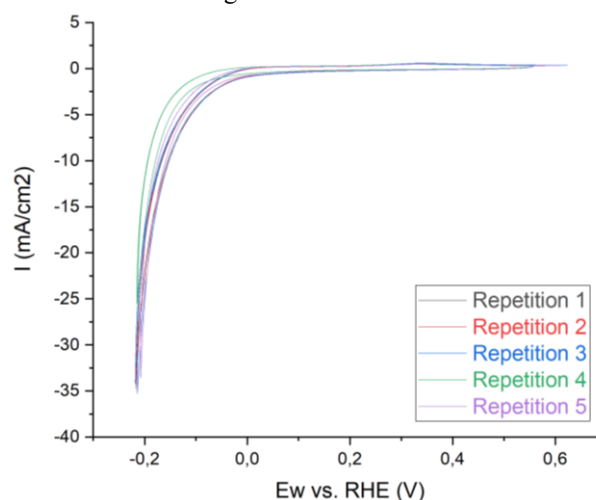
The growing concerns over climate change and environmental degradation caused by carbon dioxide emissions highlight the urgent need to transition toward sustainable energy sources. Among the promising alternatives to fossil fuels, hydrogen stands out due to its high energy density per mass and the fact that its use results in zero emissions.<sup>1</sup>

Efficient electrocatalysts are required for hydrogen production via electrolysis. Under laboratory conditions, catalytic activity is typically studied using a rotating disk electrode (RDE), which enables controlled environments and straightforward material comparison. However, RDE has a significant limitation, poor mass transport of gaseous reactants to the catalytic site, which restricts the maximum attainable current densities and deviates from the conditions typical of industrial systems.<sup>2</sup>

As an alternative, gas diffusion electrode (GDE) systems are gaining prominence. These systems enable the direct diffusion of the gaseous phase through a porous layer to the catalyst, maintaining a high local concentration of the reactant and significantly improving mass transport. GDE setups allow for higher current densities, comparable to those in industrial systems, while preserving experimental simplicity. Additionally, GDE cells incorporate a membrane, facilitating the formation of a three-phase boundary between gas, electrolyte, and catalyst, reminiscent of membrane electrode assemblies (MEA).<sup>3</sup> The stability of this interface is critical for reproducibility and long-term performance. However, it often presents a challenge, as the formation of gaseous products results in membrane detachment from the catalyst layers affecting the reproducibility of the results.

The aim of this study was to develop a GDE system that enables reliable and reproducible evaluation of the electrocatalytic activity of materials for the hydrogen evolution reaction (HER) under conditions comparable to those in real electrolyzers. In this context, we employed the GDE configuration to investigate nickel-based electrocatalysts as a cost-effective and environmentally sustainable catalyst for HER in alkaline conditions,

focusing on its efficiency, stability and repeatability as can be seen on the figure below.<sup>4</sup>



**Figure 1:** Repeatability of Electrocatalytic Activity for HER under Identical Conditions

## References:

1. Roquea, B. A. C.; Cavalcanti, M. H. C.; Brasileiro, P. P. F.; Gama, P. H. R. P.; dos Santos, V. A.; Converti, A.; Benachour, M.; Sarubbo, L. A. Hydrogen-powered future: Catalyzing energy transition, industry decarbonization and sustainable economic development: A review. *Gondwana Res.* **2025**, *140*, 159-180.
2. Nösberger, S.; Du, J.; Quinson, J.; Berner, E.; Zana, A.; Wiberg, G. K.H.; Arenz, M. The gas diffusion electrode setup as a testing platform for evaluating fuel cell catalysts: A comparative RDE-GDE study. *Electrochem. Sci. Adv.* **2022**, *3* (1), e2100190.
3. Rabiee, H.; Ge, L.; Zhang, X.; Hu, S.; Li, H.; Yuan, Z. Gas diffusion electrodes (GDEs) for electrochemical reduction of carbon dioxide, carbon monoxide, and dinitrogen to value-added products: a review. *Energy Environ. Sci.* **2021**, *14*, 1959–2008.
4. Pérez-Estrada, D.E., Sernaqué-Villagómez, M.A., Molina-Conde, L.H. et al. A comparison of Ni, Pt, and NiPt catalysts supported on SBA-15 in anisole hydrodeoxygenation: Exploring the effect of platinum addition to a nickel catalyst. *MRS Commun.* **2024**, *14*, 1191–1200.

# Development of SPE method for bisphenols

Endis Aletić\*,<sup>1</sup> Helena Prosen<sup>1</sup>

<sup>1</sup> Faculty of Chemistry and Chemical Technology, University of Ljubljana, Večna pot 113, SI-1000 Ljubljana, Slovenia

Bisphenols are a group of organic compounds that play a crucial role in the industrial development of polycarbonates and (epoxy) resins as well as many consumer products (e.g. thermal paper).<sup>1</sup> On the other hand, they also represent a group of emerging pollutants in (micro)plastics that have several adverse effects on the human body as they are endocrine disruptors. In addition to human health risks, they also pose a challenge when it comes to maintaining healthy aquatic ecosystems. Their effects have been noted to play a role in fertility issues, various developmental and metabolic disorders as well as numerous other health issues.<sup>2</sup>

Our research was therefore dedicated to the development and optimisation of a solid-phase extraction method for bisphenol A (BPA) and bisphenol S (BPS). The former was the most problematic bisphenol, hence why it had been systematically replaced by BPS over the past years. Unfortunately, it has since been discovered that the latter is no less harmful to humans.<sup>3</sup>

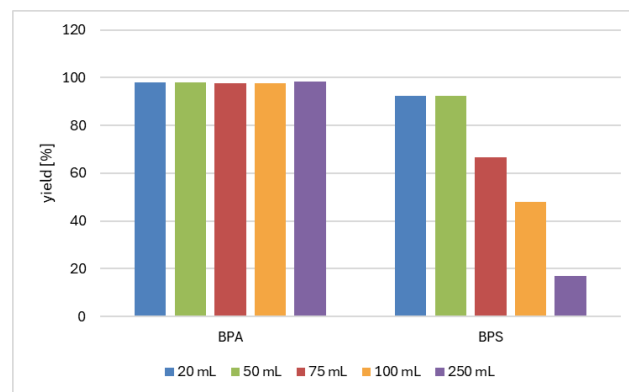
We studied the influence of different extraction parameters in order to achieve the highest possible yields. The influence of six parameters was tested, namely the suitability of the sorbent, choice and volume of elution solvent, varying pH values and ionic strength as well as whether the change in volume of MQ water (during the intermediate wash-out phase) affects the extraction yield. Furthermore, the breakthrough volume for both compounds and the method's repeatability were determined.

First, conditioning of the SPE columns was performed with 5 mL of both methanol and MQ water, before applying 20 mL of sample solution (4x5 mL). This was followed by an intermediate wash-out phase with MQ water and a 10-minute drying step. Analytes were then eluted with 5 mL of 100% acetonitrile. The eluate was analysed with pre-optimised HPLC-DAD method.

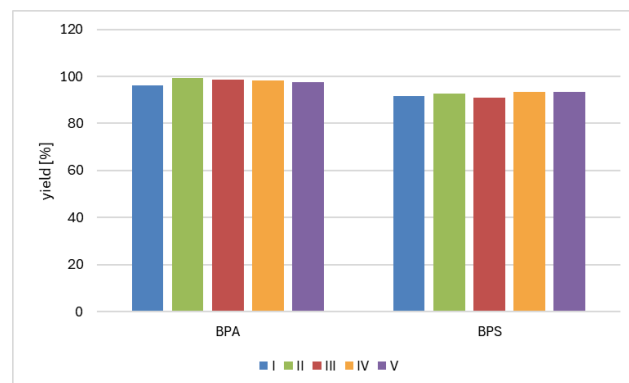
The most suitable sorbent was LC-8 (Supelco), and the highest extraction yields were achieved using 5 mL of 100% acetonitrile. Salting-out did not affect the yields, nor did the variance in pH (the experiments were continued with the original sample pH of 5.60). The change in volume of MQ water during wash-out step also had no effect on the yield.

The breakthrough volumes were more than 250 mL for BPA and around 75 mL for BPS (**Figure 1**) and the repeatability was excellent for both compounds as

the coefficients of variations were 1.12% for BPA and 1.21% for BPS. The average extraction yields were 98.0% for BPA and 92.4% for BPS (**Figure 2**).



**Figure 1:** Determination of breakthrough volumes for both compounds



**Figure 2:** Determination of method's repeatability

## References:

1. Staples, C. A.; Dorn, P. B.; Klecka, G. M.; O'Block, S. T.; Harris, L. R. A review of the environmental fate, effects, and exposures of bisphenol A. *Chemosphere* **1998**, *36*, 2149-2173.
2. Rochester, J. R., Bisphenol A and human health: A review of the literature. *Reprod. Toxicol.* **2013**, *42*, 132-155.
3. Eladak, S.; Grisin, T.; Moison, D.; Guerquin, M. J.; N'Tumba-Byn, T.; Pozzi-Gaudin, S.; Benachi, A.; Livera, G.; Rouiller-Fabre, V.; Habert, R. A new chapter in the bisphenol A story: bisphenol S and bisphenol F are not safe alternatives to this compound. *Fertil. Steril.* **2015**, *103*, 11-21.

# Genome-scale metabolic modelling of pancreatic ductal adenocarcinoma

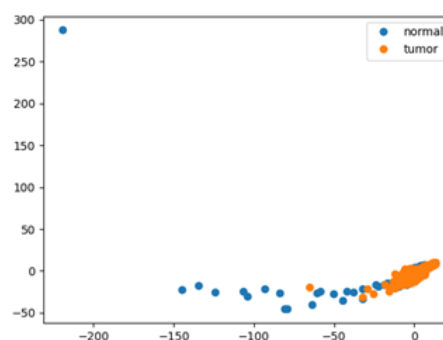
Filip Petrovič,<sup>1</sup> Ana Halužan Vasle,<sup>2</sup> Juan Solano,<sup>3</sup> Sima Tozandehjani,<sup>3</sup> Klementina Fon Tracer,<sup>3</sup> Miha Moškon,<sup>2</sup>

<sup>1</sup> Faculty of Chemistry and Chemical Technology, University of Ljubljana, Večna pot 113, SI-1000 Ljubljana, Slovenia

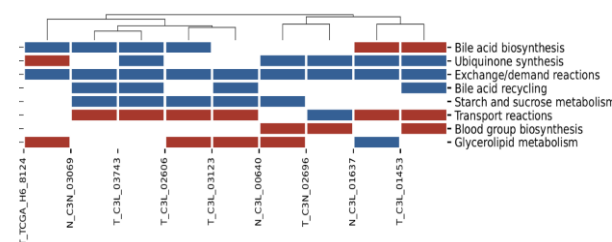
<sup>2</sup> Faculty of Computer and Information Science, University of Ljubljana, Večna pot 113, SI-1000 Ljubljana, Slovenia

<sup>3</sup> School of Veterinary Medicine, Texas Tech University, 7671 Evans Drive, Amarillo, Texas 79106, United States of America

Pancreatic cancer is one of the most lethal malignancies, with a mortality rate nearing 95%. In a significant proportion of cases, tumors arise in the pancreatic ducts, classifying the disease as pancreatic ductal adenocarcinoma (PDAC). Due to the asymptomatic nature of early-stage PDAC and the lack of effective screening methods, diagnosis often occurs at advanced stages, limiting treatment options and contributing to poor patient outcomes<sup>1</sup>. A deeper understanding of the metabolic alterations associated with pancreatic cancer is crucial for elucidating disease progression. In this study, we utilized RNA transcriptomic data from PDAC patients to construct context-specific genome-scale metabolic models (GEMs) using the fast task-driven integrative network inference for tissues (ftINIT) algorithm<sup>2</sup>. We systematically applied ftINIT to multiple input combinations to identify the optimal parameters for generating biologically relevant metabolic models. Furthermore, we investigated the metabolic impact of melanoma associated antigen A3 (MAGE-A3) overexpression in pancreatic cancer cells. MAGE-A3 is known to contribute to tumorigenesis and is associated with poor clinical outcomes<sup>3</sup>; however, its role in cancer cell metabolism remains largely unexplored. By characterizing the metabolic consequences of MAGE-A3 upregulation, we aimed to provide novel insights into its potential functional impact on pancreatic cancer metabolism, paving the way for further research into its role in disease progression.



**Figure 1:** Principle component analysis (PCA) results of constructed context-specific GEMs using the determined optimal parameters



**Figure 2:** Heatmap showing the most upregulated (blue) and downregulated metabolic subsystems of MAGE-A3 positive transcriptomic samples

## References:

1. Sarantis, P.; Koustas, E.; Papadimitropoulou, A.; Papavassiliou, A. G.; Karamouzis, M. V. Pancreatic Ductal Adenocarcinoma: Treatment Hurdles, Tumor Microenvironment and Immunotherapy. *World J. Gastrointest. Oncol.* **2020**, *12* (2), 173–181.
2. Gustafsson, J.; Anton, M.; Roshanzamir, F.; Jörnsten, R.; Kerkhoven, E. J.; Robinson, J. L.; Nielsen, J. Generation and Analysis of Context-Specific Genome-Scale Metabolic Models Derived from Single-Cell RNA-Seq Data. *Proc. Natl. Acad. Sci. U. S. A.* **2023**, *120* (6), e2217868120.
3. Florke Gee, R. R.; Chen, H.; Lee, A. K.; Daly, C. A.; Wilander, B. A.; Fon Tracer, K.; Potts, P. R. Emerging Roles of the MAGE Protein Family in Stress Response Pathways. *J. Biol. Chem.* **2020**, *295* (47), 16121–16155.

# Selective separation of model compounds from aqueous solution using a microfluidic pervaporation device

Helena Potočnik,<sup>1</sup> Rok Ambrožič\*,<sup>1</sup>

<sup>1</sup> Faculty of Chemistry and Chemical Technology, University of Ljubljana, Večna pot 113, SI-1000 Ljubljana, Slovenia

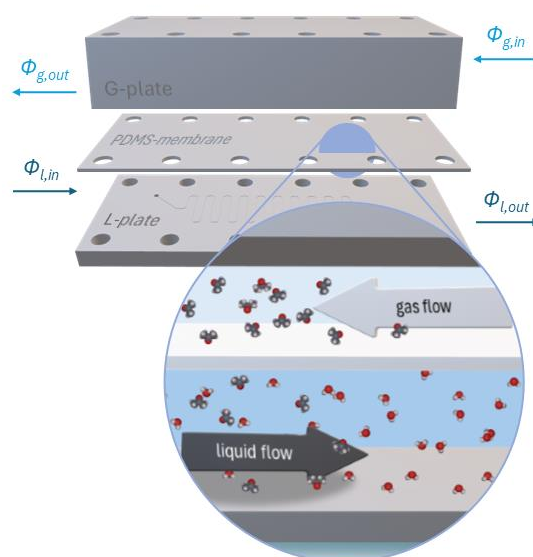
Currently, industries such as the chemical and pharmaceutical sectors are irreplaceable components of the modern economy. However, certain production strategies, for example the use of conventional metal catalysts, are gradually becoming obsolete and/or incompatible with the goals of establishing a more sustainable economy due to the depletion of limited natural resources. Therefore, there is an increasing emphasis on adopting more environmentally friendly solutions, for example bioprocesses that utilize enzymes also known as biocatalysts<sup>1</sup>. Nevertheless, there is significant potential for improvement of bioprocesses, particularly in the downstream processes (DSPs), considering many production processes currently exhibit inefficiencies in separation and purification steps, which also tend to consume a substantial portion of the overall material and financial resources<sup>2a</sup>.

One of the separation techniques applicable within DSPs for (bio)chemical processes is pervaporation. This membrane-based method enables the separation of multi-component mixtures and operates under relatively mild conditions, which can lead to reduced energy consumption compared to other methods such as distillation<sup>3</sup>.

Described phenomena can also be enhanced through the use of microfluidics, a valuable tool for process intensification that has gained significant recognition since the late 20th century<sup>2</sup>. This technology enables precise manipulation of small fluid volumes within channels ranging from micrometers to hundreds of micrometers in size, contributing to more efficient, safer and environmentally friendly process designs<sup>2b</sup>.

In our research, we developed and utilized a continuous pervaporation-based separation in a microfluidic device, enabling *in situ* removal of model molecules – specifically, acetone and acetophenone, common volatile organic compounds (VOCs) and industrial by-products – that may interfere with (bio)processes. Therefore, systematic removal of these compounds can significantly enhance operational efficiency. The effect of various operating parameters – including retention time, pressure, initial concentration, and the presence of a deep eutectic solvent (DES) – was examined using a laboratory-scale microfluidic setup.

Additionally, a mathematical model was developed to better understand and describe the separation process.



**Figure 1:** Molecular-level schematic of pervaporation in a microfluidic device

## References:

1. Satyawali, Y.; Fernandez del Pozo, D.; Vandezande, P.; Nopens, I.; Dejonghe, W. Investigating Pervaporation for *In Situ* Acetone Removal as Process Intensification Tool in  $\omega$ -Transaminase Catalyzed Chiral Amine Synthesis. *Biotechnol. Prog.* **2019**, *35*, e2731.
2. (a) Vicente, F. A.; Plazl, I.; Ventura, S. P. M.; Žnidaršič-Plazl, P. Separation and purification of biomacromolecules based on microfluidics. *Green Chem.* **2020**, *22*, 4379–4708, (b) Baccin, P.; Leng, J.; Salmon, J.-B. Microfluidic Evaporation, Pervaporation, and Osmosis: From Passive Pumping to Solute Concentration. *Chem. Rev.* **2022**, *122*, 6938–6985.
3. Jungbauer, A.; Satzer, P.; Duerauer, A.; Azevedo, A.; Aires-Barros, R.; Nilsson, B.; Farid, S.; Goldrick, S.; Ottens, M.; Sponchioni, M.; Fernandez Lahore H. M. Continuous downstream processing. *Sep. Purif. Technol.* **2024**, *338*, 126439.

**Funding information:** The author acknowledges the financial support from the Slovenian Research Agency (research core funding No. P2-0191 and projects J7-50041, J2-4562 and J2-60044).

# Atom-economical synthesis and functional diversification of pyridazinone-type heterocycles

Ines Babnik,<sup>1</sup> Nejc Petek,<sup>1</sup> Jurij Svete,<sup>1</sup> Uroš Grošelj,<sup>1</sup> Bogdan Štefane\*,<sup>1</sup>

<sup>1</sup> Faculty of Chemistry and Chemical Technology, University of Ljubljana, Večna pot 113, SI-1000 Ljubljana, Slovenia

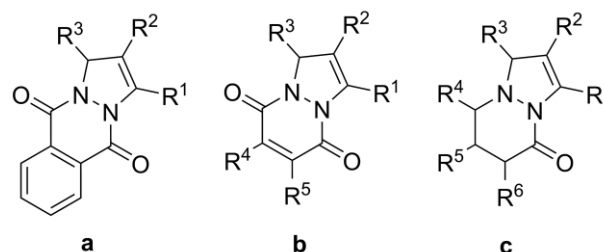
Pyrazolone-based heterocycles are valuable structural motifs in medicinal chemistry, agrochemicals, and functional materials. Due to their potent biological activity, they have been implemented as antimicrobial, antidiabetic, anticancer, anti-inflammatory, and antifungal agents.<sup>1</sup> Among pyrazolone-based heterocycles, bicyclic pyrazolonepyridazinone systems have emerged as promising enzyme inhibitors, for example as phosphodiesterase 4 (PDE4) inhibitors for the treatment of inflammatory disorders.<sup>2</sup>

Despite their biological value, some pyrazolopyridazinone derivatives remain challenging to synthesize, especially those of the [1,2]-type. While pyrazolo[1,2-*b*]phtalaiznes<sup>3</sup> and pyrazolo[1,2-*a*]pyridazine-5,8-diones<sup>4</sup> are easily accessed via multicomponent reactions, pyrazolo[1,2-*a*]pyridazinones are more difficult to prepare. This is due to the susceptibility of tetrahydropyridazinones to ring contraction under various conditions.<sup>5</sup>

In this work, we present a novel one-pot methodology for the synthesis of pyrazolo[1,2-*a*]pyridazinones under mild conditions and with excellent atom economy. The one-pot procedure enables efficient synthesis of desired compounds from easily accessible starting materials, while bypassing the problems of ring-contraction issues.

The products were further explored as substrates for photochemical transformations. By simply adjusting the reaction parameters, we achieved diverse structural modifications. These light-driven processes are rapid and do not require the use of external photocatalysts, making them highly atom-economical. Various sterically demanding pyridazinone frameworks can be accessed, which are otherwise challenging to obtain using conventional synthetic approaches.

The developed synthetic pathways are environmentally friendly, compatible with a wide range of functional groups, and offer an efficient route to novel pyridazinone derivatives.



**Figure 1:** a: pyrazolo[1,2-*b*]phtalazines, b: pyrazolo[1,2-*b*]pyridazine-5,8-diones, c: pyrazolo[1,2-*a*]pyridazinones.

## References:

1. Dubey, S. Bhosle, P. A. Pyridazinone: An Important Element of Pharmacophore Possessing Broad Spectrum of Activity. *Med. Chem. Res.* **2015**, 24 (10), 3579–3598.
2. Biagini, P., Biancalani, C., Graziano, A., Cesari, N., Giovannoni, M. P., Cilibrizzi, A., Piaz, V. D., Vergelli, C., Crocetti, L., Delcanale, M., Armani, E., Rizzi, A., Puccini, P., Gallo, P. M., Spinabelli, D., Caruso, P. Functionalized Pyrazoles and Pyrazolo[3,4-*d*]Pyridazinones: Synthesis and Evaluation of Their Phosphodiesterase 4 Inhibitory Activity. *Bioorg. Med. Chem.* **2010**, 18 (10), 3506–3517.
3. Buabeng, E. R., Shamim, M., Henary, M. Bicyclic Systems With Two Bridgehead (Ring Junction) Nitrogen Atoms. *Compr. Heterocycl. Chem. IV* **2022**, 311–338.
4. Teimouri, M. B., Mansouri, F., Bazhrang, R. Facile Synthesis of 1*H*-Pyrazolo[1,2-*a*]Pyridazine-5,8-Dione Derivatives by a One-Pot, Three-Component Reactions. *Tetrahedron* **2010**, 66 (1), 259–264.
5. Kiledal, S. A., Jourdain, R., Vellalath, S., Romo, D. Multicomponent Enantioselective Synthesis of Tetrahydropyridazinones Employing Chiral  $\alpha,\beta$ -Unsaturated Acylammonium Salts. *Org. Lett.* **2021**, 23 (17), 6622–6627.

**Funding information:** The authors gratefully acknowledge the financial support from the Slovenian Research Agency (grant P1-0179).



# From cells to genes:

## Evaluating the (geno)toxic potential of ferrite-based nanoparticles

Iza Rozman\*,<sup>1,2</sup> Alja Štern,<sup>1,2</sup> Álvaro Gallo-Cordova,<sup>3</sup> María del Puerto Morales,<sup>3</sup> Gerardo F. Goya,<sup>4</sup> Bojana Žegura,<sup>1,2</sup>

<sup>1</sup> Biotechnical Faculty, University of Ljubljana, Jamnikarjeva ulica 101, SI-1000 Ljubljana, Slovenia

<sup>2</sup> National Institute of Biology, Večna pot 121, SI-1000 Ljubljana, Slovenia

<sup>3</sup> Instituto de Ciencia de Materiales de Madrid, ICMM, CSIC, Spain

<sup>4</sup> Institute of Nanoscience and Materials of Aragón (INMA), CSIC-University of Zaragoza, Zaragoza, Spain

Spinel ferrites (SF) are metal oxides with the general formula  $AB_2O_4$ , where metal cations A and B occupy tetrahedral and octahedral sites within the crystal structure. They have attracted significant attention due to their wide range of applications, including biomedicine, water treatment, and electronic devices <sup>1</sup>.

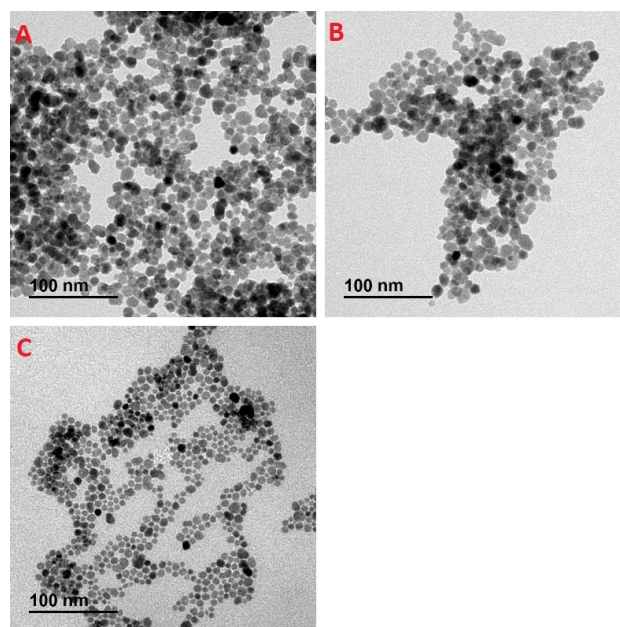
Compared to their bulk counterparts, nanomaterials (particles <100 nm), including SF, exhibit superior properties due to their small size and high surface-to-volume ratio, which enhances their reactivity, thermal stability, mechanical strength, and magnetic behaviour <sup>2</sup>. However, data on their safety and potential risks to human health remain limited.

In this study, we evaluated the potential cyto- and genotoxic effects of three spinel ferrite nanoparticles (SF NP):  $\gamma\text{Fe}_2\text{O}_3$ ,  $\text{Zn}_{0.7}\text{Fe}_{2.3}\text{O}_4$ , and  $\text{Mn}_{0.4}\text{Fe}_{2.6}\text{O}_4$ . Toxicity was assessed *in vitro* using a 3D cell model (spheroids) derived from the HepG2 human liver cancer cell line. Cell viability was measured with the CellTiter-Glo assay, while DNA damage was evaluated using the Comet assay. In addition, reactive oxygen species (ROS) levels were detected with the DCFH-DA fluorescence probe, and changes in gene expression related to DNA damage (*CDKN1a*, *GADD45A*, *TP53*, *MYC*, and *OGG1*) and oxidative stress responses (*SOD1*, *CAT*, *GPX1*, *GCLC*, and *GSR*) were analysed using qPCR.

Three-day-old HepG2 spheroids were exposed to graded concentrations of the tested nanoparticles (up to 250  $\mu\text{g/mL}$ ) for 2, 4, 24, and/or 96 hours, depending on the assay. The results showed that  $\text{Zn}_{0.7}\text{Fe}_{2.3}\text{O}_4$  and  $\text{Mn}_{0.4}\text{Fe}_{2.6}\text{O}_4$  induced greater cytotoxicity than  $\gamma\text{Fe}_2\text{O}_3$  at both 24- and 96-hour exposure points. The Comet assay indicated minimal or no significant DNA damage after 24 hours of exposure (5–50  $\mu\text{g/mL}$ ). In contrast, a considerable, dose-dependent increase in DNA damage was observed after 96 hours. Additionally, a significant dose-dependent increase in ROS generation was detected only for  $\gamma\text{Fe}_2\text{O}_3$  after 4 hours of exposure. At the transcriptome level, no clear deregulation was observed for the analysed genes, except for *MYC*, which was

consistently downregulated across all samples after 24 hours.

These findings contribute to a better understanding of the (geno)toxic potential of SF NPs and highlight the need for further investigation into their safety.



**Figure 1:** TEM micrographs of SF NP: (A)  $\gamma\text{Fe}_2\text{O}_3$ , (B)  $\text{Zn}_{0.7}\text{Fe}_{2.3}\text{O}_4$ , (C)  $\text{Mn}_{0.4}\text{Fe}_{2.6}\text{O}_4$ .

### References:

1. Salih, S. J.; Mahmood, W. M. Review on Magnetic Spinel Ferrite ( $\text{MFe}_2\text{O}_4$ ) Nanoparticles: From Synthesis to Application. *Heliyon* **2023**, *9* (6), e16601.
2. Mokhosi, S.; Mdalose, W.; Mngadi, S.; Singh, M.; Moyo, T. Assessing the Structural, Morphological and Magnetic Properties of Polymer-Coated Magnesium-Doped Cobalt Ferrite ( $\text{CoFe}_2\text{O}_4$ ) Nanoparticles for Biomedical Application. *J. Phys. Conf. Ser.* **2019**, *1310* (1), 012014.

**Funding information:** H2020-MSCA NESTOR (101007629), HE CutCancer (101079113), ARIS P1-0245, J1-4395, and MR grant to IR.

# Use of HEO as catalysts in Fenton process for treatment of wastewaters

Jaka Janežič\*,<sup>1</sup> Maša Legan,<sup>1</sup> Andreja Žgajnar Gotvajn<sup>1</sup>

<sup>1</sup> University of Ljubljana, Faculty of Chemistry and Chemical Technology, Večna pot 113, SI-1000 Ljubljana, Slovenia

High-entropy oxides (HEOs) are a recently discovered group of high-entropy materials (HEMs)<sup>1</sup>. These one-phase crystalline materials consist of five or more different metal components<sup>2</sup>. HEOs are structurally complex and can have a variety of useful and unique properties. Due to high tunability, rich magnetic properties, electrical properties and more<sup>2</sup>, they have attracted significant interest in fields such as energetics, electro-catalysis and catalysis<sup>1,2</sup>, although their capabilities as new materials need to be studied further.

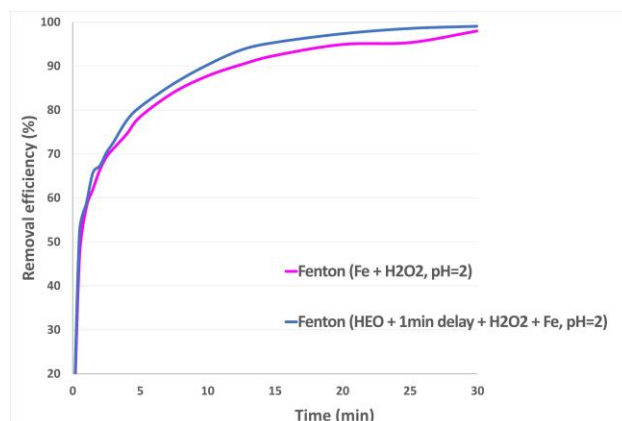
Therefore, the main idea of the work was to implement HEOs into the Fenton process with the intention of improving it. The Fenton process itself is a type of advanced oxidation process (AOP)<sup>3</sup>. That means it generates hydroxyl radicals which are used for wastewater treatment. This is achieved by adding peroxide ( $\text{H}_2\text{O}_2$ ) and iron ions ( $\text{Fe}^{2+}$ ) into the wastewater with acidic pH<sup>3</sup>.

The HEO we used for the experiments was synthesised using combustion synthesis and had a composition of  $(\text{Mg}_{0.2}\text{Co}_{0.2}\text{Ni}_{0.2}\text{Cu}_{0.2}\text{Zn}_{0.2})\text{O}$ . As a wastewater substitute we decided to use a 300 mL solution of Methylene blue (MB) with concentration of  $10 \text{ mg L}^{-1}$ . Firstly, the adsorption properties of HEO were studied. Through various experiments it was concluded, that the best results were achieved in a narrow beaker with an anchor type mixer at 160 rpm (removal percentage of 15% with 1 mg of HEO).

Subsequently, many different Fenton process experiments followed. The beaker, mixer, mixing speed and the MB concentration have remained the same, while many different initial HEO, peroxide and iron additions and ratios have been tested as well as various initial pHs, different combinations of reagents and various orders of adding them. The results so far have shown that selected HEO cannot be used as a replacement for the  $\text{Fe}^{2+}$  ions. However it has shown promise in enhancing  $\text{Fe}^{2+}$  catalytic activity. Results for an experiment at pH=2, (10 mg of HEO, 0.025 mL of  $\text{H}_2\text{O}_2$  (30 % w/w -8,25 mg) and 0.025 mL of  $\text{Fe}^{2+}$  ( $0.5 \text{ mol L}^{-1}$ )) are presented in Figure 1. 99% removal efficiency was achieved after 30 minutes using  $\text{Fe}^{2+}$ , HEO and peroxide (Figure 2).



**Figure 1:** MB solution before (left) and after (right) the Fenton process involving HEO, Fe and  $\text{H}_2\text{O}_2$ .



**Figure 2:** Removal efficiencies for experiments with and without added HEO at pH=2.

## References:

1. Sen, S.; Palabathuni, M.; Ryan, M. K.; Singh, S. High Entropy Oxides: Mapping the Landscape from Fundamentals to Future Vistas Focus Review. *ACS Energy Letters* **2024**, *9* (8), 3694–3718.
2. Kante, V. M.; Weber, L. M.; Ni, S.; van den Bosch, G. C. I.; van der Minne, E.; Heymann, L.; Falling, J. L.; Gauquelin, N.; Tsvetanova, M.; Cunha, M. D.; Koster, G.; Gunkel, F.; Nemšak, S.; Hahn, H.; Estrada, V. L.; Baeumer, C. A High-Entropy Oxide as High-Activity Electrocatalyst for Water Oxidation. *ACS Nano* **2023**, *17* (6), 5329–5339.
3. Babuponnusami, A.; Muthukumar, K. A review on Fenton and improvements to the Fenton process for wastewater treatment. *J. Environ. Chem. Eng.* **2014**, *2* (1), 557–572.



# Phenolic Azobenzenes from Lignin Precursors: Toward Sustainable Photoactive Antimicrobials

Jan Hočevar,<sup>1</sup> Estelle Leonard,<sup>2</sup> Jernej Iskra\*,<sup>1</sup>

<sup>1</sup> Faculty of Chemistry and Chemical Technology, University of Ljubljana, Večna pot 113, SI-1000 Ljubljana, Slovenia

<sup>2</sup> Université de Technologie de Compiègne, ESCOM, TIMR, F-60200 Compiègne, France

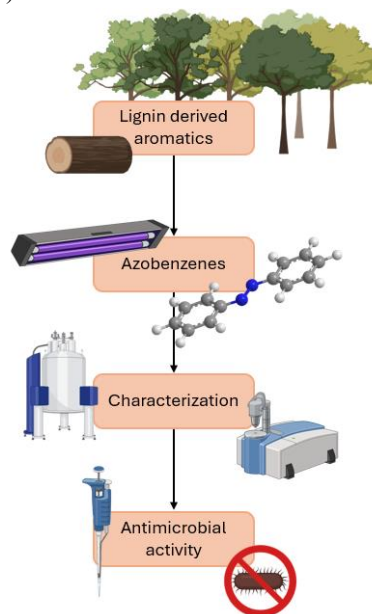
Lignin is a complex, aromatic biopolymer found in plant cell walls, where it provides structural support, water resistance and protection against decay. As the second most abundant natural polymer after cellulose, it is an important by-product of the pulp and paper industry, but unfortunately most of it is thrown away.<sup>1</sup> Globally, around 50,000,000 tonnes of lignin are produced annually and this is expected to increase to 225,000,000 tonnes by 2030. However, less than 2 % of the total lignin produced is actually utilised. Due to its richness in phenolic structures, lignin offers great potential as a renewable source for the production of valuable molecules, such as azobenzenes.

Azobenzenes are organic compounds that have an azo group (-N=N-) linking two benzene rings. Their unique properties are due to a conjugated  $\pi$ -electron system, which significantly influences their optical, electronic and structural behaviour. Of particular interest is their reversible *trans*-*cis* photoisomerisation, which makes them useful as photosensitive materials.<sup>2</sup> It is because of their unique properties that we consider azobenzenes not only as dyes, but also in everyday applications, in particular in molecular electronic and photonic devices, medicinal chemistry, photopharmacology, drug delivery, etc.

Hydroxyazobenzenes are organic compounds in which both hydroxyl (-OH) and azo functions (-N=N-) are bound to benzene rings. The position of the hydroxyl group significantly influences their properties. Various synthesis strategies have been developed for phenolic azobenzenes, which offer different advantages in terms of selectivity, efficiency and tolerance to functional groups. Common methods include azo coupling, the Mills and Wallach reaction, oxidative conversions of anilines and the reduction of nitroaromatic precursors.<sup>3</sup> While the synthesis of symmetrically substituted azobenzenes is well established, the efficient production of non-symmetrical analogues remains a major challenge.<sup>4</sup>

In this study, aromatic compounds derived from lignin were used as building blocks for azobenzene synthesis. These precursors were first converted into nitro or aniline derivatives and then converted into azobenzenes using various synthetic approaches. The resulting azobenzene compounds were thoroughly

characterised and their antimicrobial activity against various G+ and G- bacterial strains was investigated (Scheme 1).



**Scheme 1:** The pathway from lignin-based aromatics and their conversion to azobenzenes and their antimicrobial efficacy.

## References:

1. Ponnusamy, V. K.; Nguyen, D. D.; Dharmaraja, J.; Shobana, S.; Banau, J. R.; Saratale, R. G.; Chang, S. W.; Kumar, G. A review on lignin structure, pretreatments, fermentation reactions and biorefinery potential. *Bioresour. Technol.* **2019**, *271*, 462–472.
2. Hočevar, J.; Iskra, J.; Leonard, E. Phenolic Azobenzene as Ligand for Cation Complexation—Syntheses and Applications. *Molecules* **2025**, *30* (12), 2499.
3. Jerca, F. A.; Jerca, V. V.; Hoogenboom, R. Advances and opportunities in the exciting world of azobenzenes. *Nat. Rev. Chem.* **2022**, *6*, 51–69.
4. Finck, L.; Oestreich, M. Synthesis of Non-Symmetric Azoarenes by Palladium-Catalyzed Cross-Coupling of Silicon-Masked Diazenyl Anions and (Hetero)Aryl Halides. *Angew. Chem. Int. Ed.* **2022**, *61*, e202210907.

**Funding information:** This research was funded by TIMR Laboratory, UTC/ESCOM, and Slovenian Research and Innovation Agency (grant P1-0134).

# Innovative LexKan Selection System for the Discovery of Dimerization Inhibitors Targeting SARS-CoV-2 Main Protease

Jan Kogovšek,<sup>1</sup> Ana Obaha,<sup>1</sup> Marko Novinec\*,<sup>1</sup>

<sup>1</sup> Faculty of Chemistry and Chemical Technology, University of Ljubljana, Večna pot 113, SI-1000 Ljubljana, Slovenia

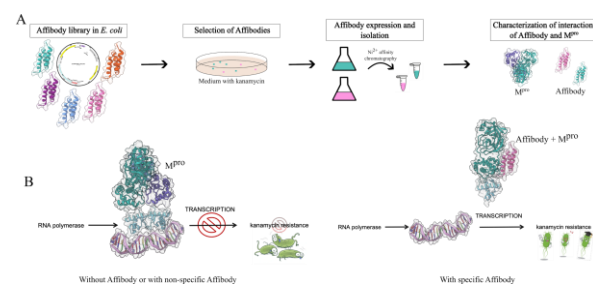
The SARS-CoV-2 main protease (M<sup>pro</sup>, or 3CL<sup>pro</sup>) is a cysteine protease responsible for cleaving viral polyproteins into individual, functional proteins required for viral replication. M<sup>pro</sup> is active only as a homodimer, making dimerization an essential prerequisite for its enzymatic function. Because its structure and function are highly conserved among coronaviruses, M<sup>pro</sup> has emerged as a promising target for antiviral drug development. Traditional inhibition strategies have focused on active site binding, but targeting dimerization offers an alternative approach that may increase specificity and limit resistance<sup>1</sup>.

To address this, we explored the use of affibody molecules, small engineered proteins derived from the Z-domain of *Staphylococcal* protein A. This domain is naturally involved in binding immunoglobulins, and through protein engineering, it has been repurposed into a versatile scaffold capable of high-affinity binding to a wide range of target proteins. Affibodies are highly stable, non-immunoglobulin binders that are easily produced in bacterial systems, making them ideal candidates for interfering with protein–protein interactions such as M<sup>pro</sup> dimerization<sup>2</sup>.

We developed and optimized the LexKan selection system in *Escherichia coli* to identify affibody binders that disrupt M<sup>pro</sup> dimer formation. The system is based on a fusion of M<sup>pro</sup> to the bacterial repressor LexA. In its dimeric form, LexA represses transcription of the kanamycin resistance gene (KanR). When M<sup>pro</sup> dimerization is inhibited, LexA repression is relieved, allowing KanR expression and bacterial growth on kanamycin-containing media (Figure 1). The concept is adapted from a prior bacterial selection system designed to detect protein–protein interactions, modified here to suit viral protease inhibition<sup>3</sup>.

From this selection, a set of affibody candidates was successfully obtained and expressed. These molecules represent promising leads for further studies aimed at assessing their ability to modulate M<sup>pro</sup> dimerization. The work demonstrates the potential of the LexKan system as

a versatile platform for discovering molecular binders, providing a foundation for the development of targeted antiviral strategies.



**Figure 1:** (A) Schematic representation of the experimental workflow. A diverse affibody library is expressed in *E. coli* and subjected to selection on medium containing kanamycin using the LexKan system. Selected clones are expressed, purified by Ni<sup>2+</sup> affinity chromatography, and analyzed for the interaction with M<sup>pro</sup>. (B) Principle of the LexKan selection system. In the absence of a specific affibody, M<sup>pro</sup> dimerization enables LexA-mediated repression of the kanamycin resistance gene, preventing bacterial growth. When a specific affibody disrupts M<sup>pro</sup> dimerization, repression is relieved, allowing transcription of the resistance gene and bacterial survival on kanamycin-containing medium.

## References:

1. Roe, M. K.; Junod, N. A.; Young, A. R.; Beachboard, D. C.; Stobart, C. C. Targeting Novel Structural and Functional Features of Coronavirus Protease Nsp5 (3CL<sup>pro</sup>, M<sup>pro</sup>) in the Age of COVID-19. *J. Gen. Virol.* **2021**, *102* (3), 001558.
2. Ståhl, S.; Gräslund, T.; Karlström, A. E.; Frejd, F. Y.; Nygren, P.-Å.; Löfblom, J. Affibody Molecules in Biotechnological and Medical Applications. *Trends in Biotechnol.* **2017**, *35* (8), 691–712.
3. Ulčakar, L. Development of a screening assay for the detection of protein homodimerization in *Escherichia coli*. Master's Thesis, University of Ljubljana, Faculty of Chemistry and Chemical Technology, **2022**.

# Characterization of lanthanum doped nickel oxide thin films for oxygen evolution reaction

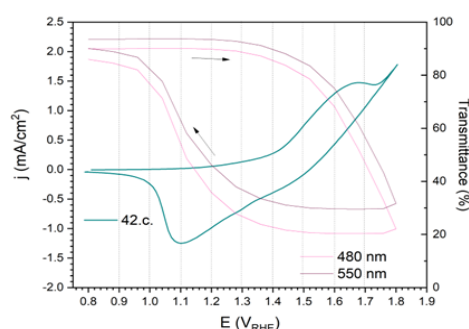
Jan Očepek\*,<sup>1,2</sup> Romana Cerc Korošec,<sup>2</sup> Marjan Bele,<sup>1</sup> Nejc Hodnik,<sup>1</sup> Angelja Kjara Surca,<sup>1</sup>

<sup>1</sup> National Institute of Chemistry, Hajdrihova 19, SI-1000 Ljubljana, Slovenia

<sup>2</sup> Faculty of Chemistry and Chemical Technology, University of Ljubljana, Večna pot 113, SI-1000 Ljubljana, Slovenia

The Ni(II)/Ni(III) redox couple has long been studied within the framework of the Bode scheme, which maps the electrochemical behavior of nickel hydroxides and oxyhydroxides through formation of  $\alpha$ -Ni(OH)<sub>2</sub>/ $\gamma$ -NiOOH  $\beta$ -Ni(OH)<sub>2</sub>/ $\beta$ -NiOOH phases [1,2]. This redox system gained attention for its reversible charge storage properties, making it a key component in Ni-based batteries (e.g., Ni-Cd and Ni-MH) and electrochromic (EC) devices. EC devices, composed of two transition oxide films and electrolyte, show distinct color change upon oxidation/reduction [1]. More recently, interest has shifted toward the role of the Ni(II)/Ni(III) transition in electrocatalysis, particularly for the oxygen evolution reaction (OER) in alkaline media [2]. Modern studies explore how structural transformations and phase evolution in the Bode scheme affect catalytic OER activity and stability, also through incorporation of additional elements like Fe, Co, Mn etc. in Ni-based samples.

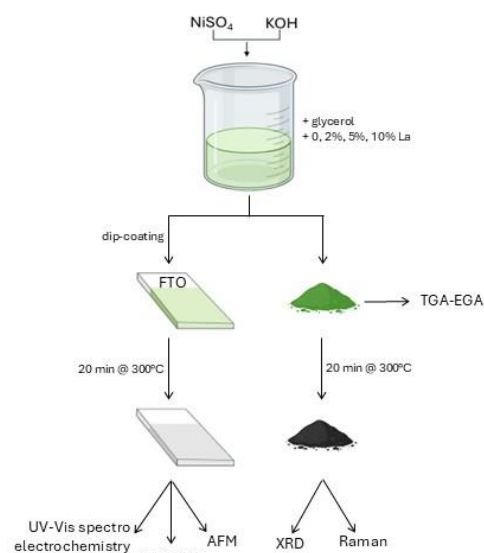
Concurrently, we leaned on the sol-gel synthesis of  $\alpha$ -Ni(OH)<sub>2</sub> electrochromic films which showed improved cyclovoltammetric cycling stability after the addition of lanthanum [1]. The films were deposited on FTO glass using the dip coating technique from sols that were synthesized from nickel(II) sulphate heptahydrate. Films were thermally treated at 300 °C for 20 min and, in addition, powders were also prepared from dried sols.



**Graph 3:** CV of Ni-oxide thin film with 10 % La and its transmittance measured during the potential step.

The *in-situ* UV-visible absorbance spectroelectrochemical measurements were made in 0.1

M KOH in a custom-made glass cell with quartz windows. The potential range employed (0.8 to 1.8 V vs. RHE) scanned the Ni(II)/Ni(III) redox transformation, as well also the OER region. Measurements were performed for pure  $\alpha$ -Ni(OH)<sub>2</sub> film and for those with intercalated lanthanum (2, 5 and 10 mol.% La) (**Graph 1**). The behavior of powders was also examined using evolved gas analysis (EGA) and Raman spectroscopy.



**Scheme 1:** Graphical abstract of synthesis and characterization of the La-doped Ni-oxides

## References:

- Šurca, A.; Orel, B.; Pihlar, B. Characterisation of Redox States of Ni(La)-Hydroxide Films Prepared via the Sol-Gel Route by ex Situ IR Spectroscopy. *J. Solid State Electrochem.* **1998**, *2*, 38–49.
- Rao, R. R.; Corby, S.; Bucci, A.; García-Tecedor, M.; Mesa, C. A.; Rossmeisl, J.; Giménez, S.; Lloret-Fillol, J.; Stephens, I. E. L.; Durrant, J. R. Spectroelectrochemical Analysis of the Water Oxidation Mechanism on Doped Nickel Oxides. *J. Am. Chem. Soc.* **2022**, *144*, 7622–7633.

**Funding information:** This study was funded by the Slovenian Research Agency (ARIS) through research program P2-0393 and project J1-4401.

# Tracking individual degradation mechanisms for Pt-Co nanoparticles

Jan Vidergar\*,<sup>1,2</sup> Ana Rebeka Kamšek\*,<sup>1</sup> Francisco Ruiz-Zepeda,<sup>1</sup> Anja Logar,<sup>1,3</sup> Goran Dražić,<sup>1</sup> Neje Hodnik<sup>1,3</sup>

<sup>1</sup> Department of Materials Chemistry, National Institute of Chemistry, Hajdrihova 19, 1000 Ljubljana, Slovenia

<sup>2</sup> Faculty of Chemistry and Chemical Technology, University of Ljubljana, Večna pot 113, 1000 Ljubljana, Slovenia

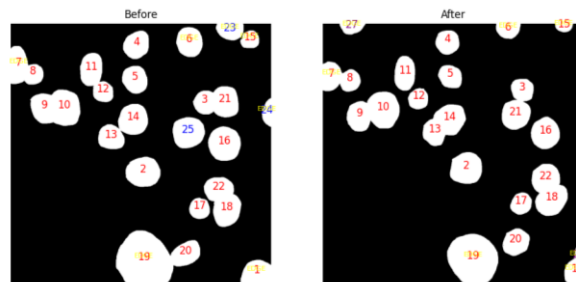
<sup>3</sup> University of Nova Gorica, Vipavska 13, 5000 Nova Gorica, Slovenia

An identical-location STEM (Scanning transmission electron microscopy) approach was used to track individual Pt–Co/C nanoparticles before and after electrochemical activation. Nanoparticles in the same field of view were segmented and then paired between the initial and post-activation images using the Hungarian assignment algorithm<sup>2</sup>, yielding a one-to-one correspondence for each particle (Figure 1). Each matched (or unmatched) nanoparticle between images was defined as an event, representing a specific outcome of degradation or stability<sup>1</sup>.

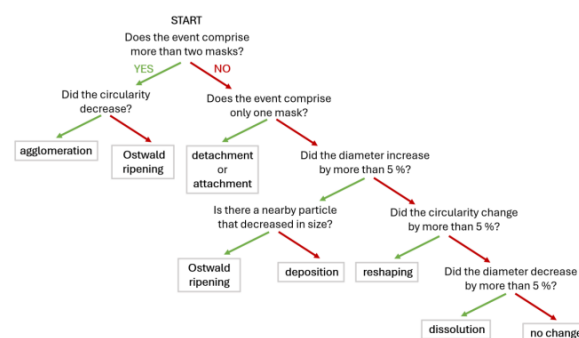
Events were categorized via a decision-tree scheme (Figure 2) that considered the number of particle masks in an event (e.g., a single mask if a particle disappeared or appeared, multiple masks if particles merged) as well as changes in particle size (equivalent diameter) and shape (circularity)<sup>3</sup>. Based on these criteria, each event was assigned to a degradation mechanism category (or marked as no significant change). Degradation modes such as dissolution, detachment, attachment, agglomeration, and Ostwald ripening were thereby distinguished. Particle properties like diameter and circularity were extracted from the IL-STEM images to quantify morphological changes for every event.

The IL-STEM analysis tracked 209 nanoparticle events, enabling quantification of their fates. Dissolution was the most frequent pathway, accounting for roughly half of all events, while about 22% of particles remained unchanged. Detachment events (loss of particles from the support) made up ~10% and predominantly involved the smallest nanoparticles. Attachments (appearance of new small particles) and agglomerations (particle coalescence) were less common (only a few percent each), with Ostwald ripening events being very scarce in this dataset. This dataset-driven analysis allowed direct quantification of particle size/shape changes and revealed the most prevalent degradation pathways, with dissolution

emerging as the dominant mechanism under the tested conditions<sup>1</sup>.



**Figure 1:** Matched Pt-Co Nanoparticles Before and After Catalytic Treatment



**Figure 2:** A decision tree showing how events are classified into degradation mechanisms.

## References:

1. Kamšek, A. R. Kristalna struktura platinskih in iridijevih nanokompozitnih elektrokatalizatorjev. Ph. D. Dissertation, University of Ljubljana, Faculty of Chemistry and Chemical Technology, 2025.
2. Reiter, F.; Reeb, D.; Sørensen, A. S. Scalable Dissipative Preparation of Many-Body Entanglement. *Phys. Rev. A* **2017**, 95 (5), 053424.
3. Đukić, T.; Pavko, L.; Jovanović, P.; Maselj, N.; Gatalo, M.; Hodnik, N. Stability Challenges of Carbon-Supported Pt-Nanoalloys as Fuel Cell Oxygen Reduction Reaction Electrocatalysts. *Chem. Commun.* **2022**, 58 (100), 13832–13854.

# Mechanical and Biological Evaluation of Alginate-TEMPO Cellulose Hydrogels

Jan Vidergar\*,<sup>1</sup> Boštjan Vihar,<sup>2</sup> Monika Belak,<sup>2</sup> Ajda Godec,<sup>2</sup> Uroš Maver,<sup>2</sup> Tilén Kopač<sup>1</sup>

<sup>1</sup> Faculty of Chemistry and Chemical Technology, University of Ljubljana, Večna pot 113, SI-1000 Ljubljana, Slovenia

<sup>2</sup> Institute of Biomedical Sciences, Faculty of Medicine, University of Maribor, Taborska ulica 8, 2000 Maribor, Slovenia

Hydrogels based on alginate and TEMPO-oxidized cellulose have gained increasing attention due to their biocompatibility and tunable mechanical properties<sup>1,2</sup>. Alginate, a naturally occurring polysaccharide, forms ionically crosslinked networks in the presence of divalent cations such as  $\text{Ca}^{2+}$ , providing a versatile matrix for biomedical applications<sup>4</sup>. The addition of TEMPO-oxidized cellulose nanofibers (TOCNF) has been shown to influence the structure and stiffness of these materials through hydrogen bonding and electrostatic interactions<sup>1,2</sup>.

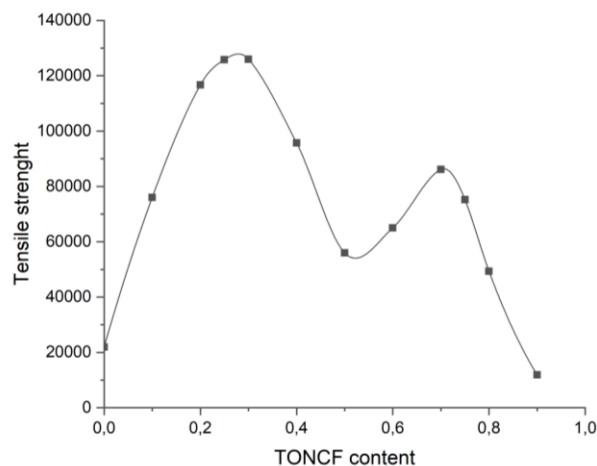
This study investigates the mechanical and biological properties of hydrogels composed of alginate and 3% TEMPO-oxidized cellulose nanofibers (TOCNF), combined in various ratios. Hydrogels were prepared by mixing alginate gels of different concentrations with TOCNF gels at a fixed 3% loading, followed by crosslinking with calcium ions ( $\text{Ca}^{2+}$ ). Mechanical properties were evaluated via tensile testing, revealing a nonlinear relationship between the alginate-to-TOCNF ratio and tensile strength (Figure 1). Optimal mechanical performance was observed at intermediate compositions. Consistent with previous findings<sup>3,5</sup>, the inclusion of TOCNF improved the elastic modulus and reinforced the network structure, particularly at higher alginate content.

Cellular responses were investigated using HaCaT keratinocytes and skin fibroblasts, employing Alamar Blue and Live/Dead viability assays. Preliminary observations suggest that HaCaT metabolic activity may be influenced by hydrogel stiffness, whereas fibroblasts appeared to favor softer, less crosslinked hydrogels. While these trends are not yet conclusive, they point toward possible cell-type-specific responses to mechanical cues in the hydrogel microenvironment<sup>4,5</sup>.

To support formulation design, a computational tool was developed to predict mechanical behavior based on experimental data. While preliminary, this tool demonstrates potential for optimizing hydrogel compositions to achieve target properties.

These findings contribute to the growing body of knowledge on hybrid hydrogels<sup>2</sup>, emphasizing the need to

tailor mechanical characteristics for specific cell types and applications in regenerative medicine and tissue scaffolding.



**Figure 1:** Tensile strength of 7.5% alginate and 3% TEMPO-oxidized cellulose hydrogels across different mixing ratios.

## References:

1. Siqueira, P.; Siqueira, É.; de Lima, A. E.; Siqueira, G.; Pinzón-García, A. D.; Lopes, A. P.; Segura, M. E. C.; Isaac, A.; Pereira, F. V.; Botaro, V. R. Three-Dimensional Stable Alginate-Nanocellulose Gels for Biomedical Applications: Towards Tunable Mechanical Properties and Cell Growing. *Nanomaterials (Basel, Switzerland)*, **2019**, 9 (1), 78.
2. Ning, X.; Huang, J.; A, Y.; Yuan, N.; Chen, C.; Lin, D. Research Advances in Mechanical Properties and Applications of Dual Network Hydrogels. *Int. J. Mol. Sci.* **2022**, 23, 15757.
3. Kamdem Tamo, A.; Wu, T.; Gaan, S.; Bandyopadhyay, A.; Basu, B. Nanocellulose-based hydrogels as versatile materials with interesting functional properties for tissue engineering applications. *J. Mater. Chem. B* **2024**, 12, 7692–7759.
4. Lee, K. Y.; Mooney, D. J. Alginate: Properties and biomedical applications. *Prog. Polym. Sci.* **2012**, 37, 106–126.
5. Rezić, T.; Perković, I.; Andlar, M.; Vrsalović Presečki, A., Kemijske modifikacije nanoceluloze. *Croat. J. Food Technol. Biotechnol. Nutr.* **2022**, 17 (1–2), 52–5.



# The influence of copper ions on the binding of N-Acetyl-D-lactosamine to hen egg white lysozyme

Jana Bregar\*,<sup>1</sup> Timotej Majdič,<sup>1</sup> Barbara Hribar-Lee,<sup>1</sup>

<sup>1</sup> Faculty of Chemistry and Chemical Technology, University of Ljubljana, Večna pot 113, SI-1000 Ljubljana, Slovenia, [jb00681@student.uni-lj.si](mailto:jb00681@student.uni-lj.si)

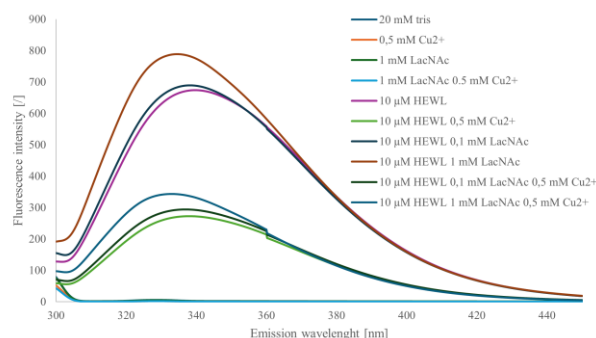
Disruption of metal ion homeostasis can lead to oxidative stress, which promotes protein misfolding and aggregation linked to several pathological conditions <sup>1</sup>. The aim of our research was to investigate the influence of copper ( $\text{Cu}^{2+}$ ) ions on the binding of N-Acetyl-D-lactosamine (LacNAc) to hen egg white lysozyme (HEWL).

Fluorescence spectroscopy was used to monitor changes in intrinsic tryptophan fluorescence of HEWL induced by the interaction between LacNAc,  $\text{Cu}^{2+}$  ions and HEWL. The effect of copper ions on the secondary structure and the thermostability of HEWL were assessed using circular dichroism (CD) spectroscopy and differential scanning calorimetry (DSC), respectively. The location of the binding site of LacNAc and the types of interactions present were studied using molecular docking.

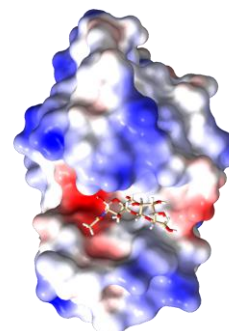
The binding of LacNAc caused an increase in fluorescence intensity and a shift of the emission maximum toward smaller wavelengths, while the addition of  $\text{Cu}^{2+}$  ions decreased the fluorescence intensity and did not cause any significant shift of the maximum. CD spectra analysis showed that  $\text{Cu}^{2+}$  ions do not cause substantial changes in the protein's secondary structure under the conditions studied. DSC experiments show only minor decrease in melting temperature ( $T_m$ ) of HEWL upon addition of  $\text{Cu}^{2+}$  ions at a concentration proportional to that used in the spectroscopic measurements, which suggests that  $\text{Cu}^{2+}$  ions do not significantly destabilize HEWL at that concentration. Molecular docking predicts that LacNAc binds in the active site cleft of HEWL. The observed binding of LacNAc to HEWL was mainly driven by hydrophobic, van der Waals, and H-bond interactions formed by the residues in the active site cleft. The electrostatic potential map for HEWL shows an area with negative potential within the active site cleft, which could be a possible binding site for  $\text{Cu}^{2+}$  ions, which is consistent with a previous study that showed potential  $\text{Cu}^{2+}$  ion binding sites within the same cleft <sup>2</sup>.

Since  $\text{Cu}^{2+}$  ions do not induce significant changes in the protein's secondary structure and their binding site overlaps with that of LacNAc, we suggest that  $\text{Cu}^{2+}$  ions

modulate the binding of LacNAc by competing for a common binding site.



**Figure 1:** Fluorescence emission spectra ( $\lambda_{\text{exc}} = 295 \text{ nm}$ ) of HEWL in the presence or absence of LacNAc and  $\text{Cu}^{2+}$  ions.



**Figure 2:** Electrostatic potential (ESP) map of HEWL with docked LacNAc <sup>3</sup>.

## References:

1. Leal, S. S.; Botelho, H. M.; Gomes, C. M. Metal Ions as Modulators of Protein Conformation and Misfolding in Neurodegeneration. *Coord. Chem. Rev.* **2012**, 256 (19–20), 2253–2270.
2. Jing, M.; Song, W.; Liu, R. Binding of Copper to Lysozyme: Spectroscopic, Isothermal Titration Calorimetry and Molecular Docking Studies. *Spectrochim. Acta, Part A* **2016**, 164, 103–109.
3. Meng, E. C.; Goddard, T. D.; Pettersen, E. F.; Couch, G. S.; Pearson, Z. J.; Morris, J. H.; Ferrin, T. E., UCSF CHIMERAX: Tools for Structure Building and Analysis. *Protein Sci.* **2023**, 32 (11), e4792.

# Design and development of fluorescent molecular probes for the detection of Alzheimer's disease biomarkers

Jerneja Kladnik,<sup>1</sup> Matic Rogan,<sup>1</sup> Ross D. Jansen-van Vuuren,<sup>1</sup> Damijana Urankar,<sup>1</sup> Janez Košmrlj<sup>1,\*</sup>

<sup>1</sup> Faculty of Chemistry and Chemical Technology, University of Ljubljana, Večna pot 113, SI-1000 Ljubljana, Slovenia, [Janez.kosmrlj@fkkt.uni-lj.si](mailto:Janez.kosmrlj@fkkt.uni-lj.si)

Alzheimer's disease (AD) is a neurodegenerative disorder, characterized primarily by cognitive decline and dementia. Despite intensive research, there remains a lack of effective therapeutic options and, critically, no widely accessible, non-invasive, and reliable diagnostic methods for early detection and monitoring of disease progression. The development of such a diagnostic tool would represent a paradigm shift, enabling identification of at-risk yet asymptomatic individuals and offering the possibility of earlier intervention with existing or future therapeutics. Furthermore, early and precise diagnosis would significantly accelerate the discovery and clinical validation of new treatment strategies.<sup>1</sup>

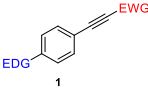
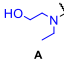
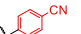
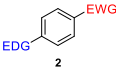
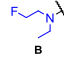
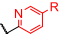
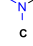
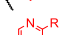

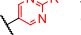
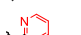
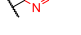

The Košmrlj research group is addressing this unmet need through the design and synthesis of novel fluorescent molecular probes for the *ex vivo* detection of AD-related proteins, particularly amyloid  $\beta$  (A $\beta$ ) and tau. These probes comprising three essential components: (a) an electron-donating group (EDG), (b) a  $\pi$ -conjugated aromatic linker, and (c) an electron-withdrawing group (EWG) (Table 1). This push-pull configuration facilitates intramolecular charge transfer (ICT), resulting in distinct and tunable photophysical properties. Importantly, the probes should exhibit optical changes – specifically, in absorption, excitation, and emission wavelengths as well as quantum yields – upon binding to their target proteins.<sup>2</sup>

A total of 21 rod-shaped fluorophores were synthesized via a modular synthetic strategy, allowing for rapid diversification of substituent patterns and  $\pi$ -system extension. Structures and purity were confirmed by NMR spectroscopy, HRMS, and HPLC analysis.<sup>2</sup> One dye, namely **1Ae**, especially stood out as it exhibited exceptionally large Stokes shifts (138–213 nm) across various solvents, effectively minimizing self-absorption. Its high quantum yield ratio ( $\phi_{\text{DCM}}/\phi_{\text{MeOH}} = 104$ )

further ensures low background fluorescence in aqueous environments, enabling high sensitivity for target detection.

Looking forward, by integrating rational molecular design this work lays the groundwork for the development of a next-generation “smart molecular probe” for AD diagnosis – an essential step toward improved patient outcomes and therapeutic development.

**Table 4:** Structural motifs of an electron-donating group (EDG), a  $\pi$ -conjugated aromatic linker (HC), and an electron-withdrawing group (EWG) of prepared fluorescent molecular probes.<sup>2</sup>

HC framework	EDG	EWG
		
		
		
		
		
		
		
		

## References:

- Chimthanawala, N.M.A., Haria, A., Sathaye, S., Non-invasive Biomarkers for Early Detection of Alzheimer's Disease: a New-Age Perspective. *Mol Neurobiol.* **2024**, *61*, 212–223.
- Rejc, L., Probing Alzheimer's pathology: Exploring the next generation of FDDNP analogues for amyloid  $\beta$  detection. *Biomed. Pharmacother.* **2024**, *175*, 116616.

**Funding information:** The study was supported by the Slovenian Research and Innovation Agency (ARIS; Research Core Funding grant P1-0230).

# To Coordinate New Things

Jure Jakoš,<sup>1</sup> Elisabeth M. Huf,<sup>2</sup> Jakob Kljuna\*<sup>1</sup>

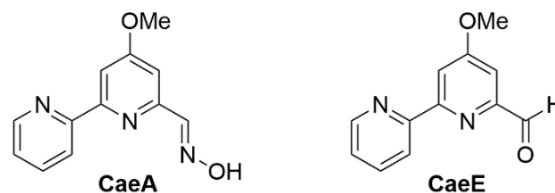
<sup>1</sup> Faculty of Chemistry and Chemical Technology, University of Ljubljana, Večna pot 113, SI-1000 Ljubljana, Slovenia

<sup>2</sup> Institute of Inorganic Chemistry, Universität Regensburg, Universitätsstraße 31, DE-93053 Regensburg, Germany

For centuries, humans have battled microbial infections, initially employing metal-based treatments such as silver, arsenic, and mercury salts, with varying degree of effectiveness. The discovery of antibiotics by Alexander Fleming in the early 20th century changed the medical paradigm and thus helped save millions of lives. However, the widespread and sometimes inappropriate use of antibiotics and other antimicrobials has driven the emergence of antimicrobial resistance—a major public health concern identified by the World Health Organization. To counter this, efforts are focusing on smarter use of antibiotics, improving existing drugs, searching for new potential therapeutics and exploring innovative solutions such as metal-based compounds.<sup>1</sup>

In 1959, a new compound with great potential was discovered while studying an extract of *Streptomyces caeruleus*. The researchers noticed that something in this extract inhibited the growth of various filamentous fungi, yeasts and even some bacteria. After closer inspection of the extract and subsequent isolation and characterization, they discovered a novel asymmetric 2,2'-bipyridine. They named this new compound caerulomycin (Cae), later after the discovery of some derivatives they renamed it to caerulomycin A (CasA) (**Figure 1**).<sup>2</sup> Further research has shown that these compounds not only have antifungal and antibacterial activity, but also exhibit good anticancer, immunoregulatory and other potential therapeutic properties.<sup>2–4</sup>

The first synthesis of CaeA was achieved in 1969. Later, in 1998, a route to produce CaeE, a precursor convertible to CaeA, was developed.<sup>5</sup> We succeeded in optimizing and improving the yield of this synthesis on a gram scale in combination with newer published procedures.<sup>6</sup> With the synthesized CaeE, we have successfully prepared the first rhenium(I) complex containing CaeE as a ligand to our knowledge.



**Figure 1:** Structure of two Caerulomycins

## References:

1. Salam, M. A.; Al-Amin, M. Y.; Salam, M. T.; Sigh Pawar, J.; Akhter N.; Rabaan, A. A.; Alqumber, M. A. Antimicrobial Resistance: A Growing Serious Threat for Global Public Health. *Healthcare* **2023**, *11*, 1946.
2. Funk, A.; Divekar, P. V. Caerulomycin, a New Antibiotic from *Streptomyces Caeruleus* Baldacci, I. Production, Isolation, Assay. and Biological Properties. *Can. J. Microbiol.* **1959**, *5*, 317–321.
3. Tong, L.; Sun, W.; Wu, S.; Han, Y. Characterization of Caerulomycin A as a DualTargeting Anticancer Agent. *Eur. J. Pharmacol.* **2022**, *922*, 174914.
4. Singla, A. K.; Krishna Gurram, R.; Chauhan, A.; Khatri, N.; Vohra, R. M.; Jolly, R. S.; Agrewala, J. N. Caerulomycin A Suppresses Immunity by Inhibiting T Cell Activity. *PLOS ONE*, **2014**, *9*
5. Trécourt, F.; Gervais, B.; Mongin, O.; Le Gal, C.; Mongin, F.; Quéguiner, G. First Syntheses of Caerulomycin E and Collismycins A and C. A New Synthesis of Caerulomycin A. *J. Org. Chem.* **1998**, *63*, 2892–2897
6. Bobrov, D. N.; Tyvorskii V. I. Facile synthesis of caerulomycin e by the formation of 2, 2'-bipyridine core via a 2-pyridyl substituted 4H-pyran-4-one. Formal synthesis of caerulomycin A. *Tetrahedron* **2010**, *66*, 5432–5434

**Funding information:** We are grateful for the financial support from the junior research grant for Jure Jakoš and program grant P1-0175 of the Slovenian Research and Innovation Agency (ARIS). The authors also acknowledge the support of the Centre for Research Infrastructure at the University of Ljubljana, Faculty of Chemistry and Chemical Technology, which is part of the Network of Research and Infrastructural Centers UL (MRIC UL) and is financially supported by ARIS; Infrastructure program No. I0-0022.



# Understanding Fluorination Effects on Butanol Derivatives Using Molecular Simulations and X-ray Scattering

Jure Kovač,<sup>1</sup> Andrej Jamnik,<sup>1</sup> István Szilágyi,<sup>2</sup> Matija Tomšič\*,<sup>1</sup>

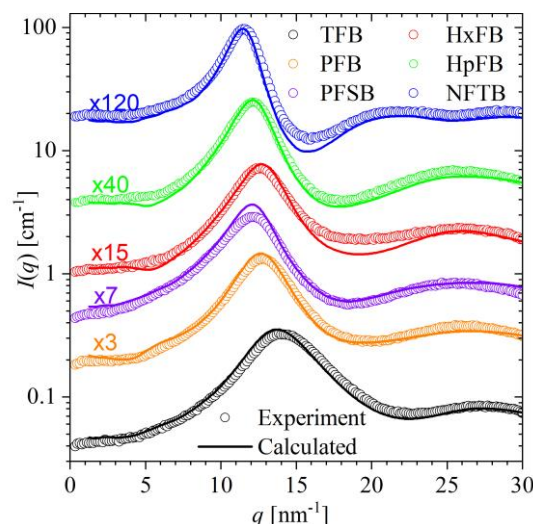
<sup>1</sup> Faculty of Chemistry and Chemical Technology, University of Ljubljana, Večna pot 113, SI-1000 Ljubljana, Slovenia

<sup>2</sup> Department of Physical Chemistry and Materials Science, University of Szeged, Rerrich Béla sq 1., HU-6720 Szeged, Hungary

Per- and polyfluoroalkyl substances (PFAS) are a large class of synthetic compounds known for their chemical stability and persistence in the environment. Their widespread use and toxicity have made them a growing concern for environmental science. Among them, fluorinated alcohols can serve as valuable model systems for studying the effects of fluorination on molecular structure and dynamics. In this study, we investigate a series of fluorinated butanol derivatives to determine how variations in fluorine content and substitution patterns affect the organisation of molecules in the liquid phase. We use molecular dynamics (MD) simulations using the OPLS-AA force field in combination with small and wide-angle X-ray scattering (SWAXS) measurements. Theoretical scattering intensities were calculated from the MD trajectories using the complemented system approach.<sup>1,2</sup>

The force field model was validated by comparing the simulated SWAXS curves with experimental data. A good agreement was found for both the peak positions and the overall shape. This confirms that the OPLS-based models reliably capture the most important structural features of the systems. With increasing fluorination, we observe a consistent shift of the main scattering peak to lower  $q$  values, indicating that the length-scales of the correlations within the local hydrophobic environment increase.<sup>3</sup> Hydrogen bonding is also significantly affected, especially when fluorination occurs on the carbon close to the hydroxyl group. Radial and spatial distribution functions show that these changes lead to fewer hydrogen bonds per molecule, altered hydrogen bond geometries and smaller hydrogen-bonded aggregate structures. The dynamic properties derived from MD — such as viscosity and self-diffusion — also vary within the series, with the more fluorinated compounds generally exhibiting higher viscosity and slower diffusion.

Our results show how even small molecular modifications can lead to significant changes in liquid structure and dynamic properties. These results improve our understanding of fluorinated alcohols and the physicochemical behaviour of PFAS molecules.



**Figure 1:** Experimental and calculated SWAXS intensities from MD simulation results for 4,4,4-trifluorobutan-1-ol (TFB), 4,4,4,3,3-pentafluorobutan-1-ol (PFB), 4,4,4,3,3-pentafluorobutan-2-ol (PFSB), 4,4,4,3,2,2-hexafluorobutan-1-ol (HxFB), 4,4,4,3,3,2,2-heptafluorobutan-1-ol (HpFB) and nonafluorotert-butanol (NFTB). The theoretical data were numerically smeared to allow direct comparison with the experimental data.

## References:

1. Lajovic, A.; Tomšič, M.; Jamnik, A. The complemented system approach: A novel method for calculating the x-ray scattering from computer simulations. *J. Chem. Phys.* **2010**, *133*, 174123.
2. Cerar, J.; Jamnik, A.; Pethes, I.; Temleitner, L.; Pusztai, L.; Tomšič, M. Structural, rheological and dynamic aspects of hydrogen-bonding molecular liquids: Aqueous solutions of hydrotropic tert-butyl alcohol. *J. Colloid Interface Sci.* **2020**, *560*, 730–742.
3. Tomšič, M.; Jamnik, A.; Fritz-Popovski, G.; Glatter, O.; Vlček, L. Structural properties of pure simple alcohols from ethanol, propanol, butanol, pentanol, to hexanol: Comparing Monte Carlo simulations with experimental SAXS data. *J. Phys. Chem. B.* **2007**, *111*, 1738–1751.

**Funding information:** Slovenian Research Agency (research core funding no. P1-0201 and project no. N1-0308).

# Synthesis of fluorinated homoserine derivatives via Mitsunobu reaction

Karin Rot,<sup>1</sup> Jure Gregorc,<sup>1</sup> Jernej Iskra\*,<sup>1</sup>

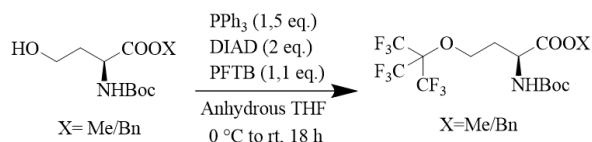
<sup>1</sup> Faculty of Chemistry and Chemical Technology, University of Ljubljana, Večna pot 113, SI-1000 Ljubljana, Slovenia

Fluorine is the most electronegative atom with a large inductive effect<sup>1</sup>. <sup>19</sup>F is a ½ spin nucleus, which occurs at 100 % natural abundance<sup>2</sup>. Because of its spin, it can be used in magnetic resonance techniques (NMR, MRI, MRS)<sup>2</sup>. <sup>19</sup>F has NMR sensitivity that is similar to that of the <sup>1</sup>H. Unlike <sup>1</sup>H, <sup>19</sup>F is absent in water and biological molecules, which makes it a particularly sensitive probe because of the absence of background or competing signals from solvent or from other molecules<sup>3</sup>.

Most amino acids used as NMR probes are monofluorinated or have a trifluoromethyl group in their structure. In order to improve the signal sensitivity, perfluoro-*tert*-butyl group can be introduced to natural amino acids. The perfluoro-*tert*-butyl group introduces nine chemically equivalent fluorine atoms that, because they are not coupled to adjacent protons, result in a sharp singlet. The best approach to install a perfluoro-*tert*-butyl group on an OH-bearing side chain, is to use Mitsunobu reaction with perfluoro-*tert*-butanol<sup>4</sup>.

Mitsunobu reaction is a method for the dehydrative coupling of alcohols with acids or pronucleophiles by using a combination of an oxidizing azo reagent (DIAD, DEAD, etc.) and a reducing phosphine reagent (PPh<sub>3</sub>, *n*-Bu<sub>3</sub>P, etc.) under mild conditions<sup>5</sup>.

The main focus of this study was to expand and improve procedures for the synthesis of perfluoro-*tert*-butyl-L-homoserine. First part of the study focused on the synthesis of appropriately protected L-homoserine. Synthesis of protected L-homoserine reported in literature has its drawbacks: low yields and formation of side products, as well as use of toxic reagents (e.g. diazomethane).

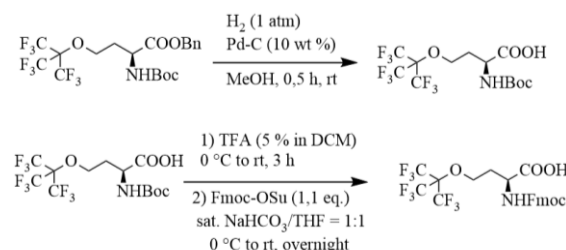


**Scheme 1:** Synthesis of perfluoro-*tert*-butyl-L-homoserine derivative using optimized Mitsunobu conditions.

In this study, I tested several procedures for the synthesis of *N*-(*tert*-butoxycarbonyl)-L-homoserine methyl and benzyl esters. After successful synthesis, these compounds were subjected to the Mitsunobu

reaction in the presence of fluorinated alcohols (primarily perfluoro-*tert*-butanol).

A further aim of this study was to prepare an *N*-Fmoc-protected building block for subsequent use in solid-phase peptide synthesis. For this reason, I exchanged the protective groups of the fluorinated derivative of protected L-homoserine, affording *N*-Fmoc-*O*-(perfluoro-*tert*-butyl)-L-homoserinate.



**Scheme 2:** Removal of the benzyl protecting group and exchange of the Boc group for Fmoc.

## References:

- Marsh, E. N. G.; Suzuki, Y. Using (19)F NMR to probe biological interactions of proteins and peptides. *ACS Chem. Bio.* **2014**, 9 (6), 1242–1250
- Danielson, M. A.; Falke, J. J. Use of 19F NMR to probe protein structure and conformational changes. *Annu. Rev. Biophys. Biomol. Struct.* **1996**, 25, 163–195.
- Tressler, C. M.; Zondlo, N. J. Perfluoro-*tert*-butyl Homoserine Is a Helix-Promoting, Highly Fluorinated, NMR-Sensitive Aliphatic Amino Acid: Detection of the Estrogen Receptor·Coactivator Protein–Protein Interaction by 19F NMR. *Biochem.* **2017**, 56 (8), 1062–1074
- Buer, B. C.; Levin, B. J.; Marsh E. N. Perfluoro-*tert*-butyl-homoserine as a sensitive 19F NMR reporter for peptide-membrane interactions in solution. *J. Pept. Sci.* **2013**, 19 (5), 308–314
- But, T. Y. S.; Toy, P. H. The Mitsunobu reaction: origin, mechanism, improvements, and applications. *Chem. Asian J.* **2007**, 2 (11), 1340–1355

**Funding information:** The authors gratefully acknowledge the financial support from the Slovenian Research Agency (ARIS) – research core funding grants P1-0134, and the Eutopia and CY Initiative of Excellence (grant Investissements d’Avenir, ANR-16-IDEX-0008).

# PMMA-Siloxane Silica Coating for Corrosion Protection of AA2024-T3 in NaCl solution

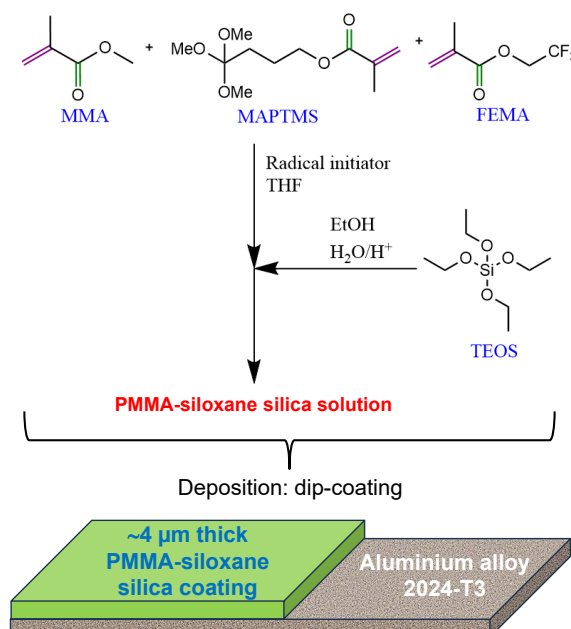
Nina Kovač,<sup>1,2</sup> Ana Kraš,<sup>1</sup> Karolina Mulec,<sup>1</sup> Ingrid Milošev,<sup>1</sup> Peter Rodič\*,<sup>1</sup>

<sup>1</sup> Jožef Stefan Institute, Department of Physical and Organic Chemistry, Jamova cesta 39, 1000 Ljubljana, Slovenia

<sup>2</sup> Jožef Stefan International Postgraduate School, Jamova c. 39, SI-1000 Ljubljana, Slovenia

Aluminium alloy (AA)2024-T3 is widely used in the aerospace industry due to its low weight, high mechanical strength, and cost-effectiveness. Despite these advantages, its susceptibility to corrosion in chloride-rich environments, primarily due to the presence of alloying elements (such as Cu, Fe, and Mn), remains a significant drawback. Traditionally, corrosion protection has relied on chromium(VI)-based compounds; however, their use is increasingly restricted worldwide due to their harmful impact on human health and the environment. As a safer and more sustainable alternative, poly(methyl methacrylate) PMMA-siloxane silica sol-gel coatings have gained attention.<sup>1,2,3</sup>

In this study, the corrosion resistance of AA2024-T3 protected with a siloxane-silica sol-gel coating was evaluated. The sol-gel system was synthesised using tetraethyl orthosilicate (TEOS), methyl methacrylate (MMA), 3-(trimethoxysilyl)propyl methacrylate (MAPTMS), and 2,2,2-trifluoroethyl methacrylate (FEMA), as schematically presented in Scheme 1.



**Scheme 1:** Stepwise procedure of PMMA siloxane-silica synthesis. The prepared solution was then deposited on the AA2024-T3 surface.

The preparation reactions of the coatings were monitored by *real-time* Fourier transform infrared (FTIR) spectroscopy. Following deposition onto AA2024-T3 substrates, the coatings were analysed using a scanning electron microscope equipped with an energy-dispersive spectrometer (SEM/EDS) to assess their surface morphology, topography, elemental composition, and thickness. Corrosion performance was evaluated in a 0.1 M NaCl solution using electrochemical impedance spectroscopy (EIS). Additionally, the salt spray testing was performed in accordance with the ASTM B117-07A standard. The findings confirmed the formation of a uniform coating layer, several micrometers thick, providing continuous coverage of the alloy surface. These coatings exhibited long-lasting barrier properties against corrosion, as indicated by stable EIS responses maintained more than 3 months.

## References:

1. Rodič, P.; Korošec, R.C.; Kapun, B.; Mertelj, A.; Milošev, I. Acrylate-Based Hybrid Sol-Gel Coating for Corrosion Protection of AA7075-T6 in Aircraft Applications: The Effect of Copolymerization Time. *Polymers* **2020**, *12*, 948.
2. Rodič, P.; Lekka, M.; Andreatta, F.; Fedrizzi L.; Milošev, I. The effect of copolymerisation on the performance of acrylate-based hybrid sol-gel coating for corrosion protection of AA2024-T3, *Prog. Org. Coat.* **2020**, *147*, 105701
3. Kovač, N.; Kapun, B.; Može, M.; Golobič, I.; Kralj, S.; Milošev, I.; Rodič, P. Superhydrophobic Coatings Based on PMMA-Siloxane-Silica and Modified Silica Nanoparticles Deposited on AA2024-T3. *Polymers* **2025**, *17*, 195.

**Funding information:** The authors acknowledge their gratitude for the financial support provided by the Slovenian Research and Innovation Agency (ARIS) under research core funding P1-0134, P2-0393. This research was also funded through the ARIS projects: No. L2-60141.

# Problem-based learning in polymer chemistry using the context of firefighter protective clothing

Katja Gubič,<sup>1\*</sup> Peter Rodič,<sup>2</sup> Miha Slapničar<sup>1,3</sup>

<sup>1</sup> University of Ljubljana, Faculty of Education, Kardeljeva ploščad 16, 1000 Ljubljana, Slovenia

<sup>2</sup> Jožef Stefan Institute, Department of Physical and Organic Chemistry, Jamova 39, 1000 Ljubljana, Slovenia

<sup>3</sup> BEC Ljubljana, Cesta v Mestni log 47, SI-1000 Ljubljana, Slovenia

Educational psychology shows that authentic, real-life contexts can significantly increase students' motivation to learn<sup>1</sup>. Situational interest triggered by appealing content can, under the right conditions, develop into a lasting individual interest<sup>2</sup>. Problem-based learning builds on this principle by confronting students with complex and realistic problems, fostering deeper understanding, problem-solving skills, collaboration and intrinsic motivation<sup>3</sup>.

In secondary school, scientific concepts such as polymers, wettability, hydrophobicity and surface tension are often presented in abstract terms, making it difficult for students to recognize their practical significance.

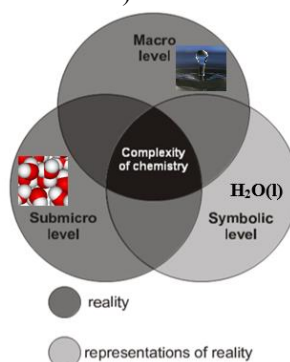
This study presents a problem-orientated learning module that embeds these topics in the authentic example of firefighters' protective clothing. These multi-layer garments, with an outer layer typically made of high-performance aramid fibres such as Nomex® and Kevlar, provide fire resistance and ballistic protection. To enhance protective properties, the surface is treated with fluorinated finishes that provide water repellency, fire resistance or antimicrobial performance. Such surface treatments can create superhydrophobic properties by lowering the surface free energy. As a result, water contact angles of more than 150° are achieved, similar to those found on lotus leaves. However, in real operational use these finishes are not permanent. Repeated cleaning cycles, especially under harsh conditions, can gradually degrade or remove the low-energy coating, exposing the underlying fibres and reducing water repellency<sup>4</sup>.

The module was conducted with 4th grade high school students. The module was designed to engage students at all three levels of science concepts: the macroscopic level, the submicroscopic level, and the symbolic level. Activities included measuring contact angles with a goniometer, analysing the effects of solvent polarity and pH on contact angles and estimating surface tension. Pre- and post- lesson questionnaires assessed situational and individual interest.

Results showed increased engagement and improved conceptual understanding when learning took place using a realistic, interdisciplinary problem scenario.

The analysis of textbooks revealed that applied polymer science related to personal protective equipment is largely absent from Slovenian secondary education. This work suggests that contextualised PBL can enrich learning by linking theory to safety, materials science and environmental responsibility.

In the future, the model could also be extended to lower grades and different fields (e.g., technical or non-technical oriented schools).



**Scheme 1:** Model representing interdependence of three levels of chemistry concepts<sup>5</sup>.

## References:

- Schraw, G.; Flowerday, T.; Lehman, S. Increasing situational interest in the classroom. *Educ. Psy. Rev.* **2001**, *13*(3), 211–224.
- Juriševič, M. *Motiviranje učencev v šoli*; Pedagoška fakulteta, **2012**.
- Hmelo-Silver, C. E. Problem-based learning: what and how do students learn? *Educ. Psy. Rev.* **2004**, *16* (3), 235–266.
- Ghosh, J.; Rupanty, N. S.; Noor, T.; Asif, T. R.; Islam, T.; Reukov, V. Functional coatings for textiles: advancements in flame resistance, antimicrobial defense, and self-cleaning performance. *RSC Advances* **2025**, *15* (14), 10984–11022.
- Slapničar, M. Ribič, L., Devetak, I. Using eye-movements to explain processing triple level of chemical information: systematic review. *Acta. Chim. Slov.* **2025**, *72* (3), 1–14.

**Funding information:** The authors acknowledge the financial support from the Slovenian Research and Innovation Agency (ARIS) research core funding Nos. P2-0393, P1-0134

# Postsynthetic Ligand Exchange Effects on CO<sub>2</sub> Performance

Klara Klemenčič,<sup>1,2</sup> Nataša Zabukovec Logar,<sup>1,2</sup> Matjaž Mazaj,<sup>1</sup>

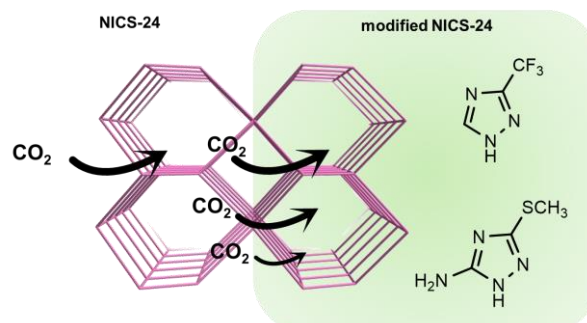
<sup>1</sup> National Institute of Chemistry, Hajdrihova 19, 1000 Ljubljana, Slovenia

<sup>2</sup> School of Science, University of Nova Gorica, Vipavska 13, 5000 Nova Gorica, Slovenia

Metal–Organic Frameworks (MOFs) are a versatile class of porous crystalline materials characterized by unique chemical and physical properties, making them suitable for a broad range of applications. In recent years, MOFs have gained considerable attention as promising candidates for selective CO<sub>2</sub> capture and separation<sup>1</sup>. One of the most compelling features of MOFs lies in their tunable synthesis. Their highly ordered structures, large surface areas, and adjustable porosity allow for precise tailoring to enhance CO<sub>2</sub> affinity<sup>2</sup>. A widely adopted strategy to improve CO<sub>2</sub> uptake involves functionalizing the framework by introducing additional functional groups into the organic linkers. For example, the incorporation of amino groups has been shown to significantly increase CO<sub>2</sub> adsorption capacity<sup>3</sup>.

This enhancement has been demonstrated in a series of functionalized triazolate-based MOFs, including CALF-20, CALF-15, and NICS-24<sup>4</sup>. The introduction of an extra amine group in NICS-24 resulted in superior CO<sub>2</sub> capture performance compared to CALF-15, with both materials outperforming CALF-20 under low CO<sub>2</sub> concentration conditions.

To further enhance the performance of NICS-24, we propose functionalizing the framework with linkers exhibiting greater hydrophobicity (Figure 1). This modification aims to systematically tune the pore properties, such as size, shape, and volume – as well as host-guest interactions (i.e., surface chemistry), thereby optimizing the material for CO<sub>2</sub> capture.



**Figure 1:** Illustration of the fine-tuning approach applied to the NICS-24 structure.

## References:

1. Yang, S. Q.; Hu, T. L.; Chen, B. Microporous metal-organic framework materials for efficient capture and separation of greenhouse gases. *Sci. China Chem.* **2023**, *66*, 2181–2203.
2. Achenbach, B.; Yurdusen, A.; Stock, N.; Maurin, G.; Serre, C. Synthetic Aspects and Characterization Needs in MOF Chemistry – from Discovery to Applications. *Adv. Mater.* **2025**, 2411359.
3. Lee, G.; Ahmed, I.; Jhung, S. H. CO<sub>2</sub> adsorption using functionalized metal–organic frameworks under low pressure: Contribution of functional groups, excluding amines, to adsorption. *Chem. Eng. J.* **2024**, *481*, 148440.
4. Klemenčič, K.; Krajnc, A.; Puškarić, A.; Huš, M.; Marinič, D.; Likozar, B.; Logar, N. Z.; Mazaj, M. Amine-Functionalized Triazolate-Based Metal–Organic Frameworks for Enhanced Diluted CO<sub>2</sub> Capture Performance. *Angew. Chem., Int. Ed.* **2025**, *64*, e202424747.

**Funding information:** Slovenian Research Agency (Research programme P1-0021 and Young Researcher Grant).



# Investigating Protein Interactors of the TDP-43 Pathology-Linked Protein

Klara Razboršek,<sup>1</sup> Jerneja Nimac,<sup>2</sup> Boris Rogelj\*,<sup>1,2</sup>

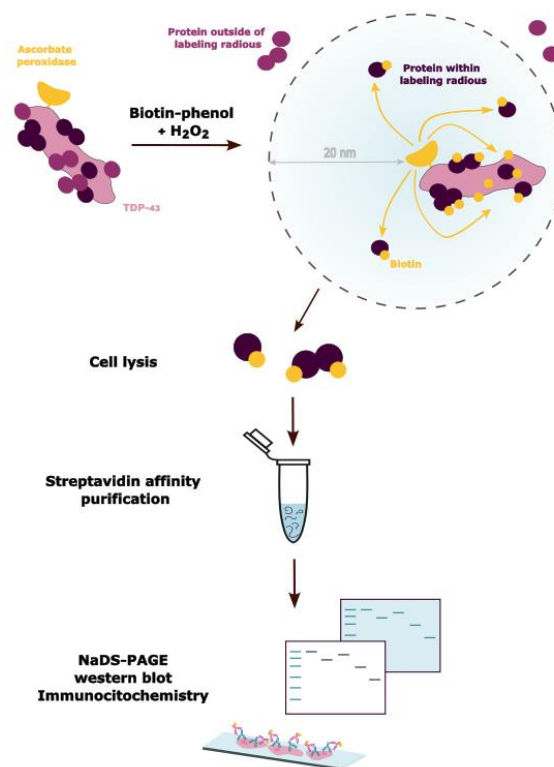
<sup>1</sup> Faculty of Chemistry and Chemical Technology, University of Ljubljana, Večna pot 113, SI-1000 Ljubljana, Slovenia

<sup>2</sup> Department of Biotechnology, Jozef Stefan Institute, Jamova cesta 39, SI-1000 Ljubljana, Slovenia, ([boris.rogelj@ijs.si](mailto:boris.rogelj@ijs.si))

Amyotrophic lateral sclerosis (ALS) is a progressive neurodegenerative disease primarily affecting motor neurons. Initial symptoms typically present as muscle weakness, often starting in distal limbs and progressing with disease advancement. The average survival time post-onset is approximately three years, with respiratory failure being the most common cause of death. Around 50 % of patients also exhibit non-motor symptoms, with 10–15% diagnosed with frontotemporal dementia (FTD), and an additional 35–45 % showing mild cognitive and/or behavioral changes<sup>1</sup>.

To date, more than 20 genes have been associated with ALS. The most frequent genetic causes include hexanucleotide repeat expansions in *C9orf72* and mutations in *SOD1*, *TARDBP*, *FUS*, and *TBK1*. A key neuropathological hallmark of ALS is the accumulation of cytoplasmic aggregates of the TDP-43 protein, which are also found in patients with FTD and other neurodegenerative diseases<sup>1,2</sup>. TDP-43 is an essential DNA/RNA-binding protein from the heterogeneous nuclear ribonucleoprotein (hnRNP) family, involved in RNA metabolism, mRNA transport, stress granule formation, and central nervous system development. Mislocalization of TDP-43 to the cytoplasm is closely linked to both gain- and loss-of-function pathogenic mechanisms<sup>2,3</sup>.

The primary aim of our work was to validate TDP-43 protein interaction partners, which were previously detected using the APEX method. We evaluated these interactions using stable cell lines expressing wild-type TDP-43 and TDP-43dNLS. Analyses included NaDS-PAGE, western blotting, and immunodetection of selected interactors. Localization and expression of fusion proteins were examined via immunocytochemistry and fluorescence microscopy. We have identified SFPQ, NUP93, hnRNPK, and ATXN2L as interaction partners of TDP-43 in both pathological conditions and normal cellular function.



**Scheme 1:** Overview of the experiments using ascorbate peroxidase for labelling protein interactors of TDP-43.

## References:

1. Masrori, P.; Van Damme, P. Amyotrophic Lateral Sclerosis: A Clinical Review. *Eur. J. Neurol.* **2020**, *27* (10), 1918–1929.
2. de Boer, E. M. J.; Orie, V. K.; Williams, T.; Baker, M. R.; De Oliveira, H. M.; Polvikoski, T.; Silsby, M.; Menon, P.; van den Bos, M.; Halliday, G. M.; van den Berg, L. H.; Van Den Bosch, L.; van Damme, P.; Kiernan, M.; van Es, M. A.; Vucic, S. TDP-43 Proteinopathies: A New Wave of Neurodegenerative Diseases. *J. Neurol. Neurosurg. Psychiatry* **2021**, *92* (1), 86–95.
3. Suk, T. R.; Rousseaux, M. W. C. The Role of TDP-43 Mislocalization in Amyotrophic Lateral Sclerosis. *Mol. Neurodegener.* **2020**, *15*, 45.

# Synthesis and characterization of niobium-doped titania photocatalysts

Klara Urankar,<sup>1</sup> Andrijana Sever Škapin,<sup>2,3</sup> Urška Lavrenčič Štangar\*,<sup>1</sup>

<sup>1</sup> Faculty of Chemistry and Chemical Technology, University of Ljubljana, Večna pot 113, 1000 Ljubljana, Slovenia

<sup>2</sup> Slovenian National Building and Civil Engineering Institute, Dimičeva ulica 12, 1000 Ljubljana, Slovenia

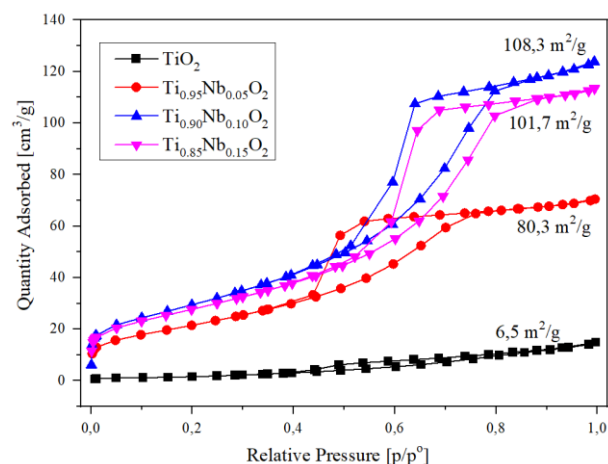
<sup>3</sup> Faculty of Polymer Technology, Ozare 19, 2380 Slovenj Gradec, Slovenia

Water pollution is a global problem that affects ecosystems, the economy and human health. The most common pollutants include microplastics, persistent organic compounds, heavy metals and other compounds that enter water systems through domestic and industrial wastewater. These compounds are difficult to degrade in the environment, and some of them are not even degradable by conventional water treatment methods. One of the methods for degradation of persistent micropollutants is heterogeneous photocatalysis, in which irradiation and suitable catalysts (usually metal oxides) are used to convert poorly degradable compounds into smaller and less harmful compounds<sup>1</sup>. Titanium(IV) oxide (TiO<sub>2</sub>) is a commonly used catalyst due to its good photocatalytic properties. Its modifications, such as doping with different metal ions, can enhance its efficiency<sup>2</sup>.

The purpose of this work was to synthesize TiO<sub>2</sub> modified with various amounts of niobium (Nb) dopants using the sol-gel method and then to characterize them<sup>3</sup>. The characterization involved nitrogen physisorption analysis, X-ray powder diffraction, UV-Vis diffuse reflection spectroscopy, Fourier transform infrared spectroscopy and scanning electron microscopy. In order to determine the catalytic activity, the degradation reaction of the water pollutant phenytoin, a representative of very poorly degradable pharmaceuticals, was carried out using UV-A light. BET adsorption isotherms showed that the Ti<sub>0.90</sub>Nb<sub>0.10</sub>O<sub>2</sub> and Ti<sub>0.85</sub>Nb<sub>0.15</sub>O<sub>2</sub> catalysts had a larger specific surface area than the other prepared samples (Figure 1). These two samples emerged as the most active catalysts, degrading 42 % of phenytoin in solution (Table 1).

## Acknowledgements:

The authors acknowledge the financial support by the Slovenian Research and Innovation Agency (project J2-4441 and programme P1-0134).



**Figure 1:** Nitrogen adsorption-desorption isotherms of the analyzed catalysts

**Table 5:** Phenytoin degradation (%) after 3 hours of reaction

Catalyst	Phenytoin degradation [%]
TiO <sub>2</sub>	33
Ti <sub>0.95</sub> Nb <sub>0.05</sub> O <sub>2</sub>	34
Ti <sub>0.90</sub> Nb <sub>0.10</sub> O <sub>2</sub>	42
Ti <sub>0.85</sub> Nb <sub>0.15</sub> O <sub>2</sub>	42

## References:

- Matoh, L.; Žener, B.; Kovačič, M.; Kušič, H.; Arčon, I.; Levstek, M.; Lavrenčič Štangar, U. Photocatalytic Sol-Gel/P25 TiO<sub>2</sub> Coatings for Water Treatment: Degradation of 7 Selected Pharmaceuticals. *Ceram. Int.* **2023**, *49*, 24395–24406.
- Wang, C.-C.; Ying, J. Y. Sol-Gel Synthesis and Hydrothermal Processing of Anatase and Rutile Titania Nanocrystals. *Chem. Mater.* **1999**, *11*, 3113–3120.
- Jiang, Y.; Ge, H.; Yang, Z.; Ji, Z.; Zhang, G.; Su, C.; Liu, Q.; Ran, X. Insight into the Enhanced Tolerance of Mo-Doped CeO<sub>2</sub>-Nb<sub>2</sub>O<sub>5</sub>/TiO<sub>2</sub> Catalyst towards the Combined Effect of K<sub>2</sub>O, H<sub>2</sub>O and SO<sub>2</sub> in NH<sub>3</sub>-SCR. *Fuel* **2023**, *346*, 128339.

# Comparison of GATK and Deep Learning-Based DeepVariant in diagnostic Next-generation Sequencing (NGS) Variant Calling

Klemen Klopčič\*,<sup>1</sup> Aleš Maver,<sup>2</sup>

<sup>1</sup> Biotechnical Faculty, University of Ljubljana, Jamnikarjeva 101, SI-1000 Ljubljana, Slovenia, ([kk80756@student.uni-lj.si](mailto:kk80756@student.uni-lj.si))

<sup>2</sup> Clinical Institute of Genomic Medicine, University Medical Centre Ljubljana, Šlajmerjeva 4, SI-1000 Ljubljana, Slovenia

Analysis of next-generation sequencing (NGS) requires comprehensive bioinformatic analysis to derive meaningful results. Genome analysis toolkit (GATK)<sup>1</sup> has long been the standard for variant calling, but deep learning tools like DeepVariant<sup>2</sup> are increasingly used for their strong performance.

Since each tool utilises different algorithms, their outputs can differ significantly. While previous studies have compared GATK and DeepVariant on trio exome sequencing (ES)<sup>3</sup> and whole genome sequencing (GS)<sup>4</sup> datasets, the critical challenge remains the accurate identification of pathogenic variants that enable precise genetic diagnoses in the clinical setting.

We compared GATK and DeepVariant on 782 exomes and 69 genomes from patients without previously identified pathogenic variants. In addition to comparing variant count, we searched for clinically relevant variants that might explain the patients' phenotypes.

As shown in Figure 1, GATK and DeepVariant identified a similar total number of variants in the GS datasets, with a large overlap between the two. However, each tool also detected a distinct subset of variants, with GATK identifying a higher proportion of unique calls than DeepVariant (8.19 % and 3.79 % of algorithm-specific variants respectively). All observed differences were statistically significant ( $p < 0.001$ ).

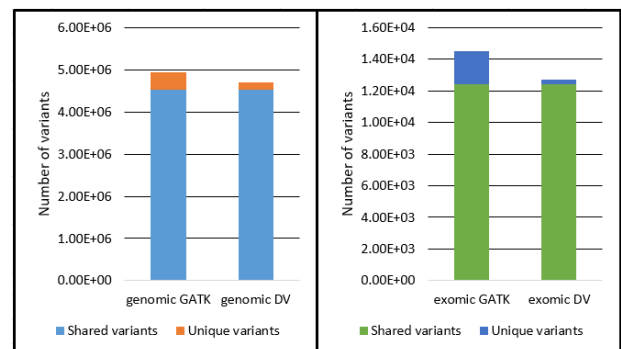
In the ES datasets GATK again reported a higher percentage of algorithm-specific calls than DeepVariant (14.67% and 2.63%, respectively). DeepVariant, therefore, showed greater concordance with shared variants than GATK.

To assess potential artefacts among variants, we compared variant calls to the dbSNP database (Single Nucleotide Polymorphism database). GATK showed a higher rate of non-dbSNP variants (2.21%) than DeepVariant (1.15%), suggesting more possible artefacts.

DeepVariant also identified 37 additional potentially pathogenic variants not found by GATK. Later they were ruled out as disease-causing due to high population frequency or lack of phenotype association.

Both GATK and DeepVariant detect substantial amount of algorithm-specific variants. While GATK reports higher number of total variants, DeepVariant's lower artefact rate suggests greater precision and

potentially reduced interpretation workload. Notably, DeepVariant did not identify any new pathogenic variants in our cohort, indicating comparable clinical sensitivity.



**Figure 1:** Comparison of discovered variants (GATK = Genome analysis toolkit, DV = DeepVariant)

## References:

1. McKenna, A.; Hanna, M.; Banks, E.; Sivachenko, A.; Cibulskis, K.; Kernytsky, A.; Garimella, K.; Altshuler, D.; Gabriel, S.; Daly, M.; DePristo, M. A. The Genome Analysis Toolkit: A MapReduce Framework for Analyzing next-Generation DNA Sequencing Data. *Genome Res.* **2010**, *20* (9), 1297–1303.
2. Poplin, R.; Chang, P.-C.; Alexander, D.; Schwartz, S.; Colthurst, T.; Ku, A.; Newburger, D.; Dijamco, J.; Nguyen, N.; Afshar, P. T.; Gross, S. S.; Dorfman, L.; McLean, C. Y.; DePristo, M. A. A Universal SNP and Small-Indel Variant Caller Using Deep Neural Networks. *Nat. Biotechnol.* **2018**, *36* (10), 983–987.
3. Lin, Y.-L.; Chang, P.-C.; Hsu, C.; Hung, M.-Z.; Chien, Y.-H.; Hwu, W.-L.; Lai, F.; Lee, N.-C. Comparison of GATK and DeepVariant by Trio Sequencing. *Sci. Rep.* **2022**, *12* (1), 1809.
4. Supernat, A.; Vidarsson, O. V.; Steen, V. M.; Stokowy, T. Comparison of Three Variant Callers for Human Whole Genome Sequencing. *Sci. Rep.* **2018**, *8*, 17851.

**Funding information:** This research received no external funding.



# Comparison of mechanical properties of alkali-activated materials made of different alternative alkali activators

Kaja Zupančič,<sup>1</sup> Liam Manevski,<sup>1</sup> Majda Pavlin\*,<sup>2</sup>

<sup>1</sup> Faculty of Chemistry and Chemical Technology, University of Ljubljana, Večna pot 113, SI-1000 Ljubljana, Slovenia

<sup>2</sup> Slovenian National Building and Civil Engineering Institute, Dimičeva ulica 12, SI-1000 Ljubljana, Slovenia

The construction industry is recognized as one of the most significant contributors to global greenhouse gas emissions, and within this sector, the cement industry alone is responsible for approximately 8% of global carbon dioxide (CO<sub>2</sub>) emissions. The production process of ordinary Portland cement is highly carbon-intensive: for every tone of cement produced, approximately 0.7 to 1 tone of CO<sub>2</sub> is emitted into the atmosphere. In response to growing concerns about climate change and environmental degradation, researchers and engineers have been actively seeking more sustainable alternatives. One such promising alternative is the use of alkali-activated materials (AAMs)<sup>1</sup>, which are emerging as potential low-carbon binders to replace traditional cement.

AAMs require an alkali solution (activator) to initiate the chemical reaction that leads to hardening and strength development. In commercial applications, this activator is often a solution of potassium or sodium silicate. However, the production of these commercial alkali activators is also associated with high carbon emissions. For example, producing just one kilogram of sodium silicate can generate approximately 1.5 kilograms of CO<sub>2</sub><sup>2</sup>, which undermines some of the environmental benefits of using AAMs. To address this issue, researchers have begun exploring the use of alternative alkaline activators (AAAs). These are synthesized from industrial waste materials that are rich in amorphous silicon, such as waste glass, mineral wool, rice husk, microsilika etc. which must undergo thermal or chemical treatment to be activated.

In our study, AAAs were prepared using two different approaches: (1) hydrothermal synthesis with continuous mixing/no mixing (modified method used in previous studies<sup>3,4</sup>), (2) and microwave digestion (extraction). The raw materials included waste glass (WG), glass wool (GW), stone wool (SW) and microsilica (MS). These were alkali-activated using 5M and 10M

sodium and potassium hydroxide solutions. The resulting AAAs were used to prepare various AAM mixtures, using metallurgical slag and metakaolin as precursors. These materials were then tested for early compressive strength after three days. Additionally, FTIR (Fourier-transform infrared) spectroscopy was used to analyze the structural features of the hardened AAMs. For comparison, reference samples were also prepared using commercial activators (Geosil and Silvez) and standard sodium and potassium hydroxide solutions.



**Figure 1:** Alkali activated materials prepared of different alternative activators.

## References:

1. Provis, J.; Deventer, J. *Alkali Activated Materials: State-of-the-Art Report*, RILEM TC 224-AAM; 2014.
2. Turner, L. K.; Collins, F. G. Carbon Dioxide Equivalent (CO<sub>2</sub>-e) Emissions: A Comparison between Geopolymer and OPC Cement Concrete. *Constr. Build. Mater.* **2013**, *43*, 125–130.
3. Pavlin, M.; König, K.; König, J.; Javornik, U.; Ducman, V. Sustainable Alkali-Activated Slag Binders Based on Alternative Activators Sourced From Mineral Wool and Glass Waste. *Front. Mater.* **2022**, *9*, 902139.
4. König, K.; Traven, K.; Pavlin, M.; Ducman, V. Evaluation of Locally Available Amorphous Waste Materials as a Source for Alternative Alkali Activators. *Ceram. Int.* **2020**, *47* (4), 4864–4873.

**Funding information:** N2-0320: Waste to alkali-activated binders (WIN).

# H/D Exchange Enabled by Polystyrene-Supported Iridium Catalyst

Luka Jedlovčnik\*,<sup>1</sup> Ross Jansen-van Vuuren,<sup>1</sup> Damijana Urankar,<sup>1</sup> Janez Košmrlj<sup>1</sup>

<sup>1</sup> Faculty of Chemistry and Chemical Technology, University of Ljubljana, Večna pot 113, SI-1000 Ljubljana, Slovenia

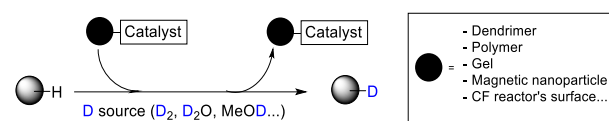
The synthesis of deuterium-labeled organic compounds typically follows two principal strategies. One involves indirect methods, such as total synthesis using deuterated substrates or reagents. The other employs direct techniques, including hydrogen/deuterium (H/D) exchange or deuterio-defunctionalization within the target molecule. Among these, direct H/D exchange is often more efficient and cost-effective, particularly when introducing deuterium into complex molecules like pharmaceutical compounds.<sup>1,2</sup>

In both direct and indirect methods, catalysts based on precious metals are commonly employed, with iridium being among the most prevalent due to its high activity in hydrogen isotope exchange reactions.<sup>2</sup> However, homogeneous iridium catalysts pose challenges in recovery and reuse, as they are difficult to separate from reaction mixtures and can deactivate through aggregation.

Immobilizing homogeneous catalysts onto solid supports (e.g., polymers or silica) offers a sustainable approach to catalysis by enhancing recyclability and simplifying purification.<sup>3</sup> This strategy tackles challenges like catalyst recovery, aggregation, and deactivation. Immobilized catalysts are easily separated, often by filtration, and reused with minimal activity loss, reducing precious metal use and aligning with green chemistry principles. It also limits leaching and product contamination, crucial in pharmaceutical synthesis, while combining the performance of homogeneous catalysts with the practicality of heterogeneous ones.<sup>4</sup>

With this in mind, we are exploring strategies to develop immobilized catalysts for the synthesis of deuterium-labeled organic compounds, building on established catalytic systems (**Figure 1**). In this presentation, we will demonstrate the immobilization of a Kerr-type Iridium(I) catalyst onto polystyrene beads. The

resulting heterogeneous catalyst was employed in the deuteration of a range of substrates previously investigated using the corresponding homogeneous counterpart. We will discuss the comparative performance of the homogeneous and heterogeneous systems, including recyclability and overall potential for practical applications.



**Figure 1:** General scheme for H/D exchange with immobilised catalysts.

## References:

1. Kopf, S.; Bourriquen, F.; Li, W.; Neumann, H.; Junge, K.; Beller, M. Recent Developments for the Deuterium and Tritium Labeling of Organic Molecules. *Chem. Rev.* **2022**, *122* (6), 6634–6718.
2. Jedlovčnik, L.; Košmrlj, J.; Massey, T. E.; Derdau, V. Deuterated Drugs and Biomarkers in the COVID-19 Pandemic. *ACS Omega* **2022**, *7* (46), 41840–41858.
3. Jedlovčnik, L.; Höfferle, J.; Pashaj, F.; Kladnik, J.; Košmrlj, J.; Derdau, V.; Jansen-van Vuuren, R. D. Sustainable synthetic routes to deuterium-labelled organic compounds using immobilized and recyclable (bio)catalysts. *GSC* **2025**, *6* (1), 1–35.
4. Barbaro, P.; Liguori, F. eds., *Heterogenized Homogeneous Catalysts for Fine Chemicals Production*, Springer Netherlands, Dordrecht, 2010.

**Funding information:** We gratefully acknowledge financial support from the Slovenian Research and Innovation Agency (ARIS) through Research Core Funding P1-0230, project J7-50041, and Young Researcher funding for L.J.

# Alkali-Silica Reaction in Concrete –Focus on Silicate Aggregates Used in Slovenia

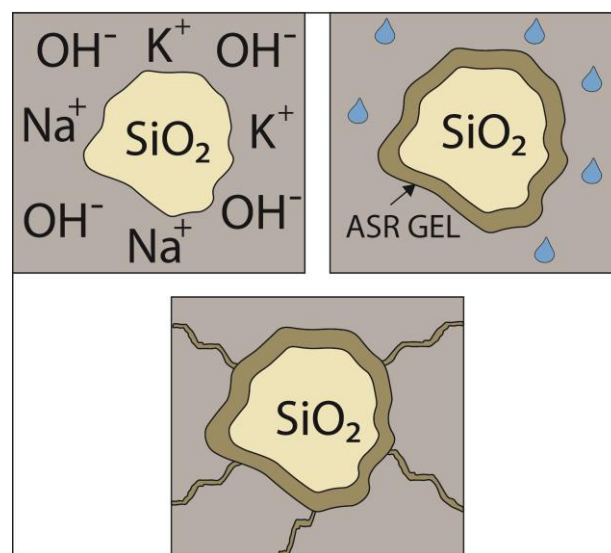
Maja Pristavec<sup>1\*</sup>, Primož Oprčkal<sup>1</sup>, Radmila Milačič Ščančar<sup>2</sup>, Janez Ščančar<sup>2</sup>, Ana Mladenovič<sup>1</sup>

<sup>1</sup> Slovenian National Building and Civil Engineering Institute, Dimičeva ulica 12, 1000 Ljubljana, Slovenia

<sup>2</sup> Department of Environmental Sciences, Jožef Stefan Institute, Jamova 39, 1000 Ljubljana

Concrete, with over 4.1 billion tonnes produced in 2023, is an essential construction material for modern infrastructure including transport, energy, and urban development, and there is no material that can replace it in the near future. Concrete is a mixture of binder (pure cement or cement with supplementary cementitious materials-SCMs) aggregate, water, and chemical admixtures.<sup>1</sup> It is usually reinforced to compensate for its low tensile strength and ductility. Among the various mechanisms affecting concrete durability, the alkali-silica reaction (ASR) is recognized as one of the most critical due to its expansive nature and long-term progression. ASR is a chemical reaction between reactive silica in aggregates and alkalis ( $\text{Na}^+$ ,  $\text{K}^+$ ) in concrete pore solution, forming crystalline or amorphous gel products that expand and cause micro- and later macrocracks in concrete.<sup>1,2</sup> The later act as physical catalysts for further degradation processes. Reactivity of silica depend on the silica type – it is – high in amorphous forms (e.g. opal, volcanic glass), moderate in cryptocrystalline or microcrystalline quartz, and lower in deformed quartz found in metamorphic rocks. In Slovenian aggregate, microcrystalline and deformed quartz are prevalent. Geology in Slovenia is predominantly carbonate-based (limestone, dolomite), but in the northeast (Pohorje, Mura and Drava basins), silicate-rich igneous, metamorphic, and alluvial deposits are common, with silicate content ranging from 40–60% in the Drava Basin, whereas the Mura Basin entirely consists of silicate-rich sediments. Aggregates from these regions, containing quartz, quartzite, gneiss, siltstone, and sandstone, are potentially alkali-silica reactive. Potentially reactive are also certain carbonate sources with silica-rich impurities like chert.<sup>3</sup> ASR in new concrete is mostly mitigated by incorporating sufficient quantity of SCMs, which lower pore solution alkalinity, bind alkalis, and reduce permeability of concrete through pozzolanic reactions.<sup>4</sup> Other methods include limiting alkali content or using lithium admixtures, though these are less practical due to material limitations and cost. Although ASR has long been

neglected in Slovenia, recent degradation of high-performance concretes has highlighted its relevance and the urgent need for systematic assessment. In collaboration with Alpacem Cement we will aim to develop innovative concrete mixes using silicate aggregates and appropriate cement-SCM combinations that will effectively mitigate ASR without compromising its durability and long-term performance.



**Scheme 1:** Simplified presentation of ASR (modified from Thomas et. al. 2011).

## References:

1. Mehta, P. K.; Monteiro, P. J. M. *Concrete: Microstructure, Properties, and Materials*, 3rd ed.; McGraw-Hill: New York, **2006**, pp 168–176.
2. Sims, I.; Poole, A. *Alkali-Aggregate Reaction in Concrete: A World Review*, 1st ed.; CRC Press: Boca Raton, FL, USA, **2017**.
3. Mladenovič, A.; Pristavec, M.; Oprčkal, P. Alkalijsko-silikatna reakcija v betonu - manifestacija in preprečevanje. *Gradbenik* **2025**, 3, 35–37.
4. Thomas, M. D. A. The Effect of Supplementary Cementing Materials on Alkali-Silica Reaction: A Review. *Cem. Concr. Res.* **2011**, 41, 209–216.

# Determination of Liquid Products from Electrochemical CO<sub>2</sub> Reduction using GC-MS

Maja Svete,<sup>1</sup> Blaž Tomc\*,<sup>1,2</sup> Dušan Strmčnik,<sup>1</sup> Nejc Hodnik<sup>1,2,3</sup>

<sup>1</sup> Laboratory for Electrocatalysis, Department of Materials Chemistry, National Institute of Chemistry, 1000 Ljubljana, Slovenia

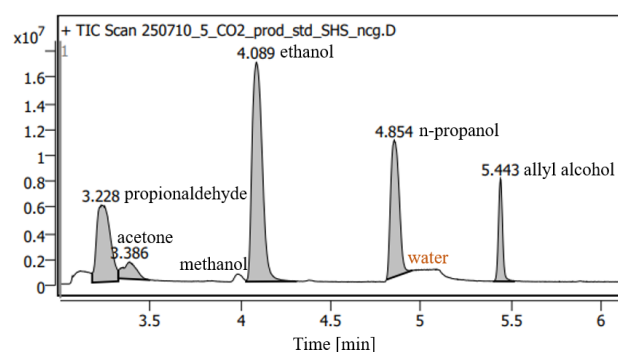
<sup>2</sup> University of Nova Gorica, 5000 Nova Gorica, Slovenia

<sup>3</sup> Institute of Metals and Technology, 1000 Ljubljana, Slovenia

CO<sub>2</sub> is a major greenhouse gas, whose rising concentration in the atmosphere is the primary driver of today's climate change.<sup>1</sup> Reducing CO<sub>2</sub> emissions and producing valuable chemicals are key goals for sustainable development.<sup>2</sup> Electrochemical CO<sub>2</sub> reduction (CO<sub>2</sub>RR) offers a promising route to reduce CO<sub>2</sub> concentrations while producing value-added products such as ethanol. Accurate quantification of liquid products formed during this process is essential.<sup>1</sup>

Typically techniques for this determination are nuclear magnetic resonance (NMR), high performance liquid chromatography (HPLC), and gas chromatography coupled with mass spectrometry (GC-MS).<sup>1</sup> NMR is widely used due to its high sensitivity and ability to detect unknown products, however, it has limitations when it comes to detecting products at very low concentrations. HPLC, on the other hand, has limited sensitivity for volatile aldehydes and alcohols, which are the primary products.<sup>1,3</sup>

In this work, we explore the capabilities of headspace GC-MS, a well-established method that is less commonly used in CO<sub>2</sub>RR, for the detection of volatile products with lower detection limits.<sup>3</sup> We found that alcohols, aldehydes, and ketones are clearly identifiable with the analysis, while carboxylic acids such as formic and acetic are poorly detected due to their low volatility. To address this, we explore derivatization of the acids to its corresponding ester, aiming to improve their detection by HS-GC-MS.



**Figure 1:** Chromatogram of liquid products from CO<sub>2</sub>RR using GC-MS

## References:

1. Nitopi, S.; Bertheussen, E.; Scott, S. B.; Liu, X.; Engstfeld, A. K.; Horch, S.; Seger, B.; Stephens, I. E. L.; Chan, K.; Hahn, C.; Nørskov, J. K.; Jaramillo, T. F.; Chorkendorff, I. Progress and Perspectives of Electrochemical CO<sub>2</sub> Reduction on Copper in Aqueous Electrolyte. *Chem. Rev.* **2019**, *119* (12), 7610–7672.
2. Tomc, B.; Bele, M.; Azeezulla Nazrulla, M.; Šket, P.; Finšgar, M.; Surca, A. K.; Kamšek, A. R.; Šala, M.; Šiler Hudoklin, J.; Huš, M.; Likozar, B.; Hodnik, N. Deactivation of Copper Electrocatalysts during CO<sub>2</sub> Reduction Occurs via Dissolution and Selective Redeposition Mechanism. *J. Mater. Chem. A* **2025**, *13* (6), 4119–4128.
3. Bertheussen, E.; Abghoui, Y.; Jovanov, Z. P.; Varela, A.-S.; Stephens, I. E. L.; Chorkendorff, I. Quantification of Liquid Products from the Electroreduction of CO<sub>2</sub> and CO Using Static Headspace-Gas Chromatography and Nuclear Magnetic Resonance Spectroscopy. *Catal. Today* **2017**, *288*, 54–62.

**Funding information:** The authors would like to acknowledge the Slovenian Research and Innovation Agency (ARIS) through programs P2-0393, P1-0034 and I0-0003; the projects N2-0257, N2-0337, J7-4636, J7-4638, and J7-50227; the grant Artificial Intel-ligence for Science (GC-0001); and European Research Council (ERC) Starting Grant 123STABLE (grant agreement ID: 852208).

# Use of specific pyrazole derivatives for characterization of *L*-threonine dehydrogenase

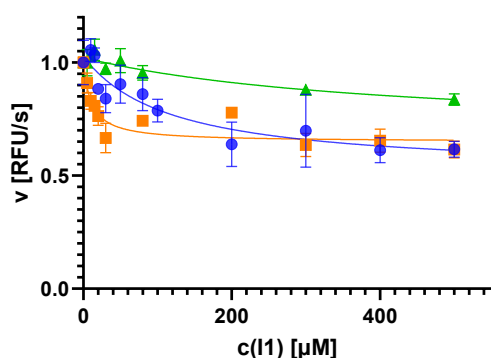
Marcel Tušek,<sup>1</sup> Marko Novinec\*,<sup>1</sup>

<sup>1</sup> Faculty of Chemistry and Chemical Technology, University of Ljubljana, Večna pot 113, SI-1000 Ljubljana, Slovenia

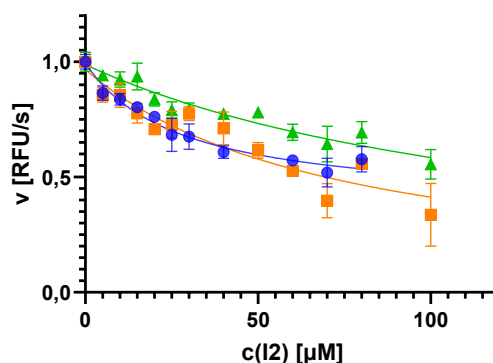
Pyrazole-based compounds are gaining prominence in pharmaceutical research due to their notable antimicrobial effects. The synthesis of new pyrazole derivatives offers promising ways for the development of novel antibiotics<sup>1</sup>. An example of such a compound is 4-(2-aminoethyl)-1-(pyridine-2-yl)-1H-pyrazole-5-ol (I1), which was found to inhibit the growth of *Escherichia coli* and the activity of *L*-threonine dehydrogenase (TDH). This enzyme is crucial for amino acid metabolism and biofilm production. As TDH is absent in human cells and lacks a human homologue, inhibitors like I1 present a valuable starting point for future drug discovery<sup>2</sup>.

This study focused on evaluating four types of pyrazole derivatives for their ability to inhibit TDH and influence biofilm formation. Enzyme activity was monitored through a fluorometric method, based on the conversion of NAD<sup>+</sup> to NADH, which allows for real time activity tracking<sup>3</sup>. Among the tested molecules, I1 proved to be the most effective inhibitor. A second compound, I2, showed comparable inhibition but could not be extensively analysed due to limited solubility at higher concentrations<sup>4</sup>.

Further experiments demonstrated that all tested derivatives reduced biofilm formation. However, only I1 and I2 were shown to exert a direct effect on TDH activity. These results support a potential association between TDH inhibition and impaired biofilm formation, though additional research is needed to confirm this relationship and fully assess the pharmacological potential of these compounds.



**Figure 1:** Effect of compound I1 concentration on reaction rates. The blue curve is 100 μM of L-Thr, orange curve is 250 μM of L-Thr and the green curve is 500 μM of L-Thr



**Figure 2:** Effect of compound I2 concentration on reaction rates. The blue curve is 100 μM of L-Thr, orange curve is 250 μM of L-Thr and the green curve is 500 μM of L-Thr

## References:

1. Naim, M. J.; Alam, O.; Nawaz, F.; Alam, M. J.; Alam, P. Current Status of Pyrazole and Its Biological activities. *J. Pharm. Bioallied. Sci.* **2016**, 8, 2–17.
2. Mikulič Vernik, N.: Karakterizacija interakcije med derivatom pirazola in *L*-treonin dehidrogenazo in suksinat dehidrogenazo bakterije *Escherichia coli*. Master's thesis, University of Ljubljana, Faculty of Chemistry and Chemical Technology, **2023**.
3. Mlinar, K.: Karakterizacija protibakterijskega delovanja izbranih derivatov pirazola na molekularni ravni. Master's thesis, University of Ljubljana, Faculty of Chemistry and Chemical Technology, **2024**.
4. ENZYME Database. *L*-threonine 3-dehydrogenase (EC 1.1.1.103). <https://enzyme.expasy.org/EC/1.1.1.103> (accessed March 20, 2025).



# Disulfide-based conformational locks for studies of alpha-actinin-1 actin cross-linking mechanism

Mark Loborec,<sup>1</sup> Jošt Hočevar,<sup>1</sup> Miha Pavšič\*,<sup>1</sup>

<sup>1</sup> Faculty of Chemistry and Chemical Technology, University of Ljubljana, Večna pot 113, SI-1000 Ljubljana, Slovenia

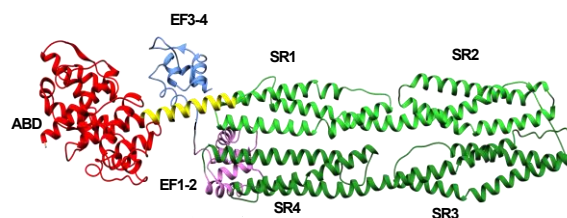
The actin cytoskeleton plays an important role in cell structure, adhesion and mobility<sup>1</sup>. Consequently, actin is one of the earliest evolved proteins, dating back to the common ancestor of life. It is also one of the most abundant proteins in many cells, accounting for up to 10 % of protein mass in most cells<sup>2</sup>.

Alpha-actinin is an actin-binding protein of the spectrin family, and likely also its originator. It consists of three major domains: an actin-binding domain (ABD), a calcium-binding calmodulin-like domain consisting of two EF-hand motifs (CaM-like domain) and a rod domain which connects the two<sup>3</sup>. It dimerizes in an anti-parallel fashion, with the CaM-like domain of one monomer regulating the ABD of the other. There are four human isoforms of alpha-actinin, two of which are calcium-sensitive (isoforms 1 and 4) and can be found in most cells, while the other two are calcium-insensitive (isoforms 2 and 3) and can be found only in muscle cells, localized to the Z-disc of the sarcomeres<sup>3</sup>.

As there is currently no accurate model of the conformational changes responsible for loss of actin-bundling activity upon calcium binding in non-muscle isoforms of alpha actinin, we have set to identify mutations which would conformationally lock parts of the structure, and measure its actin-bundling activity in the presence and absence of calcium, allowing us to determine in which region the conformational change responsible for the loss of actin-bundling activity occurs. For that purpose, we have introduced disulfide-bond forming cysteine pairs into the rod domain at selected locations, informed by previous experiments, structure models and crystal structure of related protein alpha-actinin-2 (Figure 1). A mutant with aspartate residues replacing glutamate residues in the 278 and 285 positions was also designed, as aspartate residues are absolutely conserved in calcium-insensitive human isoforms in those positions, while glutamate residues take their place in calcium-sensitive isoforms.

The mutations were introduced via the QuickChange method for site-directed mutagenesis and sequenced for

verification. The protein was then expressed in *E. coli* and purified via nickel-affinity, ion-exchange and size-exclusion chromatography. SDS-PAGE of the mutants under reducing vs. non-reducing conditions was then used to check for the formation of cross-chain disulfide bonds. Formation of such bonds was confirmed in one of the mutants, while actin-bundling activity tests are ongoing.



**Figure 1:** A model of a special "half-dimer form" of human actinin 1 in a calcium-bound state. The ABD and SR 1 and 2 domains would belong to one chain in a typical dimer, while the EF and SR 3 and 4 domains would belong to the other chain.

## References:

1. Foley, K. S.; Young, P. W. The Non-Muscle Functions of Actinins: An Update. *Biochem. J.* **2014**, 459 (1), 1–13.
2. Pollard, T. D. Actin and Actin-Binding Proteins. *Cold Spring Harbor Perspect. Biol.* **2016**, 8 (8), a018226.
3. Virel, A.; Backman, L. Molecular Evolution and Structure of Alpha-Actinin. *Mol. Biol. Evol.* **2004**, 21 (6), 1024–1031.

**Funding information:** grant no. N1-0191 (Slovenian Research and Innovation Agency (ARIS), Slovenia; bilateral project via Austrian Science Fund (FWF)).



# Frequency up-converted white to green emission tuning in 1-D Photonic crystal (MC) structures for LED applications

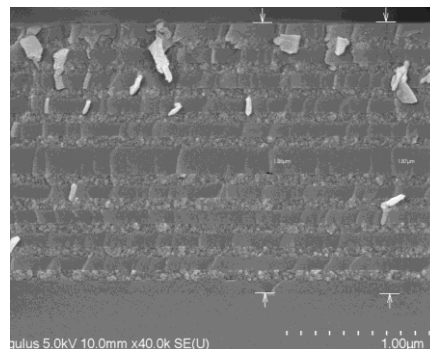
Martin Jazbec,<sup>1,2</sup> Prasenjit P. Sukul\*,<sup>1</sup> Luís F. Santos,<sup>1</sup> Rui M. Almeida,<sup>1</sup>

<sup>1</sup> Centro de Química Estrutural, Institute of Molecular Sciences and Departamento de Engenharia Química, Instituto Superior Técnico, Universidade de Lisboa, Av. Rovisco Pais, PT-1049-001, Lisboa, Portugal

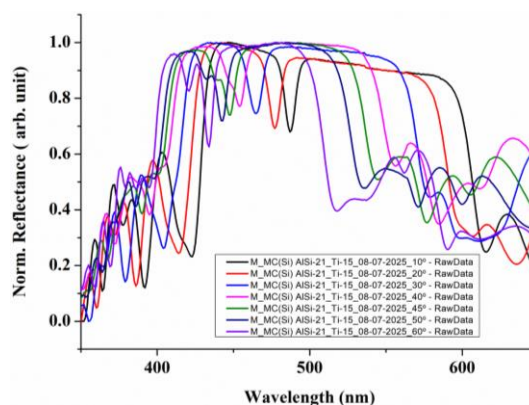
<sup>2</sup> Faculty of Chemistry and Chemical Technology, University of Ljubljana, Večna pot 113, SI-1000 Ljubljana, Slovenia

This study investigates one-dimensional photonic crystal (1D-PC) structures fabricated on silicon substrates, specifically focusing on a Fabry-Pérot microcavity (MC) designed for enhanced light emission at selected wavelengths within the white to green spectral range. The microcavity was constructed using alternating layers of titania and lanthanide (Ln)-doped aluminosilicate glass, synthesized via sol-gel (SG) processing. The aluminosilicate sols were tri-doped with  $\text{Tm}^{3+}/\text{Er}^{3+}/\text{Yb}^{3+}$  in a 0.5/0.5/5.0 mol% ratio<sup>1</sup>, serving as the low-refractive-index ( $n=1.48$ ) component, while titania sol provided the high-refractive-index counterpart. The MC structure consists of five Bragg mirror pairs on each side of a defect layer (composed of a double layer of Ln-doped<sup>2</sup> aluminosilicate). Cross-sectional SEM images of the FP MC is shown in the Figure 1 and Figure 2 shows the UV-Vis Reflectance data of the MC sample designed with defect layer targeting 525 nm for 0° angle.

In alignment with green chemistry principles, we further explored low-temperature processing methods by introducing zinc oxide ( $\text{ZnO}$ )<sup>3</sup> as an alternative high-refractive-index thin-film material. The influence of heat treatment temperature on  $\text{ZnO}$ 's crystalline structure was systematically examined. In summary, this work demonstrates the successful integration of  $\text{ZnO}$  films with Ln-doped aluminosilicate sols to fabricate optimized microcavity structures, offering a sustainable approach to photonic device fabrication.



**Figure 1:** SEM image of Fabry-Pérot microcavity (MC). It shows five Bragg mirror pairs on each side of the defect layer



**Figure 2:** Reflectance data of MC sample showing the defect layer position measured at different angles targeting 525nm defect position.

## References:

1. Almeida, R. M.; Sukul, P. P.; Maurya, S. K.; Santos, L. F. Photonic Crystal-Assisted White Light Generation in Sol-Gel Materials. *Opt. Mater. (Amst)*. **2025**, 165 (May), 117143.
2. Instrumentation for Fluorescence Spectroscopy BT - Principles of Fluorescence Spectroscopy; Lakowicz, J. R., Ed.; Springer US: Boston, MA, 2006; pp 27–61.
3. López-Mena, E.; Jiménez-Sandoval, S.; Jiménez-Sandoval, O.  $\text{ZnO}$  Thin Films Prepared at Low Annealing Temperatures, from a Novel, Simple Sol-Gel Precursor Solution. *J. Sol-Gel Sci. Technol.* **2015**, 74 (2), 419–424.

# Modeling-guided process development of a capillary force driven microfluidic distillation device

Martina Potočnik,<sup>1</sup> Rok Ambrožič\*,<sup>1</sup>

<sup>1</sup> Faculty of Chemistry and Chemical Technology, University of Ljubljana, Večna pot 113, SI-1000 Ljubljana, Slovenia

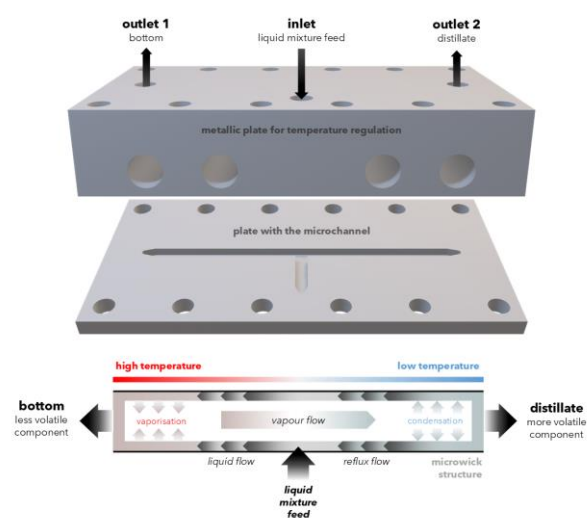
Distillation is one of the oldest and most frequently used separation processes, based on the different boiling points of components in miscible liquid mixtures. Due to its simplicity, high efficiency for various mixtures and the possibility of continuous separation, this method is widely applied in numerous industrial sectors, such as the pharmaceutical, petroleum, food and chemical industries. Despite its many advantages, distillation also has certain limitations. It is an energy-intensive process, which conflicts with sustainable development guidelines. The equipment required to ensure adequate productivity is large, meaning the process also demands significant operational space. Additionally, distillation systems are stationary, reagent consumption is relatively high even in pilot laboratories, and as a result, distillation is a relatively expensive process<sup>1</sup>.

It is possible to improve the distillation process with miniaturization, which is a promising approach for process intensification. Micro-structured systems are characterized by large specific surface areas (high surface-to-volume ratio), that enhances heat and mass transfer within the system, enabling faster separation, easier temperature regulation and, most importantly, greater energy efficiency. Firstly, due to smaller reaction volumes, the consumption of chemicals and energy is reduced, along with waste production and environmental impact. Secondly, in micro-distillation productivity can be easily increased by numbering-up the units. Microdistillation units can also be integrated with other (micro)reactors or analysers, creating a so-called "end-to-end processing" system for seamless production or analysis<sup>2</sup>.

In our research a model-based design (MBD) was used for development of a microfluidic distillation unit. In MBD of a microdistillation unit it is essential that after problem description, transport mechanisms definition, and determining the physico-chemical and other properties of the feed mixture, a model is created that mathematically describes and predicts the behaviour of the mixture within the device. After solving the model, a process simulation is carried out, allowing for a deeper understanding of the device's operation and an analysis of the impact of different variables on system performance. This enables the optimization of the process unit before its fabrication, which is one of the key advantages of the

MBD approach. Model optimization is economically more efficient and faster than empirical testing of manufactured prototypes<sup>3</sup>.

Within this research, microfluidic distillation device shown in Figure 1 was developed, and a corresponding mathematical model was created to describe the process. This was followed by numerical model solving and optimization of the distillation process to improve separation efficiency, reduce energy consumption, and enable system scale-up.



**Figure 1:** Schematic of the capillary force driven microfluidic distillation unit and illustration of its operational principle

## References:

1. Nekkanti, H.; Galam, A. K.; Vadaga, A. K. A Comprehensive Review of Distillation in the Pharmaceutical Industry. *J. Pharma Insight Res.* **2024**, *02*, 138–145.
2. Tabeling, P. *Introduction to Microfluidics*. Oxford University Press: New York, **2023**.
3. Plazl, I.; Lakner, M. Uvod v modeliranje procesov. UL, Fakulteta za kemijo in kemijsko tehnologijo: Ljubljana, **2019**.

**Funding information:** The author acknowledges the financial support from the Slovenian Research Agency (research core funding No. P2-0191).

# Synthesis and testing of molecularly imprinted polymers for electrochemical determination of neonicotinoids

Matic Plut,<sup>1</sup> Maksimiljan Dekleva,<sup>1</sup> Gregor Marolt,<sup>1</sup> Helena Prosen<sup>1</sup>

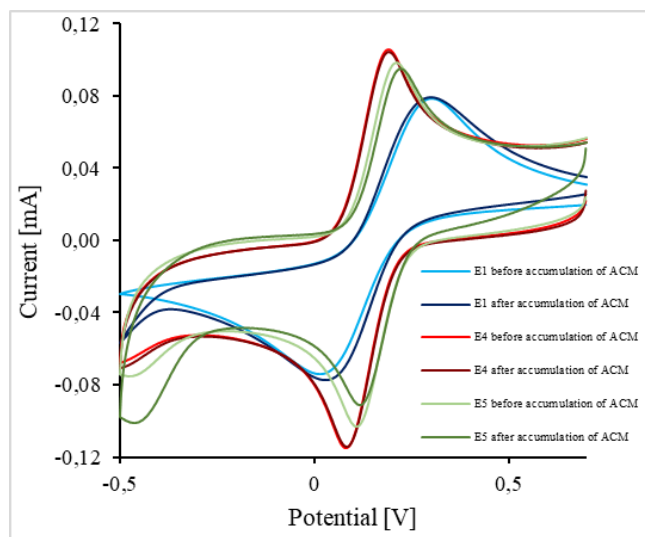
<sup>1</sup> Faculty of Chemistry and Chemical Technology, University of Ljubljana, Večna pot 113, SI-1000 Ljubljana, Slovenia

Neonicotinoids are a class of insecticides that have been in use since the end of the 20. century. Their use has increased rapidly, particularly in Africa and Asia due to their high efficiency and target specificity. However, widespread application has led to major imbalances in ecosystems, especially in insect and pollinator populations. In Europe their use has already been restricted and further restrictions are expected for the US.<sup>1–3</sup>

Thiacloprid and acetamiprid are important representatives of this group of pesticides, but their poor electroactivity due to the absence of a NO<sub>2</sub> group<sup>3</sup> makes direct electrochemical detection methods inapplicable for their determination. In our work, several molecularly imprinted polymers (MIPs) for thiacloprid and acetamiprid have been synthesised and further evaluated for electrochemical detection. The specific binding efficiencies of the polymers for the target analytes have been screened and quantified by calculating the imprinting factor (IF). The polymer with the highest IF for each analyte was applied to the working electrode of the screen-printed electrode via drop-casting.

Analysis of cyclic voltammograms of hexacyanoferrate redox probe at the i) untreated electrode, ii) modified electrode without the molecularly imprinted polymer, and iii) modified electrode with the corresponding molecularly imprinted polymer before and after accumulation in the solution of acetamiprid and thiacloprid was carried out.

The MIP-modified electrode was the only one showing decreased voltammetric signal of hexacyanoferrate, which could be the evidence of the specificity of binding of the analyte to the molecularly imprinted polymer, demonstrating the potential for further development and application to the working electrode for neonicotinoid sensing.



**Figure 1:** Cyclic voltammograms recorded by working electrodes before and after accumulation in 0.1 M acetamiprid solution (E1 – untreated electrode, E4 – modified electrode without MIP, E5 – modified electrode with MIP).

## References:

1. Jeschke, P.; Nauen, R.; Schindler, M.; Elbert, A. Overview of the Status and Global Strategy for Neonicotinoids. *J. Agric. Food Chem.* **2011**, *59* (7), 2897–2908.
2. Casida, J. E. Neonicotinoids and Other Insect Nicotinic Receptor Competitive Modulators: Progress and Prospects. *Annu. Rev. Entomol.* **2018**, *63* (1), 125–144.
3. Buszewski, B.; Bukowska, M.; Ligor, M.; Staneczko-Baranowska, I. A Holistic Study of Neonicotinoids Neuroactive Insecticides—Properties, Applications, Occurrence, and Analysis. *Environ. Sci. Pollut. Res.* **2019**, *26* (34), 34723–34740.

**Funding information:** This work was supported by the Slovenian Research and Innovation Agency, grant numbers J2–3049 and P1–053.

# Analysis of Air Pollutants in Ljubljana Bežigrad and Murska Sobota during Summer 2025

Tai Lupscha,<sup>1</sup> Matjaž Dlouhy\*,<sup>2</sup>

<sup>1</sup> Srednja poklicna in tehniška šola Murska Sobota, Šolsko naselje 12, SI-9000 Murska Sobota, Slovenia

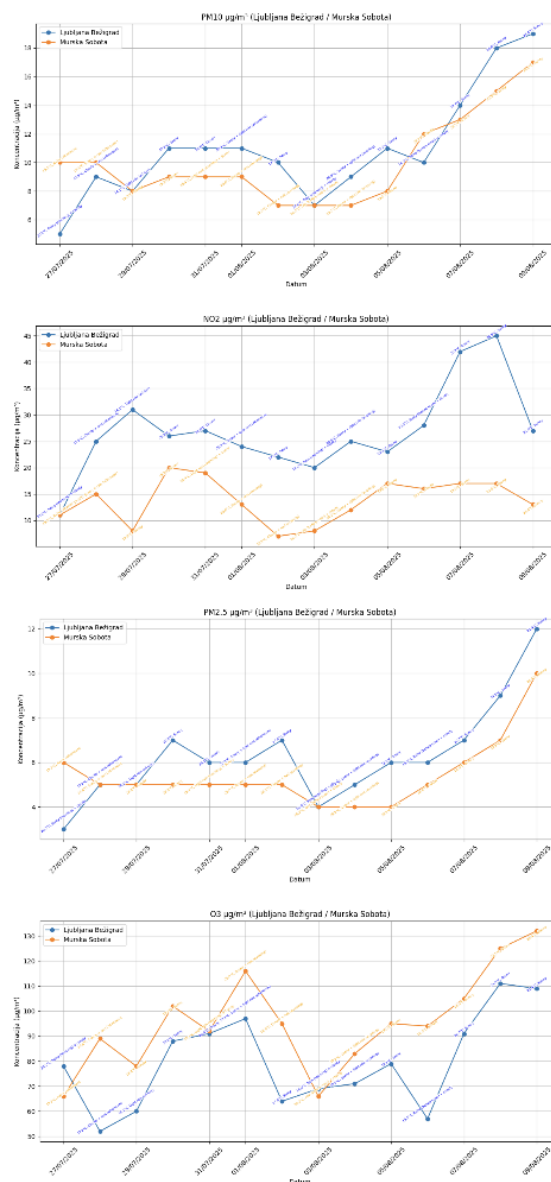
<sup>2</sup> Gimnazija Ledina, Resljeva cesta 12, SI-1000 Ljubljana, Slovenia

Environmental chemistry examines the chemical composition, transformations, and fate of substances in the natural environment, with atmospheric chemistry forming a critical branch that investigates pollutant generation, transport, and removal. Air quality research is central to this field, as atmospheric pollutants undergo complex chemical reactions affecting both human health and climate. Between July 27 and August 9, 2025, we conducted a comparative study of atmospheric pollutants at two Slovenian weather stations: Ljubljana Bežigrad (urban) and Murska Sobota (less urban/rural). Concentrations of PM<sub>10</sub>, PM<sub>2.5</sub>, NO<sub>2</sub>, and O<sub>3</sub> were measured alongside meteorological parameters such as temperature, wind, and precipitation. Ljubljana exhibited higher mean concentrations of PM<sub>10</sub>, PM<sub>2.5</sub>, and NO<sub>2</sub>, attributable to more intense anthropogenic emissions from traffic and heating systems.

In contrast, Murska Sobota consistently displayed higher ozone (O<sub>3</sub>) concentrations, illustrating the “ozone paradox” where urban areas with elevated nitrogen oxide (NO) emissions promote O<sub>3</sub> depletion through the titration reaction  $\text{NO} + \text{O}_3 \rightarrow \text{NO}_2 + \text{O}_2$ .<sup>1</sup>

Rural areas, with fewer NO sources, have less ozone destruction, allowing photochemically generated ozone to persist. During the study period, anticyclonic conditions with high solar irradiance enhanced the photolysis of NO<sub>2</sub> ( $\text{NO}_2 + h\nu \rightarrow \text{NO} + \text{O}$ ) and subsequent reaction of atomic oxygen with molecular oxygen to form ozone ( $\text{O} + \text{O}_2 \rightarrow \text{O}_3$ ). Limited vertical mixing and weak winds further allowed pollutant accumulation.

Temporal analysis revealed of data shown in Figure 1 reveals short-term peaks in PM and NO<sub>2</sub> linked to traffic surges, temperature inversions, and stagnant air masses, while rain and wind generally reduced concentrations through wet and dry deposition. Weekday pollutant levels exceeded weekend values due to commuting and industrial schedules. These findings underscore the importance of understanding the chemical kinetics of pollutant formation and removal in both urban and rural contexts. Elevated rural ozone, as observed in Murska Sobota, highlights that regional air quality policies must address not only primary emissions but also secondary pollutants formed through complex atmospheric chemistry.



**Figure 1:** Variation of Air Pollutants in Ljubljana Bežigrad and Murska Sobota (July–August 2025).

## References:

1. Sicard, P.; De Marco, A.; Agathokleous, E.; Feng, Z.; Xu, X.; Paoletti, E.; Diéguez Rodríguez, J. J.; Calatayud V. Amplified ozone pollution in cities during the COVID-19 lockdown. *Atmos. Environ.* **2020**, *239*, 117806.

# Optimization of horseradish peroxidase immobilization into cross-linked enzyme aggregates using microfluidics

Natalija Tomažin,<sup>1</sup> Marko Božinović,<sup>1</sup> Polona Žnidaršič-Plazl\*,<sup>1</sup>

<sup>1</sup> Faculty of Chemistry and Chemical Technology, University of Ljubljana, Večna pot 113, SI-1000 Slovenia, [polona.znidarsic@fkkt.uni-lj.si](mailto:polona.znidarsic@fkkt.uni-lj.si)

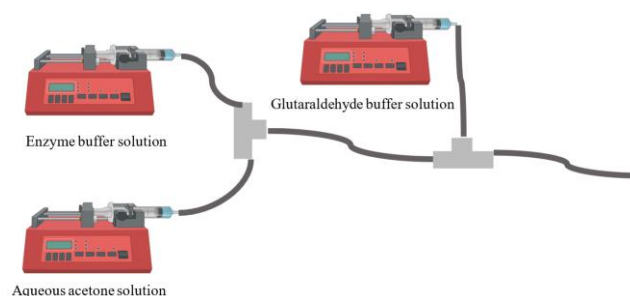
Efficient, carrier-free immobilization is pivotal for building robust biocatalysts that can be reused and operated continuously. Cross-linked enzyme aggregates (CLEAs) are attractive because they combine high volumetric activity with simple, low-cost preparation via precipitation followed by intra-aggregate crosslinking, while typically enhancing stability and enabling catalyst recycling<sup>1</sup>. However, conventional batch-scale precipitation and crosslinking that requests centrifugation for CLEAs separation from the reaction mixture often suffer from poorly controlled mixing and agglomeration, leading to highly polydisperse particle populations, variable recovered activity, and mass-transfer limitations that hamper reproducibility and scale-up. Microfluidic platforms mitigate these issues by imposing well-defined residence times and rapid micromixing, which narrow particle size distributions, improve transport, and seamlessly interface with continuous-flow operation<sup>2</sup>.

Leveraging these advantages, we aimed to optimize the immobilization of horseradish peroxidase (HRP) into CLEAs within a microfluidic platform, generating highly uniform, high-activity, and reusable nanoparticles suitable for cost-effective continuous biocatalytic processes. Immobilization in this setup not only enhances operational stability and catalyst reuse but also enables precise control over particle formation and supports seamless integration into continuous-flow oxidation reactions<sup>3</sup>.

Process optimization involved screening precipitation solvents, adjusting glutaraldehyde concentrations, and determining residence times for both precipitation and crosslinking. Dynamic light scattering was used to determine particle size distribution. The objective was to maximize the recovered activity of the enzyme, i.e. the activity after immobilization compared to that of the free enzyme, determined *via* the model reaction of 2,2'-azino-bis(3-ethylbenzothiazoline-6-sulfonic acid) (ABTS) oxidation by hydrogen peroxide, monitored spectrophotometrically at 405 nm. The best recovered

activity of 99 % was achieved at a retention time of 0.34 min with acetone and glutaraldehyde concentrations of 90 % (v/v) and 1 mM, respectively. The resulting CLEA-HRPs exhibited an average particle radius of 150 nm, determined using dynamic light scattering.

The optimized CLEA-HRP preparation provides a robust, reusable biocatalyst suitable for future continuous oxidation reactions. These findings demonstrate the potential of microfluidics-assisted CLEA generation for creating high-activity immobilized enzymes tailored for advanced biocatalytic applications.



**Figure 1:** Set-up for a continuous CLEA-HRP generation in a microfluidic system.

## References:

1. Sheldon, R. A.; van Pelt, S. Enzyme Immobilisation in Biocatalysis: Why, What and How. *Chem. Soc. Rev.* **2013**, *42* (15), 6223–6235.
2. Žnidaršič-Plazl, P. Biocatalytic process intensification *via* efficient biocatalyst immobilization, miniaturization, and process integration. *Curr. Opin. Green Sustain. Chem.* **2021**, *32*, 100546.
3. Menegatti, T.; Lavrič, Ž.; Žnidaršič-Plazl, P. Microfluidics-based preparation of cross-linked enzyme aggregates. [WO2023175002A1](#).

**Funding information:** This work was supported by Slovenian Research and Innovation Agency (ARIS) through Grants J4-4562 and P2-0191. MB was financed through Horizon Europe MSCA Doctoral Network project GreenDigiPharma (Grant 101073089).



# Synthesis, characterization and interaction between lignin nanoparticles and nanoplastics

Neja Lesinšek\*,<sup>1</sup> Azmat Ullah,<sup>1</sup> Jan Hočevar,<sup>1</sup> Boštjan Žener,<sup>1</sup> Jelena Papan Djaniš,<sup>1,2</sup> Jernej Iskra,<sup>1</sup>

<sup>1</sup> Faculty of Chemistry and Chemical Technology, University of Ljubljana, Večna pot 113, SI-1000 Ljubljana, Slovenia

<sup>2</sup> Centre of Excellence for Photoconversion, Vinča Institute of Nuclear Sciences, National Institute of the Republic of Serbia, University of Belgrade, RS-11351 Belgrade, Serbia

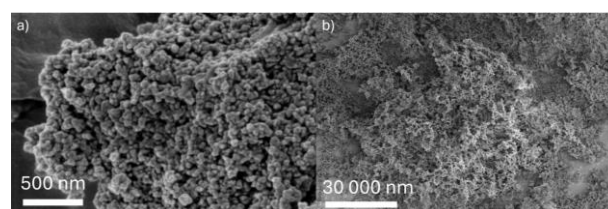
Plastic pollution is a global problem and has a major impact on the environment. While plastic materials improve everyday life and are widely used across industries due to their resilience and durability, these properties also contribute to their persistence in the environment for centuries. Humans are exposed to micro- and nanoplastics through tap and bottled water, personal care products and contaminated marine organisms that have ingested plastic particles present in aquatic environments. Marine-based sources of plastic pollution include recreational cruises, oil extraction, product transportation and fishing activities<sup>1</sup>. Nanoplastics in water can interact with naturally occurring polyphenolic compounds, such as lignin. In this study, we focused on the synthesis and characterization of lignin nanoparticles (LNPs) and nanoplastics (NPs) to establish a model system for studying their potential interactions.

Lignin was isolated from milled straw biomass using an organosolv extraction method. Biomass was mixed with ethyl acetate and hydrochloric acid and heated at 130°C for 3 hours. After cooling, the mixture was filtered, and the solvent was removed using a rotary evaporator. The resulting residue was treated with acetone and distilled water to precipitate lignin, which was then filtered and dried. Lignin nanoparticles (LNPs) were prepared via a hydrotropic synthesis method reported in <sup>2</sup>.

Nanoplastics (NPs) were synthesized by dissolving polystyrene foam in ethyl acetate and stirring the mixture at 80°C for 2 hours. The solution was dripped using a glass Pasteur pipette into stirred ethanol. The dispersion was centrifuged, and the particles were washed three times with Milli-Q water. The product was stored at 4°C <sup>3</sup>.

For characterization, FTIR, SEM, DLS, NMR and zeta potential measurements were performed to determine the chemical structure, morphology, particle size distribution and surface charge of the synthesized

nanoparticles. Representative SEM images of lignin nanoparticles and nanoplastics are shown in Figure 1. Interactions will be studied using zeta potential measurements and DLS at various pH values. This study is a starting point for future research on the interaction between lignin nanoparticles and nanoplastics. A better understanding of these interactions could help reduce environmental pollution.



**Figure 1:** Representative SEM images of : a) Lignin nanoparticles from organosolv lignin, b) nanoplastic particles

## References:

1. Almeida, M.; Oliveira, M. The why and how of micro(nano)plastic research. *TrAC, Trends Anal. Chem.* **2019**, *114*, 196–201.
2. Pourbaba, R.; Abdulkhani, A.; Rashidi, A.; Ashori, A. Lignin nanoparticles as a highly efficient adsorbent for the removal of methylene blue from aqueous media. *Sci. Rep.* **2024**, *14*, 9039.
3. Hunter, J. R.; Qiao, Q.; Zhang, Y.; Shao, Q.; Crofcheck, C.; Shi, J. Green solvent mediated extraction of micro- and nano-plastic particles from water. *Sci. Rep.* **2023**, *13*, 10585.

**Funding information:** The authors gratefully acknowledge the financial support from the Slovenian Research Agency (ARIS) – research core funding grants P1-0134, and P1-0418, and research project J2-50061.



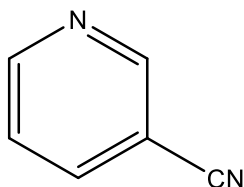
# Heptanuclear zinc(II) complex with 3-cyanopyridine

Nejc Virant,<sup>1</sup> Nina Podjed Rihtaršič,<sup>1</sup> Barbara Modec\*<sup>1</sup>

<sup>1</sup> Faculty of Chemistry and Chemical Technology, University of Ljubljana, Večna pot 113, SI-1000 Ljubljana, Slovenia

Zinc(II) plays a crucial biological role, acting as an essential cofactor in over 300 enzymes, enabling proper functioning of protein synthesis, nucleic acid metabolism, and cellular signaling etc. Additionally, zinc(II) contributes to the structural stability of proteins, which is vital for precise regulation of gene expression and the maintenance of functionality in various biological systems<sup>1</sup>.

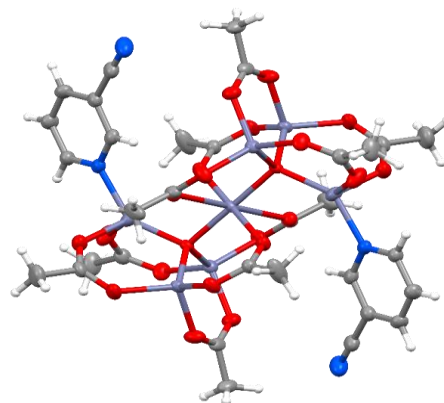
3-Cyanopyridine (3-PyCN) is a solid, colorless organic compound with the molecular formula C<sub>6</sub>H<sub>4</sub>N<sub>2</sub>. The molecule consists of a pyridine ring with a cyano group (–CN) attached at the third position.



**Scheme 1:** Structural formula of 3-cyanopyridine (3-PyCN).

3-Cyanopyridine can bind to transition metal ions in a monodentate manner through the ring nitrogen or, less commonly, also through the cyano group in a bridging manner. Surprisingly, the coordination chemistry of zinc(II) with 3-cyanopyridine is relatively poorly explored. Therefore, our goal was to prepare new zinc(II) coordination compounds with this ligand.

The reactions of zinc(II) acetate dihydrate with 3-cyanopyridine resulted in two new crystalline products, [Zn<sub>7</sub>O<sub>2</sub>(CH<sub>3</sub>COO)<sub>10</sub>(3-PyCN)<sub>2</sub>] (**1**) and [Zn<sub>7</sub>O<sub>2</sub>(CH<sub>3</sub>COO)<sub>10</sub>(3-PyCN)<sub>2</sub>]·4CH<sub>3</sub>CN (**2**). Their compositions were determined by X-ray structure analysis on single-crystal. Both compounds contain the heptanuclear core where bridging oxides and acetates link zinc(II) ions. The structure of the novel heptanuclear zinc(II) complex is shown in Figure 1.



**Figure 1:** ORTEP drawing of the heptanuclear complex molecule [Zn<sub>7</sub>O<sub>2</sub>(CH<sub>3</sub>COO)<sub>10</sub>(3-PyCN)<sub>2</sub>], as found in **1**.

Analogous heptanuclear zinc(II) complexes with acetate and nitrogen donor ligands such as 1-methylimidazole or pyrazine were prepared before<sup>2,3</sup>.

Herein, we will present the crystal structures of both compounds, along with the infrared and <sup>1</sup>H NMR spectra, as well as the TG-DSC and elemental analysis of compound **1**.

## References:

1. Parkin G. Synthetic analogues relevant to the structure and function of zinc enzymes. *Chem. Rev.* **2004**, *104*, 699.
2. Lalioti, N.; Perlepes, S. P.; Manessi-Zoupa, E.; Raptopoulou, C. P.; Terzis, A.; Aliev, A. E.; Gerothanassis, I. P. Rare M<sub>7</sub>O<sub>2</sub> double tetrahedral core in molecular species: preparation, structure and properties of [Zn<sub>7</sub>O<sub>2</sub>(O<sub>2</sub>CMe)<sub>10</sub>(1-Meim)<sub>2</sub>] (1-Meim = 1-methylimidazole). *Chem. Commun.* **1998**, 1513.
3. Waheed, A.; Jones, R. A.; McCarty, J.; Yang, X.; Synthesis and structure of Zn<sub>7</sub>(μ<sub>4</sub>-O)<sub>2</sub>(OAc)<sub>10</sub>(Pz)<sub>2</sub> (OAc = acetate; Pz = pyrazine). *Dalton Trans.* **2004**, 3840.

**Funding information:** The Slovenian Research and Innovation Agency through the Research Core Program Grant P1-0134 and Infrastructure programme No. 10-0022.

# Cyclic anhydrides as multi-purpose compounds

Nina Krašovec,<sup>1</sup> Matic Rogan,<sup>1</sup> Jerneja Kladnik,<sup>1</sup> Damijana Urankar,<sup>1</sup> Janez Košmrlj\*,<sup>1</sup>

<sup>1</sup> Faculty of Chemistry and Chemical Technology, University of Ljubljana, Večna pot 113, SI-1000 Ljubljana, Slovenia, ([janez.kosmrlj@fkkt.uni-lj.si](mailto:janez.kosmrlj@fkkt.uni-lj.si))

Cyclic anhydrides are commonly 5- or 6-member ring molecules, conventionally derived from corresponding dicarboxylic acids by an intramolecular dehydration reaction. Normally, the use of toxic dehydration reagents and harsh conditions is required, though recently new procedures have been developed which employ Lewis acids as catalysts<sup>1</sup> or allow dicarboxylic acids to be directly transformed into cyclic anhydrides via electrolysis<sup>2</sup>.

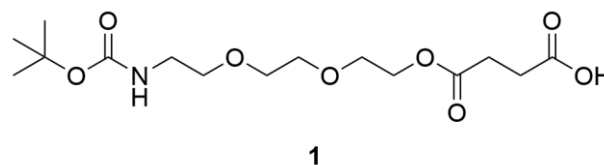
Cyclic anhydrides act as electrophiles and are able to react with nucleophilic compounds, such as amines and alcohols to form amides and esters, respectively. Due to facile activation of one carbonyl group in anhydride bond, reaction can proceed under mild conditions and without the presence of coupling reagents, which makes cyclic anhydrides valuable tools in organic and bioconjugate chemistry<sup>1</sup>.

They are commonly used for polymer functionalization, hydrogel formation and in some cases polymer synthesis. Protein modifications with cyclic anhydrides lead to increased protein solubility and can reverse the total charge of the biomolecule. Their pH-sensitivity is exploited in drug delivery systems to selectively target low pH tissues. In addition, cyclic anhydrides are often used as cross-linkers between various molecules<sup>1</sup>.

Alongside aforementioned, cyclic anhydrides have also been utilized in surface functionalization of nanoparticles. Bloemen et al.<sup>3</sup>, for instance, used succinic anhydride to end-cap a polyethylene glycol derivative, which was further linked to iron oxide nanoparticles via a siloxane group. Carboxylic acid end group served as an accessible functional group and introduced various coupling possibilities in biomedical applications, including coupling to antibodies.

In our research we used the simplest cyclic anhydride, succinic anhydride, to perform an

esterification reaction with a derivative of diethylene glycol to yield an elongated carboxyl derivative (**Figure 1**). For a successful reaction procedure an excess of triethylamine was added, which served as a base as well as a solvent. This procedure resulted in a successful synthesis of the desired compound (2,2-dimethyl-4,15-dioxo-3,8,11,14-tetraoxa-5-azaoctadecan-18-oic acid, (**1**) with little side products, which were easily removed by dissolving the reaction mixture in dichloromethane and washing it with 1 M HCl solution and brine. Synthesized molecule exhibits potential use as a linking element and in nanoparticle surface functionalization.



**Figure 1:** Synthesized compound 2,2-dimethyl-4,15-dioxo-3,8,11,14-tetraoxa-5-azaoctadecan-18-oic acid (**1**).

## References:

- Spanedda, M. V.; Bourel-Bonnet, L. Cyclic Anhydrides as Powerful Tools for Bioconjugation and Smart Delivery. *Bioconjugate Chem.* **2021**, *32*, 482–496.
- Schneider, J.; Häring, A. P.; Waldvogel, S. R. Electrochemical Dehydration of Dicarboxylic Acids to Their Cyclic Anhydrides. *Chem. Eur. J.* **2024**, *30*, e202400403.
- Bloemen, M.; Van Stappen, T.; Willot, P.; Lammertyn, J.; Koeckelberghs, G.; Geukens, N.; Gils, A.; Verbiest, T. Heterobifunctional PEG Ligands for Bioconjugation Reactions on Iron Oxide Nanoparticles. *PLoS One* **2014**, *9*, e109475.

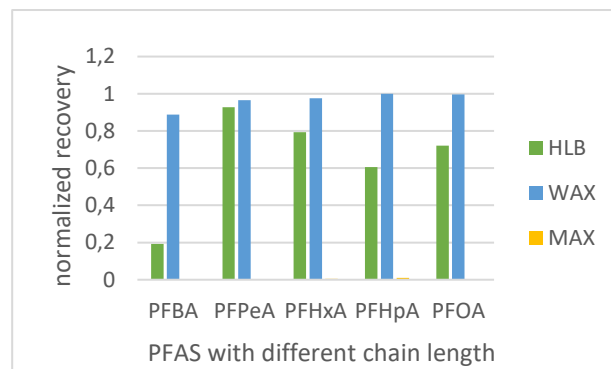
**Funding information:** The study was supported by the Slovenian Research and Innovation Agency (ARIS; Research Core Funding grant P1-0230).

# Development of extraction method for perfluoroalkyl pollutants in water

Špela Žunec,<sup>1</sup> Helena Prosen\*,<sup>1</sup> Ida Kraševac<sup>1</sup>

<sup>1</sup> Faculty of Chemistry and Chemical Technology, University of Ljubljana, Večna pot 113, SI-1000 Ljubljana, Slovenia

Per- and polyfluoroalkyl substances (PFAS) are compounds with strong carbon–fluorine (C-F) bonds that cause their exceptional stability and resistance to degradation. Therefore, they are widely used in industrial applications. However, their persistence and bioaccumulation have raised significant concerns due to their adverse effects on human health and the environment.<sup>1</sup> Determination of PFAS typically involves extraction and preconcentration, followed by analysis using sensitive techniques such as liquid chromatography–tandem mass spectrometry (LC-MS/MS).<sup>2</sup> One of the most common extraction techniques is solid-phase extraction (SPE), which was also used in this work for the extraction of five PFAS (C4-C8) from water samples. The method was optimized by evaluating sorbent type (Fig. 1), elution solvent, and extraction conditions (pH and salt concentration). The final method consisted of sample pH and salt content adjusted to 2-3 and 3.5 %, respectively. Cartridges with WAX sorbent were used with 5% NH<sub>3</sub> in methanol as the elution solvent. The breakthrough volume exceeded 500 mL and extraction recoveries were above 95% for all analytes. A seawater sample was analysed, revealing the presence of PFAS at concentrations below the limit of quantification, approximately 5-6 ng/L.



**Figure 1:** Comparison of normalized recoveries for different SPE cartridges

## References:

1. Ng, C.; Cousins, I. T.; DeWitt, J. C.; Glüge, J.; Goldenman, G.; Herzke, D.; Lohmann, R.; Miller, M.; Patton, S.; Scheringer, M.; Trier, X.; Wang, Z. Addressing Urgent Questions for PFAS in the 21st Century. *Environ. Sci. Technol.* **2021**, *55*, 2755–12765.
2. Liu, Y.; Bao, J.; Hu, X.-M.; Lu, G.-L.; Yu, W.-J.; Meng, Z.-H. Optimization of extraction methods for the analysis of PFOA and PFOS in the salty matrices during the wastewater treatment. *Anal. Bioanal. Chem.* **2020**, *412*, 1234–1245.

# Characterization of ATP-dependent amide bond synthetase for selective amidation

Tadej Menegatti\*,<sup>1</sup>, Žiga Gerdina,<sup>1</sup> András Kotschy,<sup>2</sup> Gábor Tasnádi,<sup>2</sup> Polona Žnidaršič Plazl,<sup>1</sup>

<sup>1</sup> Faculty of Chemistry and Chemical Technology, University of Ljubljana, Večna pot 113, SI-1000 Ljubljana, Slovenia

<sup>2</sup> Servier Research Institute of Medicinal Chemistry, Zahony str. 7, HU-1031 Budapest, Hungary

Amide bond formation is a central transformation in pharmaceutical synthesis, representing up to 16 % of all reactions in medicinal chemistry. Conventional approaches typically rely on stoichiometric activation of carboxylic acids with coupling reagents, which often results in poor atom economy and the generation of hazardous by-products<sup>1</sup>. In contrast, enzymatic methods operating in aqueous media without toxic reagents offer a greener and more sustainable alternative<sup>2</sup>. Among these, ATP-dependent amide bond synthetases (ABS) have emerged as promising catalysts, capable of performing both acid adenylation and subsequent amidation within a single active site, requiring only a small excess of the amine partner<sup>1,3</sup>.

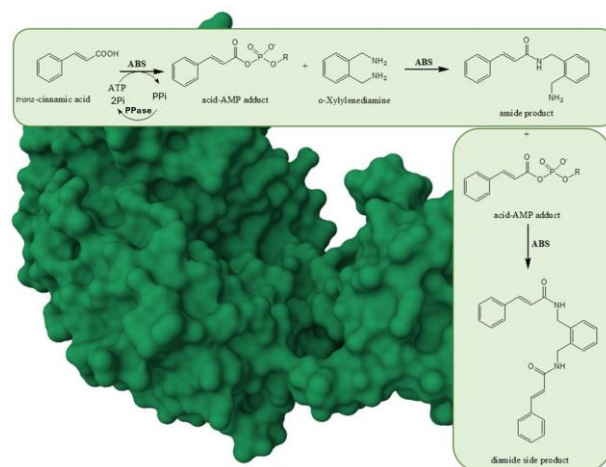
Here, we describe process development for the ATP-dependent coupling of *trans*-cinnamic acid with 1,2-phenylenedimethanamine catalyzed by an ABS from *Streptomyces* TR1341 in the presence of inorganic pyrophosphatase (PPase). The reaction proceeds through an acyl-AMP intermediate, which undergoes nucleophilic attack by the amine to form the amide product.

Higher temperatures increased activity but also diamide formation; 30 °C was chosen to balance both. The enzyme was most active at pH 7.50–7.82. At 30 % (v/v) co-solvent, DMSO severely inhibited activity (10.13 % residual), while glycerol retained 47.12 %. Gas sparging showed bubble exposure, not oxidation, caused deactivation: O<sub>2</sub> and N<sub>2</sub> reduced activity to ~57 % after 2 h, with complete loss by 3 h.

Kinetic studies with isolated acyl-AMP showed that AMP-to-amine ratios control selectivity—excess amine boosted amide yield but increased diamide via competing nucleophilic attack. Higher ratios improved yield, while lower absolute concentrations (10 mM amine, 5 mM acid) enhanced selectivity by limiting side reactions and improving solubility.

Overall, these results demonstrate that ABS-catalyzed amidation can benefit greatly from implementation in microflow systems, where precise control of residence time and reactant concentrations, along with reduced bubble formation, can minimize interfacial deactivation and improve product selectivity. This approach offers a

clear route toward intensified and scalable biocatalytic processes<sup>4</sup>.



**Figure 1:** Reaction scheme of ABS-catalyzed amide synthesis from *trans*-cinnamic acid and 1,2-phenylenedimethanamine.

## References:

- 1 Tang, Q.; Petchey, M.; Rowlinson, B.; Burden, T. J.; Fairlamb, I. J. S.; Grogan, G. Broad Spectrum Enantioselective Amide Bond Synthetase from *Streptoalloteichus* Hindustanus. *ACS Catal.* **2024**, *14* (2), 1021–1029.
- 2 Lubberink, M.; Finnigan, W.; Flitsch, S. L. Biocatalytic Amide Bond Formation. *Green Chem.* **2023**, *25* (8), 2958–2970.
- 3 Winn, M.; Richardson, S. M.; Campopiano, D. J.; Micklefield, J. Harnessing and Engineering Amide Bond Forming Ligases for the Synthesis of Amides. *Curr. Opin. Chem. Biol.* **2020**, *55*, 77–85.
- 4 Žnidaršič-Plazl, P.; Biocatalytic process intensification via efficient biocatalyst immobilization, miniaturization, and process integration. *Curr Opin Green Sustain Chem.* **2021**, *32*, 100546.

**Funding information:** The research was funded by the Interreg Central Europe project CE0200857 GreenChemForCE, co-funded by the European Union. TM and PŽP were supported also by Slovenian Research Agency (Grant P2-0191).

# Optimisation of extrusion based on a rheological analysis

Tadej Pirc\*,<sup>1</sup> Rok Ambrožič,<sup>1</sup>

<sup>1</sup> Faculty of Chemistry and Chemical Technology, University of Ljubljana, Večna pot 113, SI-1000 Ljubljana, Slovenia

This abstract summarizes research investigating the optimisation of the extrusion process for paraffin-based rodent bait using rheological analysis as a tool for systematic process improvement. The study is grounded in industrial practice and aims to address specific issues in the manufacturing process—namely, mechanical stress on the extruder, mixture inhomogeneity, and unnecessarily high production costs—while preserving product functionality and mechanical integrity<sup>1</sup>.

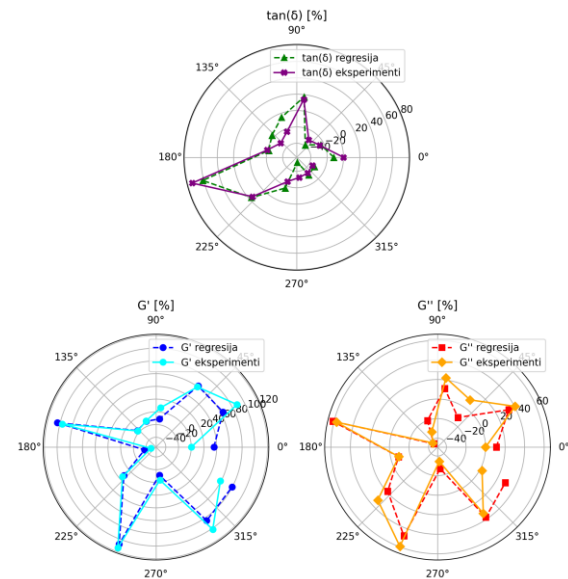
Rheological measurements were carried out using a plate–plate geometry on a rotational rheometer under controlled strain amplitude. The bait, being a viscoelastic solid, required careful sample preparation to ensure consistent results. A customized steel mold and hydraulic press were used to produce test specimens, and an optimal compaction pressure was determined through statistical evaluation of measurement repeatability. Key rheological parameters such as the elastic modulus ( $G'$ ), viscous modulus ( $G''$ ), and  $\tan(\delta)$  were used to quantify the material's response under small-strain oscillatory conditions, with  $\tan(\delta)$  serving as the principal metric for distinguishing the viscoelastic properties of various polymers<sup>1</sup>.

A Plackett–Burman design of experiments (DoE) was employed to screen nine variables: seven formulation components, extrusion temperature, and shear rate<sup>2,3</sup>. Through statistical analysis including multiple linear regression and ANOVA, the study identified the most influential factors on the viscoelastic response of the mixture<sup>2,3</sup>. These findings were used to develop a regression-based model that accurately predicts the product's rheological behavior under varying process conditions. Figure 1 illustrates the validation of this model<sup>1</sup>.

The usefulness of this approach is multifold. First, it allows for predictive control of product texture and mechanical integrity based on measurable inputs—without relying on trial-and-error methods or costly commercial software. Second, it provides a low-cost strategy for optimising formulation and processing parameters using open-source tools. Third, it enables data-driven decision-making in industrial settings where product reproducibility and equipment reliability are essential<sup>1</sup>.

The outcome includes a set of optimised parameters and a validated model capable of guiding formulation and

process changes while maintaining equivalent rheological behavior to the current product standard. The optimised formulation not only matches the mechanical and functional requirements but also results in reduced cost and greater process robustness. Examples of cost reduction with fixed  $\tan(\delta)$  are shown in Table 1<sup>1</sup>.



**Figure 1:** Comparison of regression model predictions and experimental results for rheological parameters<sup>1</sup>

**Table 6:** Relative deviations of predicted rheological parameters from experimental values for selected formulations (R1, R3, R5)<sup>1</sup>

	R1	R3	R5
$\widehat{G'}_i$	-10,30 %	2,89 %	17,06 %
$\widehat{G''}_i$	-10,30 %	2,89 %	17,06 %
$\widehat{\tan(\delta)}_i$	0,00 %	0,00 %	0,00 %
<b>Cost reduction</b>	7,23 %	6,59 %	5,07 %

## References:

1. Pirc T., Optimizacija ekstrudiranja na osnovi reološke analize. M.S. Thesis, University of Ljubljana, **2025**.
2. Durakovic B. Design of Experiments Application, Concepts, Examples: State of the Art. *PEN* **2017**, 5, 421–439.
3. Design of Experiments (DOE) in New Product Design & Development Air Academy Associates; **2014**.



# Selective Extraction of Magnesium from Slovenian Dolomite

Tal Čarman\*,<sup>1</sup> Mitja Kolar,<sup>1</sup> Vilma Ducman,<sup>2</sup> Gorazd Žibret,<sup>3</sup> Lea Žibret,<sup>2</sup>

<sup>1</sup> Faculty of Chemistry and Chemical Technology, University of Ljubljana, Večna pot 113, SI-1000 Ljubljana, Slovenia, ([tal.charman@gmail.com](mailto:tal.charman@gmail.com))

<sup>2</sup> Slovenian National Building and Civil Engineering Institute, Dimičeva ulica 12, SI-1000 Ljubljana, Slovenia

<sup>3</sup> Geological Survey of Slovenia, Dimičeva ulica 14, SI-1000 Ljubljana, Slovenia

Magnesium (Mg) is a critical metal with applications in the automotive, aerospace, electronics, chemical and pharmaceutical industries.<sup>1</sup> It is currently the third most highly produced metal globally<sup>2</sup> and demand is likely to increase as it is one of the most promising metals for the development of more sustainable batteries.<sup>3</sup> Sources of Mg range from seawater to many minerals, of which dolomite ( $\text{CaMg}(\text{CO}_3)_2$ ) is among the most suitable. Around 90 % of the world Mg supply is produced in China from dolomite, using the energy intensive and polluting Pidgeon process.<sup>2,4</sup>

The aim of our work was to develop a hydrometallurgical procedure for the selective extraction of Mg from Slovenian dolomite. The emphasis was on high efficiency and selectivity for Mg over Ca, while other impurities were only monitored.

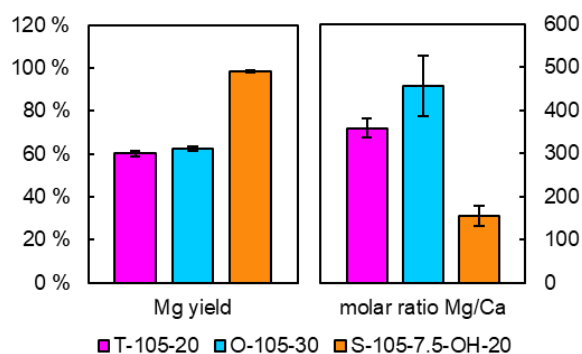
The dolomite sample, identified as dolomite rock, was collected from a Slovenian quarry and prepared by grinding to a fine powder (performed by the Geological Survey of Slovenia). The elemental composition of the sample was then determined using microwave digestion and ICP-OES analysis. The sample was close to ideal dolomite with metal impurities of less than 0.15 % by weight and the molar ratio Mg : Ca of 0.93 : 1.

Mg extraction from dolomite was performed by selective leaching and selective precipitation at room temperature on an orbital shaker. Mg was selectively leached from 1 g of the sample by sulfuric (VI) ( $\text{H}_2\text{SO}_4$ ), oxalic ( $\text{H}_2\text{C}_2\text{O}_4$ ) and tartaric ( $\text{C}_4\text{H}_6\text{O}_6$ ) acids with 50 %, 105 % and 150 % equivalent relative to the amount of Ca + Mg in 1 g of ideal dolomite. Four different sulfuric acid volumes (5 mL – 20 mL) were tried, whereas the minimum volume of oxalic and tartaric acid was limited by solubility. Selective precipitation was performed with sodium hydroxide (NaOH) from the solution obtained by the optimal leaching procedure. The amount of NaOH needed was precisely calculated for precipitation with 10 mL and 20 mL of solution.

Solutions produced by the procedures were analyzed by ICP-OES and Mg leaching and precipitation yields were calculated. Selectivity for Mg was determined by calculating the molar ratio Mg : Ca in the leachate (precipitate). The overall optimal procedure was selective

Mg leaching with 7.5 mL and 105 % equivalent of  $\text{H}_2\text{SO}_4$  followed by selective Mg precipitation with 20 mL of NaOH. It achieved an overall Mg yield of 98.3 % and a molar ratio of 155 : 1. Selective leaching with 30 mL and 105 % equivalent of  $\text{H}_2\text{C}_2\text{O}_4$  was more selective with Mg : Ca = 457 : 1, but Mg yield was only 62.5 %.

Overall, the developed procedures are highly efficient and selective for Mg. Moreover, only readily available and inexpensive reagents are needed and the energy expenditure is minimal.



**Figure 1:** Mg yield and molar ratio Mg/Ca for leaching with tartaric (T) and oxalic (O) acid. Leaching with sulfuric (VI) (S) acid was followed by precipitation with NaOH (OH). The first number stands for equivalent (%) and the second for reagent volume (mL). Only the best combination for each set of reagents is shown.

## References:

1. Tan, J.; Ramakrishna, S. Applications of Magnesium and Its Alloys: A Review. *Appl. Sci.* **2021**, *11* (15), 6861.
2. González, Y.; Navarra, A.; Jeldres, R. I.; Toro, N. Hydrometallurgical Processing of Magnesium Minerals – A Review. *Hydrometallurgy* **2021**, *201*, 105573.
3. Deng, M.; Wang, L.; Vaghefinazari, B.; Xu, W.; Feiler, C.; Lamaka, S. V.; Höche, D.; Zheludkevich, M. L.; Snihirova, D. High-Energy and Durable Aqueous Magnesium Batteries: Recent Advances and Perspectives. *Energy Storage Mater.* **2021**, *43*, 238–247.
4. Zhang, J.; Miao, J.; Balasubramani, N.; Cho, D. H.; Avey, T.; Chang, C. Y.; Luo, A. A. Magnesium Research and Applications: Past, Present and Future. *J. Magnesium Alloys* **2023**, *11* (11), 3867–3895.

# Electrochemical Monitoring of Polystyrene Nanoplastics–Fungal Biomass Interactions for Advanced Sensing Applications

Tia Kralj\*,<sup>1</sup> Andrej Gregori,<sup>2,3</sup> Gregor Marolt,<sup>1</sup>

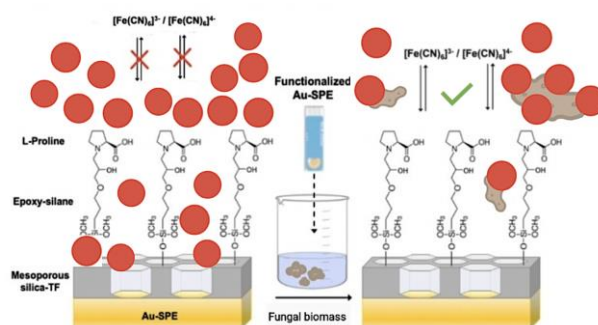
<sup>1</sup> Faculty of Chemistry and Chemical Technology, University of Ljubljana, Večna pot 113, SI-1000 Ljubljana, Slovenia

<sup>2</sup> Biotechnical Faculty, University of Ljubljana, Jamnikarjeva 101, SI-1000 Ljubljana, Slovenia

<sup>3</sup> MycoMedica Ltd, Podkoren 72, SI-4280 Kranjska Gora, Slovenia

Nanoplastics (NPs), ultrafine synthetic polymer particles, are emerging as a concerning class of pollutants due to their high mobility, persistence, and ability to penetrate biological membranes and accumulate within aquatic ecosystems<sup>1</sup>. Their nanoscale dimensions (< 1  $\mu\text{m}$ ) and intricate interactions in water make their detection challenging, often requiring complex analytical procedures and sophisticated instrumentation techniques. Their small size facilitates uptake by organisms and integration into food webs, raising concerns over ecological and human health impacts<sup>2</sup>. In this work, we present a novel, integrated approach to i) remove polystyrene nanoplastics (PSNPs) from water using fungal biomass and ii) electrochemically monitor PSNPs for the evaluation of their adsorption onto the biomass surface. The mycosorption on a medicinal fungus *Trametes versicolor* (TV) particles was systematically evaluated under various operational parameters. Its effectiveness as a sustainable and efficient biosorbent was monitored and confirmed with the electrochemical sensor, based on a gold screen-printed electrode (Au-SPE), modified with a mesoporous silica thin film via electro-assisted deposition and subsequently functionalized with epoxy silane and proline<sup>3,4</sup>, designed to interact selectively with PSNPs. The sensing process is driven by two key factors: the binding of PSNPs onto immobilized amino acid groups, and the application of a positive potential that promotes electrostatic interaction between the negatively charged PSNPs (in 0.1 M KCl) and the working electrode. The modification steps were systematically tracked and characterized via cyclic voltammetry (CV). The optimal accumulation potential was found at +0.6 V, producing the largest current decrease. All measurements were performed in 5 mM HCF, serving as a redox probe. The sensor was employed to detect 6.1 nm PSNPs based on the decrease of the anodic current peak ( $i_{\text{pa}}$ ), consistent with their ability to penetrate the mesoporous film. In this regard, a calibration curve for 6.1 nm PSNP was constructed in the range of 0.02–0.8  $\mu\text{g/mL}$ , resulting in 15–35% decrease in  $i_{\text{pa}}$ , demonstrating the sensor's sensitivity and applicability for quantitative analysis. When 0.05 mg of

TV biomass was introduced into 5.0 mL of 0.8  $\mu\text{g/L}$  PSNPs suspensions, no decrease in  $i_{\text{pa}}$  was observed, confirming a nearly-complete adsorption and thus removal of PSNPs from solution. This process was observed in real time by the sensor without any interferences of TV biomass particles, as confirmed by additional control experiments using CV. This study presents a portable electrochemical sensor for real-time detection of PSNPs and their adsorption onto TV biomass, offering a sustainable approach for on-site monitoring and mitigation of NPs pollution in aquatic environments.



**Figure 1:** PSNPs detection via pore blocking on functionalized Au-SPE and their removal by fungal biomass, preserving the electrochemical signal.

## References:

1. Sana, S. S.; Dogiparthi, L. K.; Gangadhar, L.; Chakravorty, A.; Abhishek, N. Effects of microplastics and nanoplastics on marine environment and human health. *Environ. Sci. Pollut. Res.* **2020**, *27* (36), 44743–44756.
2. Zhang, B.; Chao, J.; Chen, L.; Liu, L.; Yang, X.; Wang, Q. Research progress of nanoplastics in freshwater. *Sci. of The Tot. Environ.* **2021**, *757*, 143791.
3. Walcarius, A. Electrochem. applic. of silica-based materials. *Chem. Mater.* **2001**, *13* (10), 3351–3372.
4. Fernández, I.; Sánchez, A.; Díez, P.; Martínez-Ruiz, P.; Di Pierro, P.; Porta R.; Villalonga, R.; Pingarrón, J. M. Nanochannel-based electrochemical assay for transglutaminase activity. *Chem. Commun.* **2014**, *50*, 13356–13358.

# Establishing Enzyme Assays for the Detection of Tyrosinase and Hyaluronidase Inhibitors in Marine Algae

Tina Kosovel,<sup>1</sup> Eva Smrekar,<sup>1</sup> Petra Tavčar Verdev,<sup>1</sup> Marko Dolinar\*,<sup>1</sup>

<sup>1</sup> Faculty of Chemistry and Chemical Technology, University of Ljubljana, Večna pot 113, SI-1000 Ljubljana, Slovenia

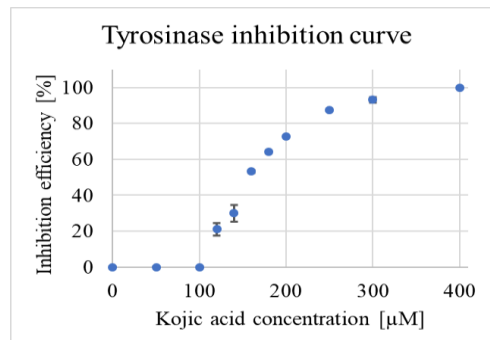
We introduced to our laboratory and adapted two simple, robust, and rapid enzyme assays to determine whether algae from Sečoveljske soline contain substances that inhibit enzymes linked to skin aging. The assays need to be sensitive to low concentrations of inhibitors while remaining resistant to interference from other algal components.

Tyrosinase catalyzes two steps in melanin production, including a rate-limiting one, making it a prime target for reducing hyperpigmentation. Hyaluronidase breaks down hyaluronic acid, and its increased activity with age contributes to wrinkles. Inhibiting these two enzymes may help prevent both skin conditions<sup>1</sup>.

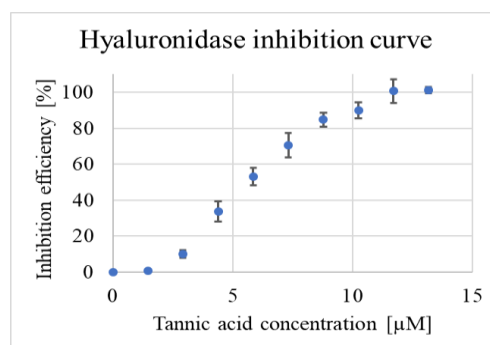
For the tyrosinase inhibitory assay, we adapted a method based on the spectrophotometric detection of the reaction product<sup>2</sup>. In this assay, tyrosinase oxidizes dopamine to dopamine quinone, which exhibits a maximum absorbance at 475 nm. We modified the original assay by replacing the substrate L-tyrosine with dopamine, which is converted to the target product in a single step. Additionally, we optimized the concentrations of both enzyme and substrate to maximize the differential absorbance value. The assay was validated using kojic acid, a well-known tyrosinase inhibitor.

For the hyaluronidase assay, we adapted the method proposed by Sigma-Aldrich<sup>3</sup>. It relies on the aggregation of hyaluronic acid with albumin in acidic conditions, producing varying degrees of turbidity measurable at 600 nm. We optimized enzyme and substrate concentrations to detect low inhibitor levels. We tested multiple known inhibitors of the enzyme: apigenin was unsuitable due to aggregation in the test solution, and copper ions were too weak to detect inhibition. On the other hand, tannic acid, a plant-derived polyphenol, proved to be a strong and reliable inhibitor for assay validation.

In conclusion, we successfully established both assays and generated inhibition curves for both enzymes (Figures 1 and 2). Optimized assays can now be used to evaluate the presence of inhibitors in algal samples.



**Figure 1:** Inhibition curve obtained by the optimized tyrosinase assay with kojic acid at an enzyme concentration of 60 U/ml. Data represent the mean  $\pm$  SD from three independent experiments.



**Figure 2:** Inhibition curve obtained by the hyaluronidase assay with tannic acid at an enzyme concentration of 12,2 U/ml. Data represent the mean  $\pm$  SD from two independent experiments.

## References:

1. Wang, H.-M. D.; Chen, C.-C.; Huynh, P.; Chang, J.-S. Exploring the Potential of Using Algae in Cosmetics. *Bioresour. Technol.* **2015**, *184*, 355–362.
2. An, B.-J.; Kwak, J.-H.; Park, J.-M.; Lee, J.-Y.; Park, T.-S.; Lee, J.-T.; Son, J.-H.; Jo, C.; Byun, M.-W. Inhibition of Enzyme Activities and the Antiwrinkle Effect of Polyphenol Isolated from the Persimmon Leaf (*Diospyros Kaki Folium*) on Human Skin. *Dermatol. Surg.* **2005**, *31* (7 Pt 2), 848–854; discussion 854.
3. *Enzymatic Assay of Hyaluronidase (3.2.1.35)*. <https://www.sigmaaldrich.com/SI/en/technical-documents/protocol/protein-biology/enzyme-activity-assays/enzymatic-assay-of-hyaluronidase?srsId=AfmBOorVSRsRKLbU-RujZYPwwPwnUcvUASU8EYYZOGoleJcuoERKkb7l> (accessed 2025-07-12).

# Investigating FHL2 and $\beta$ -catenin Interaction by Cross-Linking Mass Spectrometry

Tina Logonder<sup>1</sup>, Aljaž Gaber<sup>\*1</sup>

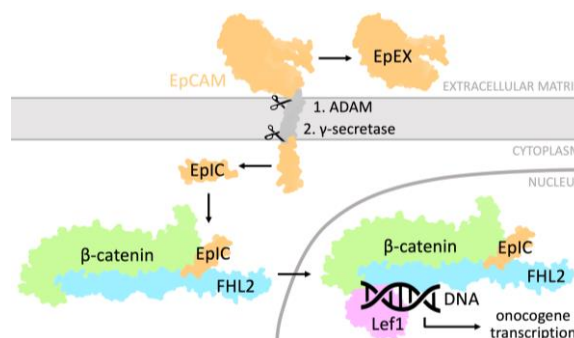
<sup>1</sup> Faculty of Chemistry and Chemical Technology, University of Ljubljana, Večna pot 113, SI-1000 Ljubljana, Slovenia

Epithelial Cell Adhesion Molecule (EpCAM) plays a crucial role in epithelial morphogenesis and carcinogenesis. It is one of the most utilized carcinoma biomarkers as its overexpression is linked to poor prognosis in various cancers. The intracellular domain of EpCAM (EpIC: aa 289–314) interacts with FHL2 and  $\beta$ -catenin, key proteins in the canonical *Wnt* signaling pathway. This complex induces the expression of oncogenes (Figure 1), making it a promising target for therapies<sup>1</sup>. Despite its functional relevance, structural information of the complex with FHL2,  $\beta$ -catenin and EpIC remains limited. We aim to elucidate the structures using an integrative structural biology approach by employing Cross-Linking Mass Spectrometry (XL-MS) with BS3 and Small-Angle X-ray Scattering (SAXS).

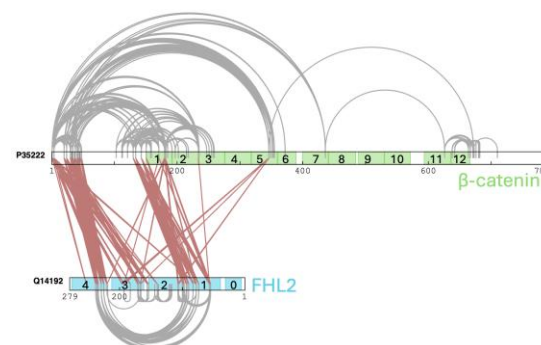
FHL2 (32.2 kDa) is composed of four and a half LIM domains, each containing 2 zinc fingers.  $\beta$ -catenin (85.4 kDa) consists of intrinsically disordered termini and the core region with 12 armadillo repeats (ARMs: aa 138–664). The interface between FHL2 and  $\beta$ -catenin has not been precisely defined. It was investigated by yeast two-hybrid assay and coimmunoprecipitation. Results from two separate studies only partly overlap. The first one showed that the N-terminus and ARM1 within  $\beta$ -catenin are crucial for binding. The second study determined that ARM1–9 is primarily involved, and ARM3–8 is essential for interaction. Both analyses concluded that deletions of any LIM domains within FHL2 significantly reduce affinity. An exception is the LIM0 domain, which is not essential, but still enhances the binding<sup>2,3</sup>.

According to our XL-MS analysis, the LIM0 domain is not included in binding, which is in agreement with previous studies. Results show FHL2 binding mostly to the N-terminus and ARM1 of  $\beta$ -catenin (Figure 2). A combination of XL-MS and SAXS data enabled us to structurally characterize FHL2, which will be important for the following steps when modeling the FHL2: $\beta$ -catenin complex. Stoichiometry (FHL2: $\beta$ -catenin = 2:1) introduces challenges as XL-MS cannot distinguish between the two molecules of FHL2.

Our work is a basis for structural characterization of EpIC binding to the FHL2: $\beta$ -catenin complex, which would provide insights into the mechanism underlying EpCAM's role in the carcinogenesis signaling pathway.



**Figure 1:** Schematic representation of intracellular signaling with EpIC



**Figure 2:** Cross-links between FHL2 and  $\beta$ -catenin detected by XL-MS analysis.

## References:

1. Maetzel D.; Denzel S.; Mack B.; Canis M.; Went P.; Benk M.; Kieu C.; Papior P.; Baeuerle P. A.; Munz M.; Gires O. Nuclear signalling by tumour-associated antigen EpCAM. *Nat. Cell Biol.* **2009**, *11*, 162–171.
2. Wei Y.; Renard C.-A.; Labalette C.; Wu Y.; Lévy L.; Neuveut C.; Prieur X.; Flajolet M.; Prigent S.; Buendia M.-A. Identification of the LIM Protein FHL2 as a Coactivator of  $\beta$ -Catenin\*. *J. Biol. Chem.* **2003**, *278*, 5188–5194.
3. Martin B.; Schneider R.; Janetzky S.; Waibler Z.; Pandur P.; Köhl M.; Behrens J.; von der Mark K.; Starzinski-Powitz A.; Wixler V. The LIM-only protein FHL2 interacts with beta-catenin and promotes differentiation of mouse myoblasts. *J. Cell Biol.* **2002**, *159*, 113–122.

**Funding information:** This work was supported by the Slovenian Research Agency, research program P1-0140 and research project Z1-2637.



# *Analysis of adhesive joint using beech wood*

Tjaša Likeb\*,<sup>1</sup> Martin Capuder,<sup>2</sup> Tina Skalar,<sup>1</sup> Andreja Pondelak,<sup>2</sup> Ermelinda Maçoas,<sup>3</sup> Amelia Almeida<sup>4</sup>

<sup>1</sup> Faculty of Chemistry and Chemical Technology, University of Ljubljana, Večna pot 113, SI-1000 Ljubljana, Slovenia ([tjasa.likeb@gmail.com](mailto:tjasa.likeb@gmail.com))

<sup>2</sup> Slovenian National Building and Civil Engineering Institute, Dimičeva ulica 12, 1000 Ljubljana, Slovenia

<sup>3</sup> CQE, Instituto Superior Técnico, Universidade de Lisboa, Av. Rovisco Pais 1, 1049-001 Lisbon, Portugal

<sup>4</sup> CeFEMA, Instituto Superior Técnico, Universidade de Lisboa, Av. Rovisco Pais 1, 1049-001 Lisbon Portugal

Wood is a porous, anisotropic material distinguished by a complex array of natural anatomical features. In softwoods, the main structural elements are longitudinal tracheids, while in hardwoods, they primarily consist of vessel elements and longitudinal fibers. The lumens of these cells are generally large enough to permit the infiltration of liquid adhesives, a process crucial for forming strong and durable bonds. Despite this, adhesive joints are often regarded as the weakest components in wooden assemblies, as they are essential for transferring loads across the bonding interface. This highlights the importance of thoroughly investigating adhesive performance and behavior in such systems.<sup>1</sup>

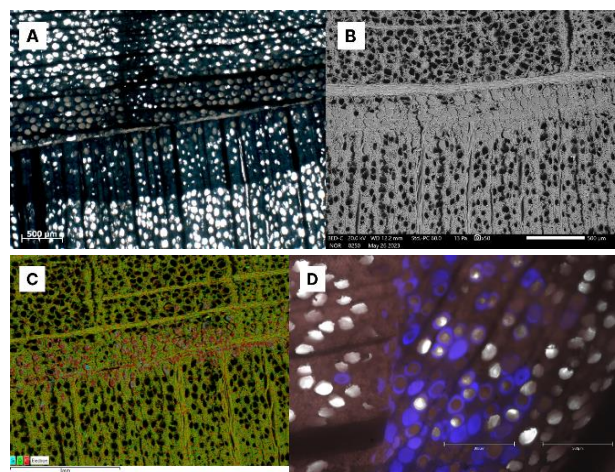
In this study, beech wood with two grain orientations (radial and tangential) was bonded using polyurethane adhesive (PUR). Specimens were prepared in accordance with the EN 302-1<sup>2</sup> standard and subjected to natural weathering for three months in Lisbon, Portugal.

The research aimed to evaluate both the depth and distribution of adhesive penetration in plates with different fiber and growth ring configurations. Additionally, the study examined the effects of aging by tracking mechanical, physical, and chemical changes in the bonded joints over time.

A comprehensive set of analytical techniques was employed, including tensile-shear testing, Scanning Electron Microscopy (SEM), Energy Dispersive Spectroscopy (EDS), X-ray Diffraction (XRD), epi-fluorescence microscopy, Fourier-transform infrared spectroscopy (FTIR,  $\mu$ FTIR), Raman microscopy, and micro-computed tomography ( $\mu$ CT). The precision and reliability of these methods in characterizing the bonded interfaces were also assessed.

The findings revealed that effective adhesive penetration is influenced by multiple factors, such as the

presence of growth rings, application time and pressure, and the intrinsic wood structure. Moreover, after three months of natural aging under the given conditions, no significant changes were observed in the physical, chemical, or mechanical properties of the joints. This suggests that extended aging studies are necessary to gain deeper insights into the long-term behavior of these bonded systems.



**Figure 1:** Optical microscopy (A), SEM (B), EDS (C), and epi-fluorescence (D) image of the PUR-RT sample after 120 minutes of pressing.

## References:

1. Kamke, F. A.; Lee, J. N. Adhesive penetration in wood – a review. *Wood and Fiber Science*, 2007, 39 (2), 205–220.
2. Karlsson, S.; Wong, M.: Experimental Evaluation of the Test Methods EN 302-1 and ASTM D905 for Wood-Adhesive Bonds.



# Where does Pb in the blood of children from the upper Meža Valley (Slovenia) come from?

Tjaša Žerdoner,<sup>1,2</sup> Darja Mazej,<sup>1</sup> Marta Jagodic Hudobivnik,<sup>1</sup> Janja Snoj Tratnik,<sup>1</sup> Neža Palir,<sup>1</sup> Ingrid Falnoga,<sup>1</sup> Milena Horvat,<sup>1,2</sup> Tea Zuliani\*,<sup>1,2</sup>

<sup>1</sup> Jožef Stefan Institute, Department of Environmental Sciences, Jamova cesta 39, SI-1000 Ljubljana, Slovenia

<sup>2</sup> Jožef Stefan International Postgraduate School, Jamova cesta 39, SI-1000 Ljubljana, Slovenia

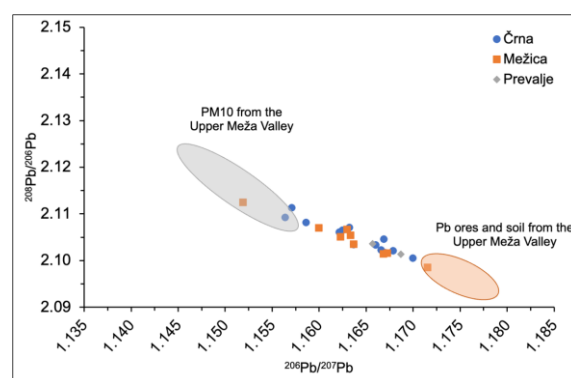
Lead (Pb) is a naturally occurring, non-essential, and toxic element. Contamination with it is both a persistent global environmental and public health issue. An area in Slovenia that has been significantly affected by Pb pollution is the upper Meža Valley. There lies the largest Pb and Zn ore deposit in Slovenia with a long history of mining and ore processing. During processing, a large amount of mine waste with high concentrations of Pb and other potentially toxic elements (PTEs) was produced and deposited in abandoned mine shafts and near small streams along the upper Meža Valley. As a result, the area was excessively polluted with Pb, Zn, and other PTEs<sup>1,2</sup>. In addition to mining, the industry for the production and recycling of Pb-batteries has been present since 1956.

As Pb is transmitted to the body through the inhalation and ingestion of contaminated dust particles, food, and water, surrounding inhabitants have had high levels of Pb in their blood. Especially at risk were young children, so the first testing for Pb concentrations in blood was carried out from 1974 to 1976, and the median Pb concentration in the blood of preschool children was over 400 µg/L<sup>3</sup>. In 1990, the concentrations decreased to (41–284) µg/L. In 2001–2002, more than one-third of tested children still had elevated blood Pb concentrations (> 100 µg/L), while in 2017, this was observed in one-fifth of three-year-olds.

Furthermore, monitoring of Pb concentrations in PM<sub>10</sub> in Žerjav, where a Pb smelter used to operate and is now a site for secondary Pb production, has been carried out since 1972. Even though Pb concentrations in PM<sub>10</sub> decreased dramatically from 1972 to 2007, annual average concentrations increased from 250 ng/m<sup>3</sup> to 700 ng/m<sup>3</sup> between 2010 and 2021. While previous studies have focused on the distribution and environmental burden of Pb in the upper Meža Valley, a detailed source apportionment of individual Pb contributions remains largely unexplored.

Therefore, this study aimed to i) develop a comprehensive database of Pb isotope ratios in environmental and anthropogenic samples from the upper Meža Valley, and ii) use Pb isotope ratios to identify the primary sources of Pb in children's blood.

Pb isotope analysis of samples from the upper Meža Valley revealed that local samples (e.g., soil, river sediment, ores, mine waste) have a distinct Pb isotope composition that differs from that of anthropogenic samples (e.g., Pb-battery components manufactured in the area). Similar to the Pb isotope composition of PM<sub>10</sub> samples, which showed a mix of local and anthropogenic sources, Pb isotope ratios in children's blood also showed mixed values (Figure 1), suggesting that inhalation of contaminated air is a significant exposure pathway alongside soil and dust ingestion.



**Figure 1:** Pb isotope ratios in the blood of children from the upper Meža Valley.

## References:

1. Gosar, M., Miler, M., Anthropogenic metal loads and their sources in stream sediments of the Meža River catchment area (NE Slovenia). *Appl. Geochem.* **2011**, 26 (11), 1855–1866.
2. Finzgar, N., Jez, E., Voglar, D., Lestan, D., Spatial distribution of metal, contamination before and after remediation in the Meža Valley, Slovenia. *Geoderma* **2014**, 217–218, 135–143.
3. Jez, E., Lestan, D., Prediction of blood lead levels in children before and after remediation of soil samples in the upper Meža Valley, Slovenia. *J. Hazard. Mater.* **2015**, 296, 138–146.

**Funding information:** This research was funded by ARIS Program (P1-0143), Young researcher program (PR-10487), HBM-National Human Biomonitoring, CRP project V1-1939, and DISCOVER project (J1-60008, PIN8195924) – with Austrian Science Fund (FWF).

# Cancer-Associated Fibroblast Overgrowth Disrupts Lung Cancer Spheroid Formation: Characterization by Flow Cytometry

Tonja Oman Sušnik,<sup>1,2</sup> Anamarija Habič,<sup>2,3</sup> Barbara Breznik\*,<sup>1,2</sup> Metka Novak,<sup>2</sup>

<sup>1</sup> Faculty of Chemistry and Chemical Technology, University of Ljubljana, Večna pot 113, SI-1000 Ljubljana, Slovenia

<sup>2</sup> National Institute of Biology, Večna pot 121, SI-1000 Ljubljana, Slovenia

<sup>3</sup> Jožef Stefan International Postgraduate School, Jamova cesta 39, SI-1000 Ljubljana, Slovenia

Non-small cell lung cancer (NSCLC) accounts for approximately 85 % of all lung cancer cases. It is characterized by high aggressiveness, late detection and difficult treatment, which often results in poor prognosis<sup>1</sup>.

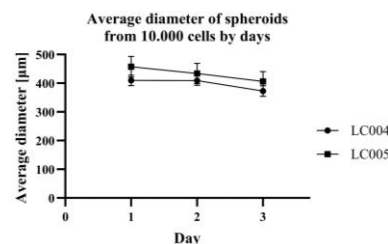
Our aim was to optimize the preparation of viable spheroids of repeatable sizes by centrifugation and to characterize cell cultures by analyzing the expression of cell markers.

Three-dimensional (3D) tumor models, such as spheroids, are important for NSCLC studies, since they better mimic tumor microenvironment in patients than adherent cell lines<sup>2</sup>. We established spheroids from different numbers of cells from cell cultures LC004 and LC005, obtained from tumor biopsies of patients with NSCLC. After optimizing the protocol, we established spheroids from 10,000 cells and then continued their cultivation in ClinoStar bioreactor. We monitored the growth of 12 spheroids from each culture using light microscopy and analyzed spheroid diameter and surface area during cultivation. The results showed that the overall growth of spheroids was negligible. We noticed reduction in spheroid size (scheme 1) and significant cell migration into the medium. Despite those results, spheroids were of repeatable sizes. After the cultivation in ClinoStar, we either observed a shrinkage of spheroids or fusion into irregular clumps.

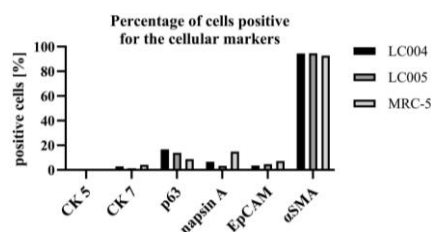
Afterwards we characterized both cell cultures and normal fibroblast cell line MRC-5 using flow cytometry. We analyzed the percentage of cells positive for tumor markers cytokeratin 5, cytokeratin 7, p63 and napsin A, the epithelial marker EpCAM, and the fibroblast marker  $\alpha$ SMA (scheme 2). The results showed that none of the cell cultures was significantly positive for tumor and epithelial markers, but both strongly expressed the  $\alpha$ SMA marker. These results also matched the MRC-5 cell line.

Based on flow results, we concluded that the cultures did not contain cancer cells, but rather cancer-associated fibroblasts (CAFs). This was also consistent with the results of spheroid formation. The shrinkage of spheroids and cell migration into the medium reflects the less pronounced proliferative nature and weaker intercellular contacts of CAFs on the account of dominant N-cadherin which improves invasive properties of CAFs<sup>3</sup>.

The outcome of the study highlights the problem of CAFs overgrowth and the importance of their exclusion from primary NSCLC cell cultures.



**Scheme 1:** Average diameter of LC004 and LC005 spheroids formed from 10,000 cells over a 3-day period.



**Scheme 2:** Percentage of cells positive for tumor markers cytokeratin 5 (CK5), cytokeratin 7 (CK7), p63, napsin A, the epithelial marker EpCAM, and the fibroblast marker  $\alpha$ SMA determined by flow cytometry.

## References:

- Miao, D.; Zhao, J.; Han, Y.; Zhou, J.; Li, X.; Zhang, T.; Li, W.; Xia, Y. Management of Locally Advanced Non-Small Cell Lung Cancer: State of the Art and Future Directions. *Cancer Commun.* **2024**, *44* (1), 23–46.
- Rozenberg, J. M.; Filkov, G. I.; Trofimenko, A. V.; Karpulevich, E. A.; Parshin, V. D.; Royuk, V. V.; Sekacheva, M. I.; Durymanov, M. O. Biomedical Applications of Non-Small Cell Lung Cancer Spheroids. *Front. Oncol.* **2021**, *11*, 791069.
- Mrozik, K. M.; Blaschuk, O. W.; Cheong, C. M.; Zannettino, A. C. W.; Vandyke, K. N-Cadherin in Cancer Metastasis, Its Emerging Role in Haematological Malignancies and Potential as a Therapeutic Target in Cancer. *BMC Cancer* **2018**, *18*, 939.

**Funding information:** ARIS program P1-0245, EU Horizon projects SPACETIME (101136552) and CutCancer (101079113).

# The effects of biodegradable and conventional microplastics on aquatic organisms

Urša Košak,<sup>1</sup> Barbara Klun,<sup>1</sup> Gabriela Kalčíkova<sup>1,2</sup>

<sup>1</sup> Faculty of Chemistry and Chemical Technology, University of Ljubljana, Večna pot 113, SI-1000 Ljubljana, Slovenia

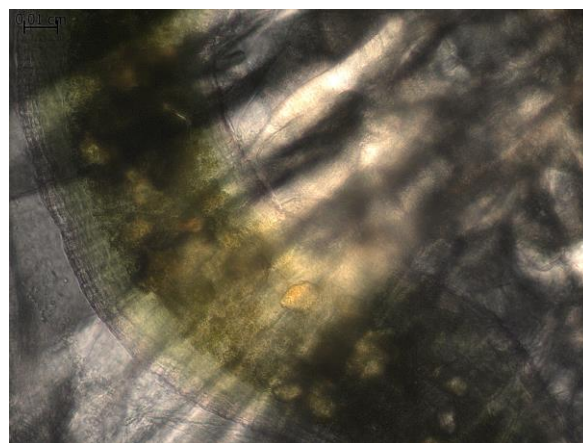
<sup>2</sup> Faculty of Mechanical Engineering, Brno University of Technology, Brno, Czech Republic

Microplastics are widespread pollutants that can negatively affect aquatic ecosystems by accumulating in the organisms, disrupting physiological functions and acting as carriers for toxic substances. While biodegradable plastics are often marketed as environmentally friendly alternatives, their degradation in aquatic environments is often incomplete and slow, allowing them to persist long enough to cause biological effects.

Our study examined the impact of three differently persistent types of microplastics polyethylene terephthalate (PET, non-biodegradable), polylactic acid (PLA, low biodegradable) and poly(3-hydroxybutyrate) (P3HB, fast biodegradable), on two freshwater organisms *Daphnia magna* and *Lemna minor*. To mimic environmentally more relevant ecosystem, both organisms were combined in one microcosm. Over a 21-day period, the organisms were exposed to a concentration of 10 mg/L of microplastics with particle size of less than 80µm for all three types. The most visible effects were found at the presence of P3HB, where the reproduction of *Daphnia magna* was noticeably increased and accelerated. P3HB also had statistically significantly more fronds, longer root length and lower chlorophyll *a* content in *Lemna minor* than control samples without microplastics after 21-day period. Analysis under scanning electron microscope (SEM) showed that P3HB particles were not present in the organisms. On the other hand, PLA and PET particles accumulated in *Daphnia magna*, but the effects on reproduction and mortality were less noticeable. Also, no significant trends were detected in *Lemna minor*, for these two plastics. Besides the effects on the organisms, basic water parameters such as pH,

oxygen and nutrients were also measured. These remained mostly stable across all groups, with only slight variations observed in the P3HB treatment.

The results indicate that the presence of microplastics can have effects on the aquatic ecosystems, even if they are biodegradable. Future studies should consider long term studies and critical evaluation of the biodegradable materials in aquatic environments.



**Figure 1:** *Daphnia magna* under the microscope (SEM) with PLA microplastics visible in the gut (100x).

## References:

1. Procházková, P.; Macová, S.; Aydın, S.; Zlamalová Gargošová, H.; Kalčíkova, G.; Kučerík, J. Effects of biodegradable P3HB on the specific growth rate, root length and chlorophyll content of duckweed, *Lemna minor*. *Heliyon* **2023**, 9, e23128

# Contaminants of Emerging Concern in the Ljubljana River Basin: A Study of the Presence of Pesticides

Veronika Plut,<sup>1,2</sup> Jan Hočevár,<sup>1,2</sup> Ester Heath,<sup>2,3,4</sup> Jurij Trontelj,<sup>5</sup> Vesna Mislej<sup>\*,2</sup>

<sup>1</sup> Faculty of Chemistry and Chemical Technology, University of Ljubljana, Večna pot 113, SI-1000 Ljubljana, Slovenia

<sup>2</sup> Slovenian Chemical Society, Section for the Environment, Hajdrihova 19, SI-1000 Ljubljana, Slovenia

<sup>3</sup> International Postgraduate School Jožef Stefan, Jamova cesta 39, SI-1000 Ljubljana, Slovenia

<sup>4</sup> Jožef Stefan institute, Jamova cesta 39, SI-1000 Ljubljana, Slovenia

<sup>5</sup> Faculty of Pharmacy, Aškerčeva cesta 7, SI-1000 Ljubljana, Slovenia

A key element of water management in Slovenia is the National River Basin Management Plan, which provides a systematic assessment of the status of water bodies. Accordingly, surface waters are evaluated in terms of their chemical and ecological status<sup>1</sup>.

In this study, we analysed publicly available surveillance monitoring data (2009–2023) on pesticides tested in the Ljubljana River, at sampling points downstream of treated municipal wastewater discharges within the Ljubljana catchment, but upstream of the confluence with the Sava River<sup>1</sup>. The dataset includes 1,994 chemical measurements of pesticides, which represent 63.8 % of all measurements carried out for 165 different groups of pollutants.

The number of pesticides tested in the given period was 75. They are grouped as follows: i) year of their measurement, ii) chemical properties and application, and iii) EU-authorised or banned<sup>1</sup>. Of these, 97.5 % of the detected pesticides were below the limit of quantification (LOQ). Parameters such as measured environmental concentration (MEC) as the highest maximum annual concentration (MAC, acute impact) and the highest annual average concentration (AA, chronic impact) in the period under consideration, predicted no-effect concentration (PNEC) and LOQ were compared<sup>2</sup>. Based on this analysis, a new proposed measuring strategy ( $PNEC \geq LOQ/2$ )<sup>2</sup>, and the scientific literature<sup>3</sup> we estimated the risk quotient ( $RQ = MEC/PNEC$ ) for tested pesticides with quantified results<sup>1</sup>. Our analysis showed (Table 1) that: i) Tebuconazole, azoxystrobin, and metalaxyl ( $RQ_{\text{chronic and acute}} < 0.01$ ) pose a negligible risk; ii) Flufenacet ( $0.01 < RQ_{\text{acute}} < 0.1$ ) and ammonium methyl phosphoric acid (AMPA) ( $0.01 < RQ_{\text{chronic}} < 0.1$ ) pose a low risk; and iii) Propiconazole ( $RQ_{\text{chronic and acute}} > 1$ ) and metazachlor ( $RQ_{\text{chronic}} > 1$ ) pose a high risk to the aquatic environment and human health. Given that the  $PNEC^3$  (acute for propiconazole; chronic for metazachlor) are less than  $LOQ/2$ , their official determination method should be improved with reducing the LLOQ (lower limit of quantification) by factor 1.2 for propiconazole and 1.8 for metazachlor<sup>1,2,3</sup>.

**Table 7:** Comparison of parameters MEC and LOQ with chronic (C) and acute (A) PNEC in 2009–2023 (Note: \*AA; \*\*MAC).

	MEC <sup>1</sup> μg L <sup>-1</sup>	PNEC <sup>3</sup> μg L <sup>-1</sup>	LOQ <sup>1</sup> μg L <sup>-1</sup>	PNEC <sup>3</sup> LOQ/2 <sup>2</sup>	RQ
Tebuconazole	0.010*	1.2 <sup>C</sup>	0.01	√	0.008 <sup>C</sup>
Azoxystrobin	<0.002*	0.676 <sup>C</sup>	0.01	√	0.0015 <sup>C</sup>
Propiconazole	0.046**	0.00085 <sup>A</sup>	0.002	X	54.1 <sup>A</sup>
AMPA	0.13*	3.0 <sup>C</sup>	0.1	√	0.043 <sup>C</sup>
Metalaxyl	<0.001*	6.25 <sup>C</sup>	0.01	√	0.0001 <sup>C</sup>
Metazachlor	0.011*	0.0022 <sup>C</sup>	0.008	X	5.0 <sup>C</sup>
Flufenacet	0.048**	4.0 <sup>A</sup>	0.01	√	0.012 <sup>A</sup>

The results contribute to a more comprehensive understanding of the chemical status of the Ljubljana River and support the development of more effective methods for monitoring and assessing water pollution.

## References:

1. Waters, Archive data - water quality, Ljubljana, Moste-Podgrad, <http://arso.si/vode/podatki/>, accessed: 2023–2025.
2. Loos, R. et al. *Review of the 1st Watch List under the Water Framework Directive and recommendations for the 2nd Watch List*. Publications Office of the European Union: Luxembourg, **2018**.
3. Fernandes Farah, I.; Carolina Rodrigues dos Santos, C.; Ferreira Pinto, M. C.; Righi Araújo, C.; Santos Amaral, M. C. Pesticides in aquatic environment: Occurrence, ecological implications and legal framework. *J. Environ. Chem. Eng.* **2024**, 12 (5), 114072.

**Funding information:** We would like to thank the Slovenian Chemical Society for making this research possible within the framework of the Section for the Environment. We would also like to thank the Ministry of Environment, Climate and Energy of the Republic of Slovenia for providing a complete database on the state of water in Slovenia.

# Pharmaceutical Contaminants in the Ljubljana River Basin: Insights from National Surveillance Monitoring

Jan Hočevar,<sup>1,2</sup> Veronika Plut,<sup>1,2</sup> Ester Heath,<sup>2,3,4</sup> Jurij Trontelj,<sup>5</sup> Vesna Mislej\*,<sup>2</sup>

<sup>1</sup> Faculty of Chemistry and Chemical Technology, University of Ljubljana, Večna pot 113, SI-1000 Ljubljana, Slovenia

<sup>2</sup> Slovenian Chemical Society, Section for the Environment, Hajdrihova 19, SI-1000 Ljubljana, Slovenia

<sup>3</sup> International Postgraduate School Jožef Stefan, Jamova cesta 39, SI-1000 Ljubljana, Slovenia

<sup>4</sup> Jožef Stefan institute, Jamova cesta 39, SI-1000 Ljubljana, Slovenia

<sup>5</sup> Faculty of Pharmacy, Aškerčeva cesta 7, SI-1000 Ljubljana, Slovenia

Pharmaceutical active compounds (PhACs) are among the major environmental pollutants in surface waters because they are designed to affect living things directly.

In this study, we analysed parameters tested in the Slovenian national surveillance monitoring used to detect new pollutants in surface waters. The study looked at publicly available data for the period between 2015 and 2023, focusing on sampling points downstream of treated municipal wastewater discharges (TMWD) in the Ljubljana catchment, before the confluence of the Ljubljana and Sava Rivers<sup>1</sup>. The dataset includes 148 chemical measurements of 58 substances, categorised by chemical properties and applications. The tested PhACs represented 35.2 % of all tested pollutants, while the proportion of their results was only 4.73 %, which indicates the technical complexity and cost of the measurement methods used<sup>1</sup>. The PhACs originating from various sources are collecting in TMWDs (Figure 1). In particular, we reviewed and compared parameters such as limit of quantification (LOQ), predicted no effect concentration (PNEC) and the risk quotient (RQ)<sup>1,2,3,4</sup>.

Determining the relevant PNEC for a specific PhAC is a complex protocol<sup>2</sup>. US regulatory guidance requires new PhACs to undergo standard acute toxicity tests (fish, *Daphnia magna*, and algae) if the predicted or measured environmental concentration (PEC, MEC) of the active ingredient is  $>1 \mu\text{g L}^{-1}$ .<sup>3</sup> In the EU, the PEC cut-off is  $0.01 \mu\text{g L}^{-1}$ , and if no obvious environmental concerns, no further testing is required<sup>3</sup>. Otherwise, the PNEC for the aquatic compartment is extrapolated by dividing the lowest Median Lethal Concentration or Median Effective Concentration (LC50, EC50) from standard tests by an assessment factor from 1 up to 1000 in the EU<sup>3</sup>. For the aquatic environment, toxicological data from the most sensitive species are used for PNEC-water calculation. If the PEC/PNEC is  $<1$ , no further assessment is necessary<sup>3</sup>. Higher PNECs are recommended for short-term exposures (days or weeks)<sup>2</sup>. In our analysis of the RQs, we focussed on 13 quantified PhACs. The RQs (based on the PNEC values from the Watch Lists and scientific

literature<sup>2,3,4</sup>) indicate that diclofenac, clarithromycin, azitromycin, venlafaxine, and O-desmethylvenlafaxine present a high risk to the aquatic environment.

The results provide a clearer understanding of the chemical status of the Ljubljana River, particularly since several PhACs covered here will be regularly analysed under the new EU Urban Wastewater Treatment Directive, requiring quaternary treatment with at least 80 % removal efficiency of the selected PhACs from wastewater.

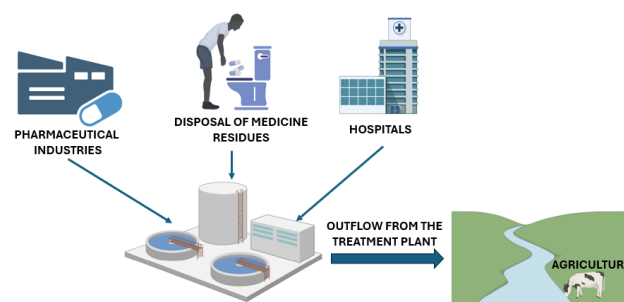


Figure 1: Sources of Pharmaceuticals in Waters.

## References:

1. Waters, Archive data - water quality, Ljubljana, Moste-Podgrad, <http://arso.si/vode/podatki/>, accessed: 2023–2025.
2. Aydin S.; Aydin M. E.; Kiliç H.; Tekinay A. Occurrence and Ecotoxicological Risk Assessment of Analgesics in Wastewater. *Environ. Ecol. Res.* **2018**, *6*, 413–422.
3. Sanderson H.; Johnson D. J.; Wilson C. J.; Brian R. A.; Solomon K. R. Probabilistic hazard assessment of environmentally occurring pharmaceuticals toxicity to fish, daphnids and algae by ECOSAR screening. *Toxicol. Lett.* **2003**, *144*, 383–395.
4. Loos, R. et al. *Review of the 1st Watch List under the Water Framework Directive and recommendations for the 2nd Watch List*. Publications Office of the European Union: Luxembourg, **2018**.

**Funding information:** We thank the Slovenian Chemical Society (Section for the Environment) and the Ministry of the Environment, Climate and Energy of Slovenia for supporting this research and providing full access to national water quality data.



# Valorization Pathways for Sodium Sulfate: Addressing One of the Abundant By-products in Battery Industry

Vinz Ymannuelle C. Tatad,<sup>1,2,3</sup> Cédric Tassel,<sup>1,2,3</sup> Jacob Olchowka\*,<sup>1,2,3</sup>

<sup>1</sup> University of Bordeaux, CNRS, Bordeaux INP, ICMCB, UMR 5026, F-33600 Pessac, France

<sup>2</sup> Réseau sur le Stockage Electrochimique de l'Energie (RS2E), CNRS FR 3459, Hub de l'Energie, Rue Baudelocque, 80039 Amiens Cedex, France

<sup>3</sup> ALISTORE-European Research Institute, CNRS FR 3104, Hub de l'Energie, Rue Baudelocque, 80039 Amiens Cedex, France

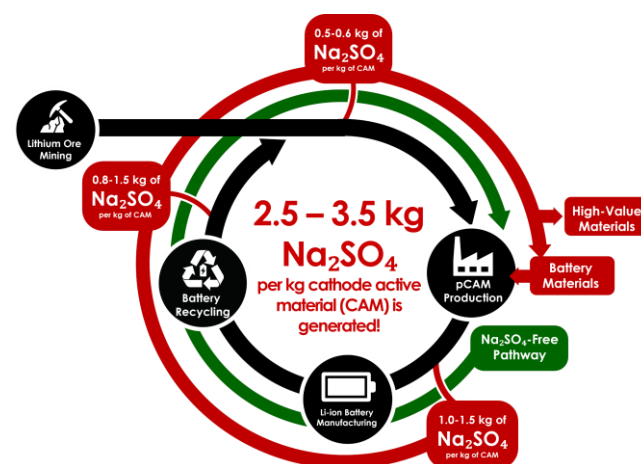
The rapid expansion of the lithium-ion battery (LIB) industry has resulted in a significant increase in sodium sulfate ( $\text{Na}_2\text{SO}_4$ ) production, making it one of the most abundant inorganic by-products across the entire battery value chain.  $\text{Na}_2\text{SO}_4$  waste production occurs at multiple stages of the LIB life cycle. The first major source is lithium refining, where hard-rock spodumene ores are processed into battery-grade  $\text{LiOH}$  or  $\text{Li}_2\text{CO}_3$ . The second is the production of precursor cathode-active materials (pCAM), such as  $\text{Ni}_{1-x-y}\text{Mn}_x\text{Co}_y(\text{OH})_2$  or  $\text{Ni}_{1-x-y}\text{Mn}_x\text{Co}_y\text{CO}_3$  for use in NMC-type batteries. A third significant source is LIB recycling, particularly during the hydrometallurgical process.

Over the full cycle of an NMC battery, approximately 2.5–3.5 kg of  $\text{Na}_2\text{SO}_4$  is generated per kilogram of NMC cathode material. Projections indicate that by 2030, the LIB sector alone could produce as much as  $8.8 \times 10^3$  metric tons of  $\text{Na}_2\text{SO}_4$  annually<sup>1</sup>. Managing this growing waste stream through conventional methods (discharge through rivers) will be both costly<sup>2</sup> and environmentally unsustainable, with potential threats to aquatic ecosystems and plant life<sup>3</sup>.

Currently, excess  $\text{Na}_2\text{SO}_4$  is mainly repurposed in traditional sectors such as detergents, glass, textiles, paper, and small industries like food additives. However, these markets are limited in growth and increasingly unable to absorb rising volumes.

To address this looming surplus, this paper identified and gave light to two main solutions for these issues (Figure 1). First, it explores upstream elimination strategies that target the prevention of  $\text{Na}_2\text{SO}_4$  formation at its source, such as redesigning existing production processes for lithium refining and pCAM synthesis to avoid sodium-based precipitation routes. Second, it presents downstream valorization approaches that recycle or convert  $\text{Na}_2\text{SO}_4$  into high-value products, with particular emphasis on closing the loop by reintegrating recovered  $\text{Na}_2\text{SO}_4$  into the battery production chain.

Together, these strategies aim to shift  $\text{Na}_2\text{SO}_4$  from a costly waste disposal problem to an opportunity for resource recovery and circular economy integration, creating both economic value and environmental benefits for the rapidly growing battery industry.



**Figure 1:** Schematic overview of  $\text{Na}_2\text{SO}_4$  generation across the LiB (NMC type) lifecycle and proposed solutions to address them.

## References:

- Hayagan, N.; Aymonier, C.; Croguennec, L.; Morcrette, M.; Dedryvère, R.; Olchowka, J.; Philippot, G. A Holistic Review on the Direct Recycling of Lithium-Ion Batteries from Electrolytes to Electrodes. *J. Mater. Chem. A* **2024**, 12, 46, 31685–31716.
- Performance Evaluation of Freeze Crystallization for Removal of Water and Sodium Sulphate from Mine Wastewater. In SETWM-20, ACBES-20 & EEHSS-20 Nov. 16-17, 2020 Johannesburg (SA); Eminent Association of Pioneers, **2020**.
- OECD SIDS, SIAR Sodium sulfate, SIAM 20, UNEP Publications, **2005**.

**Funding information:** The authors declare that no funding was received for this work.

# Design and Synthesis of Functionalized Carbazoles for Optoelectronic Applications

Vitan Šlamberger,<sup>1</sup> Griša Grigorij Prinčič,<sup>1</sup> Marko Jošt,<sup>2</sup> Jernej Iskra\*,<sup>1</sup>

<sup>1</sup> Faculty of Chemistry and Chemical Technology, University of Ljubljana, Večna pot 113, SI-1000 Ljubljana, Slovenia

<sup>2</sup> Faculty of Electrical Engineering, University of Ljubljana, Tržaška cesta 25, SI-1000 Ljubljana, Slovenia

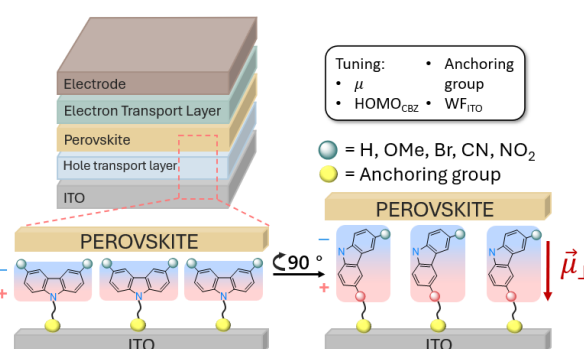
Carbazole-based molecules have emerged as versatile and high-performing materials for interface engineering in optoelectronic devices, particularly as hole-transporting self-assembled monolayers (SAMs) in p-i-n perovskite solar cells (PSCs) (Figure 1). The widespread use of these molecules can be attributed to the unique combination of favorable properties, including favorable optoelectronic characteristics, high thermal and morphological stability as well as synthetic tunability that allows precise modification of both electronic and structural features.<sup>1,2</sup>

The overall performance, efficiency, and long-term stability of PSCs are strongly influenced by the structural and electronic features of the SAM layer. Therefore, precise control over molecular orientation, electronic structure, and anchoring group design is essential for achieving efficient hole transport, maintaining indium tin oxide (ITO) integrity and stability while also ensuring optimal alignment between the SAM's highest occupied molecular orbital (HOMO) level and the electrode work function (WF).<sup>2,3</sup>

While many previous studies have focused on horizontal carbazole architectures,<sup>3</sup> less is known about the impact of orientation and dipole alignment at the molecular level. In this study, we explore structure–property relationships of vertically aligned carbazole SAMs. To support our molecular design strategy, we carried out calculations of HOMO energies and molecular dipole moments for a diverse series of functionalized carbazole derivatives.

We will present our strategy for rational molecular design via 90 ° carbazole orientation (Figure 1) and analyze how parameters such as HOMO, dipole and anchoring groups affect the properties of PSCs. Anchoring groups including phosphonic acid, boronic acid and carboxylic acid will be compared in terms of work function modulation, ITO compatibility, and long-term stability. This combined computational–

experimental approach enables the targeted optimization of carbazole-based interfacial layers for improved performance in PSCs, paving the way for more stable and efficient next-generation optoelectronic technologies.



**Figure 1:** Schematic representation of a p-i-n perovskite solar cell and SAM interface tuning. Carbazole molecules are flipped by 90 ° adopting a vertical orientation resulting in an increased dipole moment

## References:

1. Konidena, R. K.; Thomas, K. R. J.; Park, J. W. Recent Advances in the Design of Multi-Substituted Carbazoles for Optoelectronics: Synthesis and Structure-Property Outlook. *ChemPhotoChem* **2022**, 6 (10), 202200059.
2. Jiang, W.; Li, Y.; Gao, H.; Kong, L.; Wong, C.-T.; Yang, X.; Lin, F. R.; Jen, A. K.-Y. Regiospecific Halogenation Modulates Molecular Dipoles in Self-Assembled Monolayers for High-Performance Organic Solar Cells. *Angew. Chem., Int. Ed.* **2025**, 202502215.
3. Wang, S.; Guo, H.; Wu, Y. Advantages and Challenges of Self-Assembled Monolayer as a Hole-Selective Contact for Perovskite Solar Cells. *Materials Futures* **2023**, 2 (1), 012105.

# Understanding macronutrients through the three levels of chemical representation

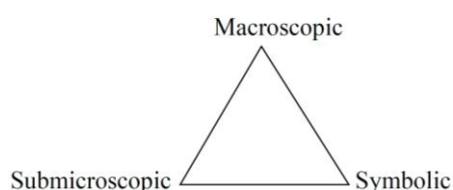
Zala Cvitanič,<sup>1</sup> Matjaž Dlouhy,<sup>2</sup> Miha Slapničar\*<sup>1,3</sup>

<sup>1</sup> University of Ljubljana, Faculty of Education, Kardeljeva ploščad 16, 1000 Ljubljana, Slovenia

<sup>2</sup> Ledina Upper Secondary School, Resljeva cesta 12, 1000 Ljubljana, Slovenia

<sup>3</sup> BEC Ljubljana, Cesta v Mestni log 47, 1000 Ljubljana, Slovenia

Learning chemical concepts is based on the observation of natural phenomena. For the correct construction of mental models of chemical concepts, it is essential that both teaching and learning involve the simultaneous integration of the three levels of representation (Figure 1).<sup>1</sup>



**Figure 1:** Johnstone's model, the triangle of the triple nature of the chemical concept<sup>1</sup>

It is known that students today tend to use learning strategies that allow them to make quick decisions with minimal cognitive effort. However, these strategies can oversimplify the learning process and lead to misconceptions or incomplete understanding of, for example, the relationship between the submicroscopic structure of a substance and its macroscopic properties. Research shows that students who have developed misconceptions often justify their reasoning with a superficial use of the macroscopic level or a misapplication of the submicroscopic level.<sup>2</sup> Motivation and interest also play an important role in memory performance and further knowledge acquisition. Some studies suggest that students with a higher level of intrinsic motivation and individual interest tend to perform better on knowledge tests.<sup>3</sup>

The aim of our study is to investigate the influence of individual interest and motivation for chemistry lessons in 9th grade primary school on students' understanding of the triple nature of macronutrients, including carbohydrates, fats and proteins.

The study is based on a causal non-experimental method in educational research using a mixed methods approach. The random sample consisted of 79 ninth grade students (31 girls and 48 boys;  $M = 1.39$ ,  $SD = .49$ ) aged

14 years ( $M = 14.63$ ,  $SD = .49$ ) from a primary school in Ljubljana in the school year 2023/2024.

Knowledge of the content of macronutrients and possible misconceptions were measured using a paper-and-pencil knowledge test. Students' individual interest in learning this content was assessed using a purposive questionnaire, while motivation was explored through structured interviews. We interviewed the top 10% of students (high achievement) and the bottom 10% (low achievement) based on their performance on the knowledge test.

The results show that half of the students (51%) achieved at least 50% of the total score in the knowledge test. A t-test revealed no statistically significant difference between the genders in the number of points achieved in the test ( $t(79) = -.87$ ,  $p > .05$ ). Almost half of the students (48%) had misconceptions in at least one question. The analysis of variance (ANOVA) showed no statistically significant effect of individual interest on the students' test results,  $F(2, 79) = .42$ ,  $p = .66$ ,  $\eta^2 = .01$ .

The surveys showed that students who scored well on the knowledge test generally had a stronger external orientation to learning chemistry. Regardless of their test scores, all students indicated that experiments were the most motivating aspect of chemistry instruction.

This suggests that there are misconceptions among students and that neither individual interest nor gender is related to test performance. Most students who achieved good test results were externally orientated.

## Reference:

1. Johnstone, A. H. Macro- and Micro-chemistry. *Sch. Sci. Rev.* **1982**, *64*, 377–379.
2. Graulich, N. Intuitive judgments govern students' answering patterns in multiple-choice exercises in organic chemistry. *J. Chem. Educ.* **2015**, *92*, 205–211.
3. Liu, Y.; Kim, E. Investigating Student Intrinsic Motivation Trends over One Semester in an Online General Chemistry II Course. *J. Chem. Educ.* **2024**, *101*, 2175–2187.

# Expression and purification of recombinant ORF1p from LINE1

Zala Kramar\*,<sup>1</sup> Vera Župunski,<sup>1</sup>

<sup>1</sup> Faculty of Chemistry and Chemical Technology, University of Ljubljana, Večna pot 113, SI-1000 Ljubljana, Slovenia

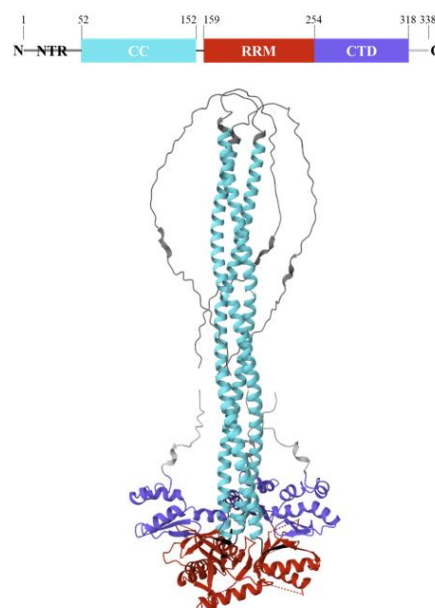
The ORF1 protein (ORF1p) is an essential component of the LINE-1 retrotransposon, acting as a high-affinity, non-sequence-specific RNA-binding protein with nucleic acid chaperone activity. It contains an intrinsically disordered N-terminal region (NTR), a coiled coil domain (CC) responsible for trimerization, a central RNA recognition motif (RRM), and a C-terminal domain (CTD), which together mediate nucleic acid binding<sup>1</sup>. Our aim was to express and purify recombinant ORF1p fused to a maltose-binding protein (MBP) tag to assess construct stability and obtain enough protein for further studies.

We constructed pMCSG7-MBP-ORF1p and pMCSG7-ORF1p-MBP vectors by PCR and *in vivo* assembly<sup>2</sup>. These constructs were expressed in *E. coli* BL21[DE3], and the resulting MBP-ORF1p and ORF1p-MBP fusion proteins were purified by immobilized metal ion affinity chromatography (IMAC), exploiting the His<sub>6</sub>-tag, or MBP affinity chromatography targeting MBP.

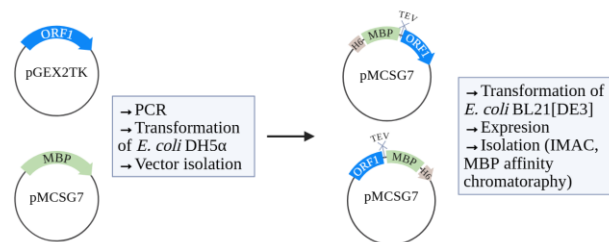
After induction, both constructs showed bands near the expected size (~83 kDa), but the C-terminal fusion (ORF1p-MBP) also displayed a lower band at ~66 kDa, suggesting possible proteolysis. We therefore focused on the MBP-ORF1p construct.

To evaluate purification efficiency, we compared isolation of MBP-ORF1p using HisTrap and MBPTrap columns. In both cases, a substantial amount of the target protein was recovered, although a significant portion remained unbound. The purity of elution fractions was similar for both methods, but neither achieved complete isolation, and several contaminating proteins were still present. A degradation product of approximately 40 kDa was detected in both cases, suggesting that partial proteolysis of MBP-ORF1p may occur during purification.

In conclusion, N-terminal fusion of ORF1p to MBP proved to be more effective for expression in *E. coli*, likely due to shielding of the disordered N-terminal region, which is prone to proteolytic degradation<sup>3</sup>. While both affinity purification approaches successfully isolated the target protein, the presence of contaminants and degradation products indicates that purification conditions require further optimization. This may include reducing purification time, adjusting buffer ionic strength, or adding specific protease inhibitors to enhance protein stability and purity<sup>4</sup>.



**Figure 1:** Structure of LINE1 ORF1p homotrimer (PDB ID: 6FIA, 2YKP; AlphaFold DB ID: AF-Q9UN81-F1).



**Figure 2:** Overview of the experiments.

## References:

1. Khazina, E.; Weichenrieder, O. Human LINE-1 Retrotransposition Requires a Metastable Coiled Coil and a Positively Charged N-Terminus in L1ORF1p. *eLife* **2018**, *7*, e34960
2. García-Nafria, J.; Watson, J. F.; Greger, I. H. IVA Cloning: A Single-Tube Universal Cloning System Exploiting Bacterial In Vivo Assembly. *Sci. Rep.* **2016**, *6* (1), 1–12.
3. Kalthoff, C. A Novel Strategy for the Purification of Recombinantly Expressed Unstructured Protein Domains. *J. Chromatogr. B: Anal. Technol. Biomed. Life Sci.* **2003**, *786* (1–2), 247–254.
4. Ryan, B. J.; Hennehan, G. T. Avoiding Proteolysis During Protein Purification. *Methods Mol. Biol.* **2017**, *1485*, 53–63

# Photoreaction of functionalized poly( $\beta$ -benzyl-L-aspartate) with tetrazole and maleimide groups

Zala Trbežnik,<sup>1</sup> Petra Utroša\*,<sup>2</sup> Jernej Iskra<sup>1</sup>

<sup>1</sup> Faculty of Chemistry and Chemical Technology, University of Ljubljana, Večna pot 113, SI-1000 Ljubljana, Slovenia

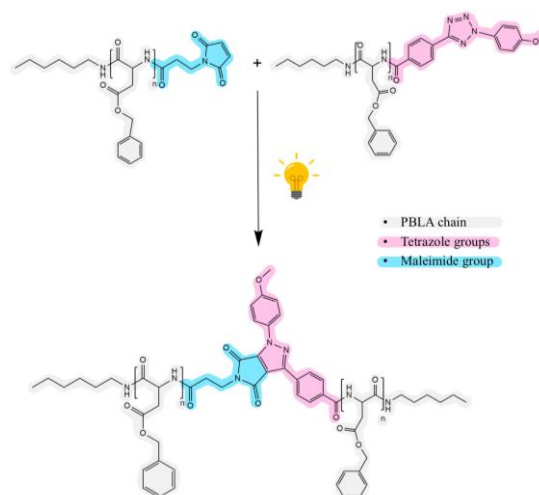
<sup>2</sup> Department of Polymer Chemistry and Technology, National Institute of Chemistry, Hajdrihova ulica 19, SI-1000 Ljubljana, Slovenia

Polypeptides are polymers with amide bonds (–CONH–) between  $\alpha$ -amino acid repeating units. Synthetic polypeptides can be efficiently, cost-effectively, and on a large scale prepared from *N*-carboxyanhydride monomers via ring-opening polymerization.<sup>1</sup> Various functional groups can be implemented into the polypeptide structure to allow further post-polymerization reactions. Especially interesting are photochemical reactions as we can control when and where new bonds are formed. In this work, we explore a light-induced nitrile imine mediated tetrazole-ene cycloaddition (NITEC). In this 1,3-dipolar cycloaddition, photoexcited tetrazoles release nitrogen to generate reactive nitrile imines in situ, which then react with various alkenes or alkynes to form pyrazoline-based covalent bonds.<sup>2</sup> The goal of our work was to functionalize polypeptide chains with a tetrazole and a maleimide group, and demonstrate linking of the two polypeptides together via NITEC reaction.

To obtain a polymer with functional groups suitable for NITEC, we first transformed our starting material,  $\beta$ -benzyl-L-aspartate, into  $\beta$ -benzyl-L-aspartate *N*-carboxyanhydridemonomer. The <sup>1</sup>H nuclear magnetic resonance (NMR) spectroscopic data of the synthesized *N*-carboxyanhydride are in agreement with the reported literature data. We polymerized the *N*-carboxyanhydride into poly( $\beta$ -benzyl-L-aspartate) and confirmed the identity of the product with <sup>1</sup>H NMR spectroscopy and matrix-assisted laser desorption/ionization time-of-flight mass spectrometry (MALDI-TOF MS). The next step was to functionalize the amino end-groups of the synthesized polypeptide with a maleimide group, for which we used *N*-succinimidyl 3-maleimidopropionate. Similarly, we functionalized the amino end-groups with a tetrazole group using (2-(4-methoxyphenyl)-2H-tetrazol-5-yl)benzoic acid. We confirmed the proposed structures with <sup>1</sup>H NMR spectroscopy and MALDI-TOF mass spectrometry. The NITEC photoreaction between polypeptide-maleimide and polypeptide-tetrazole was conducted by exposing the reaction mixture to UV irradiation. After 11 min of irradiation, we observed fluorescence of the reaction mixture, which indicates the formation of photoproducts. However, <sup>1</sup>H NMR spectroscopy did not show new signals that would

correspond to the expected pyrazoline product. Presumably, NITEC photoreaction took place and pyrazoline initially formed but then rearomatized into pyrazole.<sup>2</sup> This explains observed fluorescence, but the NMR spectra had no signals for pyrazole; since the pyrazole structure contains double bonds in positions without hydrogen atoms, there are no corresponding protons for NMR detection.

Our work demonstrates successful poly( $\beta$ -benzyl-L-aspartate) functionalization with tetrazole and maleimide groups, and shows promising results for NITEC photoreaction between the functionalized polypeptide chains.



**Scheme 1:** Linking of two polypeptide chains via NITEC reaction between poly( $\beta$ -benzyl-L-aspartate) functionalized with tetrazole and maleimide groups

## References:

1. Mazo, A. R.; Allison-Logan, S.; Karimi, F.; Chan, N. J.-A.; Qiu, W.; Duan, W.; O'Brien-Simpson, N. M.; Qiao, G. G. Ring Opening Polymerization of  $\alpha$ -Amino Acids: Advances in Synthesis, Architecture and Applications of Polypeptides and Their Hybrids. *Chem. Soc. Rev.* **2020**, 49 (14), 4737–4834.
2. Kamm, P. W.; Blinco, J. P.; Unterreiner, A.-N.; Barner-Kowollik, C. Green-Light Induced Cycloadditions. *Chem. Commun.* **2021**, 57 (33), 3991–3994.



# Coordination of deprotonated furosemide to zinc(II) ion

Zarja Uranjek,<sup>1</sup> Barbara Modec,<sup>1</sup> Nina Podjed Rihtaršič\*,<sup>1</sup>

<sup>1</sup> Faculty of Chemistry and Chemical Technology, University of Ljubljana, Večna pot 113, SI-1000 Ljubljana, Slovenia

Furosemide (IUPAC name: 4-chloro-2-(furan-2-ylmethylamino)-5-sulfamoylbenzoic acid) is a loop diuretic used to treat hypertension and edema, caused by cardiac, renal and hepatic failure. It is a weak acid with a  $pK_a$  value of 3.8<sup>1</sup>. In addition to the carboxyl group, furosemide molecule contains a chlorine-substituted phenyl ring, a furan ring, a sulphonamide group and an amine group (Figure 1). These functional groups enable the coordination of furosemide to metal centers. Surprisingly, only two crystal structures have been reported in the Cambridge Structural Database<sup>2</sup> featuring coordination compounds with furosemide anion. The latter is coordinated either in a monodentate or bidentate chelating manner *via* carboxylate oxygens.

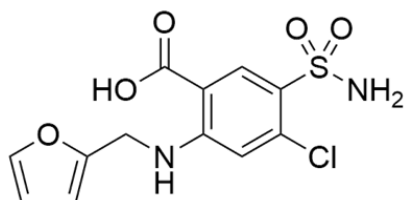


Figure 3: Structural formula of furosemide.

Zinc(II), a biologically important Lewis acid, remains relatively unexplored with this pharmaceutically active ligand. Therefore, this study investigates zinc(II) coordination chemistry with deprotonated furosemide.

The reaction systems consisted of zinc(II) oxide or chloride, furosemide and aqueous ammonia solution. Coordination complex  $[Zn(fur)_2(NH_3)_2]$  (Figure 2), where  $fur^-$  represents the deprotonated furosemide, was obtained as the main product at ambient conditions. Unfortunately, some reactions produced mixtures with ammonium salt,  $NH_4fur$ . The salt formation proved to be suboptimal as it consumed a significant amount of the ligand that could otherwise participate in the coordination with the zinc(II) ion<sup>3</sup>. Solvothermal reactions in acetonitrile or mixtures of acetonitrile and methanol yielded an unidentified microcrystalline solid. Compounds were characterized by infrared (IR) and nuclear magnetic resonance (NMR) spectroscopies, elemental analysis (CHN), thermogravimetric analysis (TGA) and single crystal X-

ray diffraction analysis. The results will be presented to shed light on the possible composition of the unidentified compound.

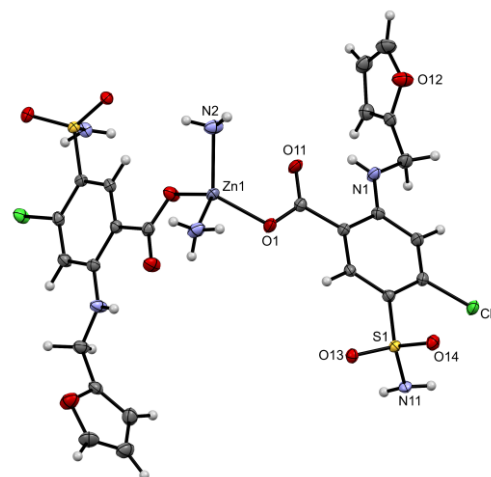


Figure 4: ORTEP drawing of  $[Zn(fur)_2(NH_3)_2]$

## References:

1. Granero, G. E.; Longhi, M. R.; Mora, M. J.; Junginger, H. E.; Midha, K. K.; Shah, V. P.; Stavchansky, S.; Dressman, J. B.; Barends, D. M. Biowaiver monographs for immediate release solid oral dosage forms: furosemide. *J. Pharm. Sci.* **2010**, *99*, 2544–2556.
2. Groom, C. R.; Bruno, I. J.; Lightfoot, M. P.; Ward, S. C. The Cambridge Structural Database. *Acta Crystallogr., Sect. B* **2016**, *72*, 171–179.
3. Podjed, N.; Uranjek, Z.; Cerc Korošec, R.; Hrast Rambaher, M.; Golob, M.; Modec, B. On zinc(II) coordination chemistry with furosemide: a journey from a mononuclear complex to a coordination polymer. *New J. Chem.* **2025**, *49*, 9113–9122.

**Funding information:** This research was funded by the Slovenian Research and Innovation Agency (Research Core Funding Grant P1-0134). The authors acknowledge the support of the Centre for Research Infrastructure at the University of Ljubljana, Faculty of Chemistry and Chemical Technology, which is a part of the Network of Research and Infrastructural Centres UL (MRIC UL) and is financially supported by the Slovenian Research and Innovation Agency (Infrastructure Program No. I0-0022).

# Immobilization of glucose oxidase into cross-linked enzyme aggregates using microfluidic system

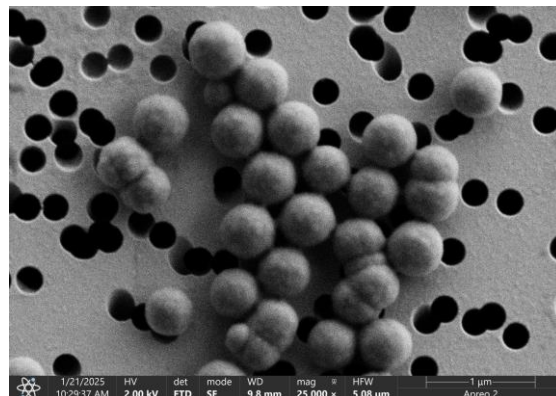
Žiga Gerdina\*,<sup>1</sup> Borut Šketa,<sup>1</sup> Polona Žnidaršič Plazl,<sup>1</sup>

<sup>1</sup> Faculty of Chemistry and Chemical Technology, University of Ljubljana, Večna pot 113, SI-1000 Ljubljana, Slovenia

Biocatalysis offers a sustainable and efficient alternative to conventional chemical synthesis, enabling reactions with high selectivity and yield under mild, environmentally friendly conditions<sup>1</sup>. However, the industrial application of enzymes is often limited by their poor operational stability, sensitivity to process conditions, and high cost<sup>2</sup>. Immobilization techniques, such as the formation of cross-linked enzyme aggregates (CLEAs), have been developed to overcome these limitations by improving enzyme robustness, simplifying product separation, and allowing enzyme reuse<sup>3</sup>. When combined with microfluidic systems, CLEA synthesis benefits from precise control over reaction parameters, rapid mixing, and scalability for continuous-flow operation<sup>4</sup>.

In this study, a microfluidics-based generation of CLEAs from glucose oxidase (GOx)—a model enzyme with broad applicability in biosensors, antimicrobial systems, and biofuel cells<sup>5</sup>—was optimized. Using the Box–Behnken experimental design, the influence of enzyme, precipitant, and cross-linker concentrations on the properties of the resulting particles was systematically investigated. At the optimized conditions, monodisperse CLEA-GOx particles with an average hydrodynamic radius of  $113 \pm 1.37$  nm were produced and an immobilization yield of 100% was reached. The recovered enzyme activity reached up to  $91.39 \pm 1.68\%$ , supporting the viability of this approach for enzyme immobilization.

Figure 1 shows a representative microscopic image of the CLEA-GOx particles, confirming the uniformity achieved under optimized synthesis conditions. These results highlight the potential of microfluidics-based CLEA generation for producing highly active and stable biocatalysts with consistent characteristics. The combination of high immobilization efficiency, excellent retained activity, and reproducibility demonstrates the suitability of this approach for scalable enzyme immobilization, particularly in continuous bioprocessing and flow chemistry applications where catalyst stability and reusability are essential. These findings support the broader application of microfluidic CLEA synthesis in industrial biocatalysis, where consistent performance, scalability, and sustainability are increasingly required.



**Figure 5:** CLEA particles synthesized under optimal conditions; observed by SEM at 25000× magnification.

## References:

1. Bai, J.; Huang, C.; Liu, Y.; Zheng, X.; Liu, J.; Zhou, L.; Liu, J.; Jiang, Y. Integrating Biocatalysis with Continuous Flow: Current Status, Challenges, and Future Perspectives. *J. Adv. Res.* **2025**.
2. Žnidaršič-Plazl, P. Biocatalytic Process Intensification via Efficient Biocatalyst Immobilization, Miniaturization, and Process Integration. *Curr. Opin. Green Sustain. Chem.* **2021**, 32 (100546), 100546.
3. Sheldon, R. A.; van Pelt, S. Enzyme Immobilisation in Biocatalysis: Why, What and How. *Chem. Soc. Rev.* **2013**, 42 (15), 6223–6235.
4. Menegatti, T.; Lavrič, Ž.; Žnidaršič-Plazl, P. Microfluidics-Based Preparation of Cross-Linked Enzyme Aggregates. WO2023175002A1. **2023**.
5. Wong, C. M.; Wong, K. H.; Chen, X. D. Glucose Oxidase: Natural Occurrence, Function, Properties and Industrial Applications. *Appl. Microbiol. Biotechnol.* **2008**, 78 (6), 927–938.

**Funding information:** The financial support from the Slovenian Research and Innovation Agency - ARIS (Grants P2-0191, J4-4562, and MR-56884) and Interreg GreenChemForCE project (Grant CE0200857) is acknowledged. The authors would like to thank U. Rozman for FE-SEM characterization of the particles and M. Božinović for assistance with statistical data analysis. The support of the Centre for Research Infrastructure at the UL FCCT, financially supported by ARIS (Infrastructure programme No. 10-0022), is also acknowledged.

# *N*-Substituted 2-phenylimidazoles as substrates in the catalytic C–H bond functionalization

Žiga Močnik,<sup>1</sup> Uroš Grošelj,<sup>1</sup> Jurij Svete,<sup>1</sup> Bogdan Štefane,<sup>1</sup> Franc Požgan\*<sup>1</sup>

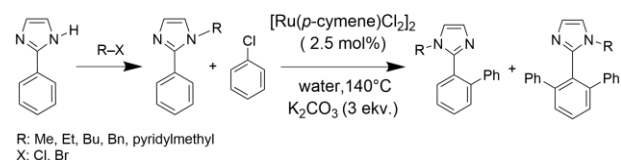
<sup>1</sup> Faculty of Chemistry and Chemical Technology, University of Ljubljana, Večna pot 113, 1000 Ljubljana, Slovenia

Catalytic C–H activation has emerged as a groundbreaking strategy for the formation of new carbon-carbon (C–C) bonds, particularly in the synthesis of biaryls, which are crucial building blocks in pharmaceuticals, agrochemicals, and materials science. This approach offers significant advantages over classical cross-coupling reactions, such as enhanced atom and step economy, and reduced waste generation. While palladium catalysts have traditionally been at the forefront of C–H activation, cheaper and air-stable ruthenium catalysts have become an attractive alternative, enabling access to otherwise challenging reaction pathways. However, the widespread application of C–H arylation still faces challenges, including issues with regioselectivity, the frequent requirement for specific directing groups, and often elevated reaction temperatures that are unsuitable for thermally labile substrates.<sup>1,2,3</sup>

The aim of our research was to investigate the influence of various *N*-substituents of 2-phenylimidazole on the outcome of catalytic *ortho* C–H arylation. We synthesized a series of *N*-functionalized 2-phenyl-1*H*-imidazoles (including *N*-methyl, *N*-ethyl, *N*-butyl, *N*-benzyl, and *N*-pyridylmethyl derivatives) starting from commercially available 2-phenylimidazole and appropriate organic halides, following established literature procedures. These products were then subjected to a C–H arylation reaction with chlorobenzene, catalyzed by [Ru(*p*-cymene)Cl<sub>2</sub>]<sub>2</sub>.

Through systematic optimization of the reaction conditions, we discovered that water serves as the optimal solvent, leading to high yields and selectivity. Unexpectedly, the addition of common ligands such as KOPiv and PPh<sub>3</sub> was found to be unnecessary, and in some cases, even inhibited the reaction, which deviates from general observations in the chemical literature. Crucially, the nature of the *N*-substituent on the imidazole ring profoundly influences the ratio between mono- and diarylated products. Specifically, while methyl and ethyl derivatives yielded a mixture of mono- and diarylated

products (with mono:di ratios ranging from approximately 2:1 to 3.7:1), the benzyl group predominantly directed the reaction towards the formation of the monosubstituted product. Furthermore, for the substrate bearing a (2-pyridyl)methyl group, we observed an intriguing additional C–H activation on the imidazole ring itself, however most of products formed in trace amounts. All resulting products were comprehensively characterized using <sup>1</sup>H NMR, <sup>13</sup>C NMR, IR spectroscopy, and high-resolution mass spectrometry (HRMS).



**Scheme 1:** Two-step reaction scheme

**Table 8:** Ratios of mono- and diaryl products

R	Mono:Di
Me	2:1
Et	3.7:1
Bu	2.8:1
Bn	Mono
pyridylmethyl	/

## References:

- Li, B.; Darcel, C.; Dixneuf, P. H. Ruthenium(II)-catalysed Functionalisation of C-H Bonds via a Six-membered Cyclometallate: Monoarylation of Aryl 2-pyridyl Ketones. *ChemCatChem* **2014**, *6*, 127–130.
- Nareddy, P.; Jordan, F.; Szostak, M. Recent Developments in Ruthenium-Catalyzed C–H Arylation: Array of Mechanistic Manifolds. *ACS Catal.* **2017**, *7*, 5721–5745.
- Yadav, P.; Velmurugan, N.; Luscombe, C. Recent Advances in Room-Temperature Direct C–H Arylation Methodologies. *Synthesis* **2023**, *55*, 1–26.



# **ABSTRACTS**

YOUNG MINDS<sup>2</sup>

# NAC supplement development for the reduction of the health gap

## Product development and business plan

Aljaž Kostevc Redek\*,<sup>1</sup> Danial Doustmohammadi,<sup>1</sup> Diana Doustmohammadi,<sup>1</sup> Mihajlo Krstić,<sup>1</sup> Andraž Velušček,<sup>1</sup> Mentor: Alenka Mozer\*<sup>1</sup>

<sup>1</sup> Gimnazija Vič, Tržaška cesta 72, 1000 Ljubljana, Slovenia

In Slovenia, only half of the low-income population is in good health, compared to only a quarter in Lithuania. 70–80% of people with high incomes report good health. Significant health gap can also be observed between different levels of education. To help reduce the health gap of the disadvantaged population, we (1) developed a product mix to address common health issues and boost the immune system, and (2) prepared a business idea, targeting those people (OECD, 2025 and Eurostat, 2025).

Primary goal was to **develop a scientifically backed, price-competitive, synergetic antioxidative mix**—a product designed for daily use that boosts the immune system and neutralizes free radicals through a carefully selected combination of antioxidants. Secondly, we have created a **synergetic mucolytic mix** that focuses on thinning mucus and supporting respiratory health, making breathing easier during respiratory discomfort. Lastly, we have established a **comprehensive customer support system**, including a website, chatbot, and live support, to provide scientifically grounded information and promote transparent communication about the products' effects and potential side effects in a user-friendly manner. Last, we prepared a comprehensive business plan, studying the customer needs, market analysis, and preparing a production and financial plan for a start-up company.


**Methodology.** We reviewed scientific literature on NAC and other ingredients, analyzed health and market data, and interviewed experts and potential customers. We developed evidence-based formulations, designed recyclable packaging, and built an online platform with an e-shop, an AI chatbot, and clear guides.

**Results:** We developed two scientifically backed products, addressing main health issues of our target population, relying on scientific literature and qualitative analysis among experts and potential customers (Table 1).

We also prepared a **business plan**. The health supplement market is growing, driven by greater health awareness, rising purchasing power, and an aging population (Statista, 2025). The EU and US have a combined potential €2.8 billion; our estimated achievable share is €2.8 million. We focus on individuals with average or lower incomes, including retirees, with, on average, poorer health. Key consumer preferences include affordability, availability, clear and easy-to-

follow instructions, and diverse sales and marketing channels that address the price-sensitive market. The business model targets value-driven consumers through retail partnerships with discount stores, online sales via our own website featuring AI chatbot support, and strategic collaborations with local pharmacies and health centers. Competitive pricing significantly differentiates us. Our sales strategy initially targets Slovenia and the EU. **We expect to reach target market in 3 years.**

**Table 1:** Developed products and supportive services

Product	
RespiraNAC	NAC Protect
400 mg N-acetilcistein (NAC)*, Vitamin B3, Vitamin A, Vitamin B7	200 mg N-acetilcistein (NAC)*, Koencim Q10, Vitamin C, Vitamin E, Vitamin B2, Selenomotionin
Support for coughing up thick mucus. Contributes to easier breathing	Strengthens the natural immune response. Works in both water and fatty environments. Restores levels of the body's antioxidant - glutathione
Supportive services	
 <a href="https://wellforall.netlify.app">https://wellforall.netlify.app</a> <b>Web page With Customer support</b> (AI chatbot and expert support) and <b>Web-shop</b>	

\*serving size is 2 capsules

### References:

1. Eurostat Database, European Commission; <https://ec.europa.eu/eurostat/web/digital-economy-and-society/data/comprehensive-database> (accessed July 11, 2025).
2. OECD, OECD Data Explorer; [https://www.oecd-ilibrary.org/economics/data/oecd-stat/data-warehouse\\_data-00900-en](https://www.oecd-ilibrary.org/economics/data/oecd-stat/data-warehouse_data-00900-en) (accessed July 11, 2025).
3. Statista, Dietary Supplements and Functional Foods Worldwide; <https://www.statista.com/study/102831/dietary-supplements-and-functional-foods-worldwide/> (accessed July 11, 2025).

**Acknowledgements:** We are grateful for help to prof. dr. Marko Anderluh from the UL Faculty of Pharmacy and prof. dr. Tjaša Redek, UL School of Economics and Business.



# Microplastics found in food from cutting boards

Brina Zver\*,<sup>1</sup> Klara Grantaša\*,<sup>1</sup> Mentors: dr. Marija Meznarič,<sup>1</sup> dr. Manca Kivač Viršek,<sup>2</sup>

<sup>1</sup> Gimnazija Franca Miklošiča Ljutomer, Prešernova ulica 34, 9240 Ljutomer

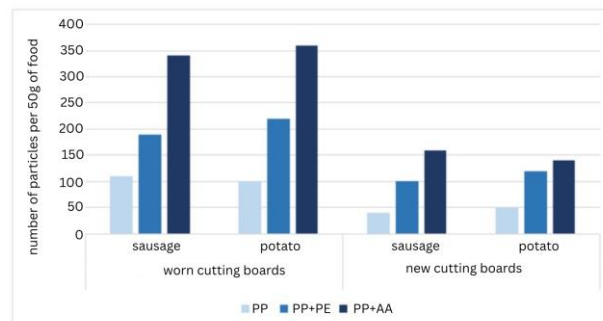
<sup>2</sup> National Institute of Biology, Marine Biology Station Piran, Fornače 41, 6330 Piran

Microplastics are all plastic particles smaller than 5 mm. Based on their shape, they are divided into six basic groups: fragments, films, pellets, granules, filaments and foams. The most common sources of it are plastic containers, cutlery, straws, tea bags, plastic food packaging and canned coatings. Traces of microplastics are also obtained to our food through plastic cutting boards. According to a study by the Chemical Association, an individual is on average exposed to up to 79.4 million microplastic particles per year.

Microplastic particles can be introduced into our body in different ways: oral (most commonly), respiratory and topical. On average (oral and respiratory intake) an individual ingests between 74,000 and 121,000 microplastic particles annually. It is present in water, milk, tea bags and seafood due to plastic pollution of the ocean. They bring physical (e.g. damage to the body when plastic particles rub against the tissue), chemically (e.g. consequences of chemicals contained in plastics) and biologically (e.g. transmission of pathogens) dangers to our body.

We found differences in the excretion of the amount and size of microplastic particles according to the wear and chemical composition of the plastic cutting boards. We compared polypropylene, a mixture of polypropylene and polyethylene, and a mixture of polypropylene and acrylic acid. On the cutting boards of the mentioned materials, example of soft (sausage) and hard (potato) food was cut into smaller pieces. We then counted the number of microplastic particles found and observed the sliced pieces of food under a stereo microscope. We then boiled the water with which we rinsed the studied boards and observed the behavior of microplastic particles during heat treatment. We planned a control experiment on a ceramic board to demonstrate microplastics that were absent there and starch with methylene blue in potato samples.

We found microplastics in the study, mostly from worn plastic boards. The quantity and shape were also affected by the material of the cutting board, but not by the food that was cut on it. The microplastic particles were small enough to be absorbed into the human body and cause potential problems.



**Figure1:** Average number of microplastic particles created depending on food hardness and cutting board wear

**Table 9:** Minimum, maximum and average size of formed particles of microplastics and their standard deviation

	PP+AA		PP+PE		PP N	PP W
	N	W	N	W		
Min. size	67,2	70,9	66,2	74,4	47,4	95,1
Max. size	1766,4	1636,4	1119,9	2166,7	728,6	3050,8
Average size	567,1	582,3	515,5	531,3	288,2	774,4
Standard deviation	532,2	434,6	268,0	488,6	200,4	682,4

## References:

- Koren, A. (2024). Mikroplastika v kuhinji: Top 5 predmetov, ki se jim morate izogibati. [https://senior24.si/mikroplastika-v-kuhinji-top-5-predmetov-ki-se-jim-morate-izogibati/#google\\_vignette](https://senior24.si/mikroplastika-v-kuhinji-top-5-predmetov-ki-se-jim-morate-izogibati/#google_vignette) (accessed 2024-12-04)
- Song, M.; Li, Y.; Tao, L.; Wang, Q.; Wang, F.; Li, G. Potential Health Impact of Microplastics: A Review of Environmental Distribution, Human Exposure, and Toxic Effects. *Environ. Health*, **2023**, *1*, 249–257
- Božič, T. Vpliv mikro- in nanoplastike iz kopenskih ekosistemov na varnost hrane in zdravje ljudi. M. S. Thesis, Univerza v Mariboru, Fakulteta za zdravstvene vede, 2024.

**Funding information:** dr. Manca Kovač Viršek, univ. dipl. biol. from Institute for Water of the Republic of Slovenia, dr. Marija Meznarič, prof. bio. and chem. from Gimnazija Franca Miklošiča Ljutomer

# Galvanic Coupling of Aluminium Alloy and Copper for Electric Vehicle Applications

Peter Rodič\*,<sup>1</sup> Eva-Arolea Trdan,<sup>2</sup> Andraž Logar,<sup>3</sup> Ingrid Milošev,<sup>1</sup> Damjan Klobčar,<sup>3</sup>

<sup>1</sup> Jožef Stefan Institute, Department of Physical and Organic Chemistry, Jamova c. 39, SI-1000 Ljubljana, Slovenia

<sup>2</sup> Gimnazija Ledina, Resljeva c. 12, SI-1000 Ljubljana, Slovenia

<sup>3</sup> University of Ljubljana, Faculty of Mechanical Engineering, Laboratory for Welding, Aškerčeva cesta 6, SI-1000 Ljubljana, Slovenia

The increasing integration of aluminium and copper components in electric vehicles (EVs) and battery systems presents significant corrosion challenges arising from galvanic coupling effects.<sup>1</sup> When two dissimilar metals are in direct electrical contact within a conductive electrolyte, the less noble metal (aluminium) acts as the anode and corrodes preferentially, whereas the more noble metal (copper) functions as the cathode and remains largely unaffected.<sup>2</sup> Such interactions are of particular concern in EV battery modules, busbars, cooling systems, and structural assemblies, where weight reduction, electrical conductivity, and thermal management are critical to performance.<sup>1</sup> While the use of aluminium offers substantial mass savings, its electrochemical activity in the presence of copper poses a durability risk, particularly in chloride-containing environments.

This study investigates galvanic corrosion between AA6068 and Cu-ETP, both widely applied in high-performance EV assemblies. Cylindrical specimens with diameters of 6.8 mm, 9.4 mm, and 11.4 mm were precision-machined and mounted in a custom 3D-printed polymer holder (Figure 1), ensuring reproducible, flush metallic contact at the coupling interface. The coupled samples were exposed to salt spray testing in accordance with ASTM B118 (5 wt.% NaCl<sub>(aq)</sub>, cabinet temperature 35 °C), replicating marine-like atmospheric conditions relevant to EV service in coastal, humid, or winter-road environments where road de-icing salts are present.

After 192 hours, AA6068 exhibited accelerated surface degradation characterised by both localised pitting and uniform material loss, while copper remained visually intact, Figure 1. The corrosion rate increased inversely with specimen diameter, indicating that smaller anodic surface areas experience higher galvanic current densities. The observed degradation patterns are consistent with literature reports for Al–Cu galvanic couples in NaCl electrolytes, in which copper serves as an efficient cathode, driving sustained anodic dissolution of aluminium.

These results underline the urgent need for targeted mitigation strategies in mixed-metal EV designs. Approaches include anodising, dielectric barrier coatings,

polymeric sealants, or mechanical design modifications to interrupt electrical continuity at dissimilar-metal junctions. Among these, anodizing is particularly promising, forming a dense, adherent oxide layer that reduces both general corrosion and the galvanic potential difference.



**Figure 1:** An example of galvanically coupled AA6082 and Cu-ETP mounted in 3D printed holder during testing in the salt spray chamber (after 192 hours).

This research is also a restudy for developing durable protective technologies to extend the operational lifespan of EV energy and power systems. Future work will include systematic evaluation of multiple surface treatments under prolonged salt spray and cyclic corrosion exposures, combined with electrochemical testing.

## References:

1. Cheng, T.; Huang, H.; Huang, G. Galvanic corrosion behavior between ADC12 aluminum alloy and copper in 3.5 wt% NaCl solution. *J. Electroanal. Chem.* **2022**, 927, 116984.
2. Logar, A.; Trdan, U.; Klobčar, D.; Trdan, E.-A.; Kovač, N.; Kapun, B.; Milošev, I.; Rodič, P.; Černivec, G. Mitigating galvanic corrosion between copper and AA6082 via anodising. *Svet strojništva* **2024**, 13 (01/06), 136–137.

**Funding information:** The authors acknowledge the financial support from the Slovenian Research and Innovation Agency (ARIS) research core funding Nos. P2-0393, P1-0134 and P2-0270 and ARIS research projects Nos. J2-60033 and N2-0328, and the Horizon Europe framework's Sustainable Blue Economy Partnership for funding the CORRASBlue project.

# Compartment-based pharmacokinetic model of phytocannabinoids in chronic users

Niko Nolimal,<sup>1</sup> Gregor Čekada,<sup>1</sup> Patricija Zupan,<sup>3</sup> Mentors: Miha Slapničar,<sup>1,2</sup> Nejc Umek,<sup>4</sup> Janez Mavri\*<sup>5</sup>

<sup>1</sup> Biotechnical Education Centre Ljubljana, Cesta v Mestni log 47, 1000 Ljubljana, Slovenija

<sup>2</sup> Faculty of Education, University of Ljubljana, Kardeljeva ploščad 16, 1000 Ljubljana, Slovenija

<sup>3</sup> Gymnasium Kranj, Koroška cesta 13, 4000 Kranj, Slovenija

<sup>4</sup> Faculty of Medicine, Institute of Anatomy, University of Ljubljana, Korytkova 2, 1000 Ljubljana, Slovenija

<sup>5</sup> National Institute of Chemistry, Hajdrihova ulica 19, 1000 Ljubljana, Slovenija

In our society, the use of marijuana is increasing among the young population. To investigate the long-term effects of marijuana on chronic users, we performed compartment-based pharmacokinetic modelling of the THC molecule and its metabolites THC-OH and THC-COOH.

The THC molecule occurs naturally in various plants of the Cannabis genus, such as Cannabis indica, Cannabis sativa and Cannabis ruderalis. The highest concentration of THC is found in Cannabis sativa.

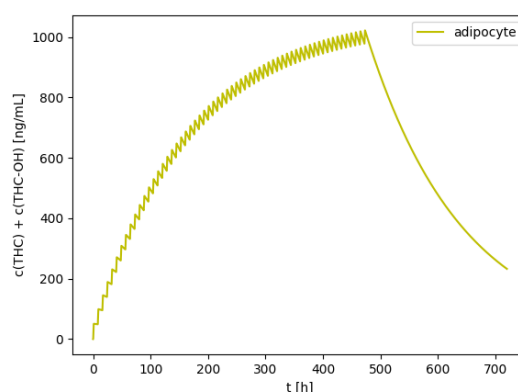
Pharmacokinetics includes ingestion, metabolism and excretion. When marijuana is smoked, the smoke is absorbed through the alveoli directly into the bloodstream, which means that smoked THC bypasses first-pass metabolism (it does not pass through the liver). It then passes directly into adipocyte tissues such as the brain and fat<sup>1</sup>. In the brain, it affects the endocannabinoid nervous system.

The endocannabinoid nervous system consists of neurotransmitters, receptors and various enzymes that synthesise and break down the neurotransmitters. A distinction is made between endogenous (2-AG and AEA<sup>2</sup>) and exogenous neurotransmitters THC and CBD. These molecules bind to CB1 and CB2 receptors. When a molecule binds to the CB1 receptor, which is most found in the CNS and PNS, it affects memory, appetite and can trigger schizophrenia. However, when a molecule binds to the CB2 receptor, which is found in microglia, immune cells, the spleen, brainstem and hippocampus, it mainly affects inflammation and has no psychotropic properties.

THC is primarily metabolised in the liver in a two-stage process. The first step produces the THC-OH metabolite, which is also psychoactive and has a similar octanol-water partition coefficient<sup>3</sup>. Due to its similarity to THC, we have excluded it from our model. In the second step, the THC-COOH metabolite is formed. This metabolite is important because it has a completely different octanol-water partition coefficient, is no longer

psychoactive and is excreted directly via the urine. For this reason, it is the only metabolite that we have included in our model.

There is virtually no gradual accumulation of THC and its metabolites THC-OH and THC-COOH in users who smoke marijuana infrequently. In chronic marijuana users, however, the amount of THC ingested is greater than the number of cannabinoids metabolised and excreted. This effect can lead to false positive results in tests for marijuana use conducted by law enforcement and medical personnel.



**Figure 1:** Accumulation of THC and THC-OH in adipocyte tissues

## References:

1. McGilveray, I. J. Pharmacokinetics of cannabinoids, pain research and management. *Pain Res. Manag.* **2005**, *10*, 15–22.
2. Lu, H.C.; Mackie, K. An introduction to the endogenous cannabinoid system. *Biol Psychiatry.* **2016**, *7*, 516–525.
3. Thomas, B. F.; Compton, D. R.; Martin, B. R. Characterization of the lipophilicity of natural and synthetic analogs of delta 9-tetrahydrocannabinol and its relationship to pharmacological potency. *The J. Pharmacol. Exp. Ther.* **1990**, *2*, 624–630.

# Optimization and study of milk protein coloration, as a sustainable alternative to traditional plastic materials

Iva Jaklin,<sup>1</sup> Anže Škrget,<sup>1</sup> Mentor: mag. Nina Žuman<sup>1</sup>

<sup>1</sup> Gimnazija Franca Miklošiča Ljutomer, Prešernova ulica 34, 9240 Ljutomer, Slovenia

Write abstract text here. Use Times New Roman; font size 10; justified; line spacing 1,15 (Normal style). Total abstract length is limited to one page. Please delete the instructions page before submission. Cite<sup>1</sup> references<sup>2a</sup> in the following<sup>2</sup> fashion<sup>3</sup>.

Plastic waste is an increasingly serious environmental problem, so the development of biodegradable materials is necessary to reduce pollution and the consumption of fossil resources. In the study, we examined the possibility of preparing a biopolymer from denatured casein, a milk protein, as a sustainable alternative to synthetic plastic. We determined how the type of milk, amount and concentration of vinegar, and milk temperature affect the utilization of casein and the properties of the resulting solid substance.

Casein is a natural phosphoprotein that forms colloidal micelles in milk that are sensitive to pH changes<sup>1</sup>. At a pH reduction to the isoelectric point (around 4.6), the micelles destabilize and precipitate. The precipitation process was carried out using alcohol vinegar, and the resulting precipitate was dried and formed into blocks. We examined the mechanical properties of the products, including strength, odor, heat resistance, and practicality.

We used different types of milk: whole, low-fat, protein (with higher protein content), soy milk, and expired milk. We achieved the highest yield and most compact biopolymer with protein milk, which we attribute to the higher casein content and denser protein network<sup>2</sup>. Whole milk also proved to be a good raw material, while the product from semi-skimmed milk was less durable. Due to the absence of casein, soy milk produced a fragile and weak material.

Milk past its expiration date yielded lower yields, but its use supports a sustainable strategy for reducing food waste. The largest decrease in casein content after the expiration date was observed in non-homogenized milk (47.6%) and full-fat long-life milk (–36.6%). The smallest decrease was in semi-skimmed long-life milk (only –4.3%), indicating greater stability during storage. Protein milk lost almost 30% of its casein, showing that even this is not resistant to degradation at acidic pH after the expiration date. At the same time, sensory testing of the

squares showed that the products made from protein milk had the best ratings in terms of strength and temperature resistance. We also formed beads from some of the samples, which we tested as dog toys – this allowed us to explore additional practical applications of the biopolymer. Overall, a reduction in the amount of precipitated casein was observed in all types of milk, likely due to protein degradation by proteases, denaturation of casein and/or formation of insoluble aggregates, and changes in the colloidal structure of milk caused by microbiological activity.

We can conclude that protein milk has the greatest potential for producing bioplastics based on casein. Incorporating surplus or waste milk into the process further enhances the environmental and economic justification for using this material<sup>3</sup>.



**Figure 1:** Condition of squares made from different types of milk after the endurance test

## References:

1. Foqara, M.; Nandi, R.; Amdursky, N.; Casein proteins as building blocks for making ion-conductive bioplastics. *J. Mater. Chem. A*, **2022**, *10*, 14529–14539
2. Chan, W. Y. Proteins in the design of sustainable plastics alternatives, *MRS Communications*, **2023**, *13*, 1009–1024
3. Hottle, T. A.; Bilec, M. M.; Landis, A. E. Biopolymer production and end of life comparisons using life cycle assessment, *Resour., Conserv. Recycl.* **2017**, *122*, 295–306.
4. Šprajcar, M.; Horvat, P.; Kržan, A. Biopolymers and Bioplastics: Plastics in Harmony with Nature; National Institute of Chemistry: Ljubljana, 2012.

# Water electrolysis in connection with fuel cells

Maj Matjašec,<sup>1</sup> Jakob Ritlop,<sup>1</sup> Mentor: Nina Žuman\*,<sup>1</sup>

<sup>1</sup> Gimnazija Franca Miklošiča Ljutomer, Prešernova ulica 34, SI-9240 Ljutomer, Slovenia

Fossil fuels and their excessive use remain one of the key problems of modern society, contributing to environmental pollution, resource depletion, and climate change. As an alternative, hydrogen offers a cleaner and more sustainable energy solution, especially when used in fuel cells, which produce only water and heat during operation. This greatly reduces waste compared to conventional energy sources and helps lower harmful emissions.

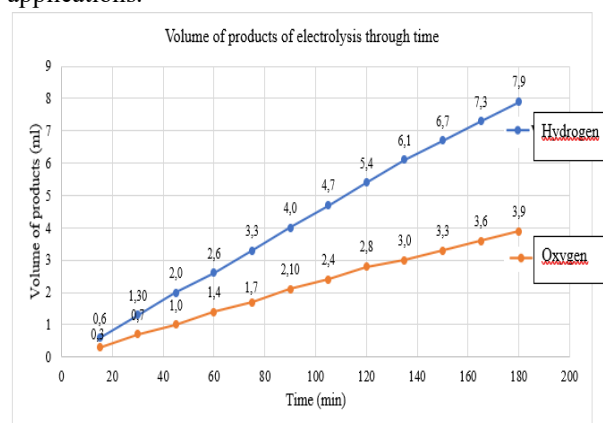
In our research project, we investigated the production of hydrogen through the electrolysis of water, where an electric current splits water into hydrogen and oxygen gases. We examined how different factors affect gas production, including the type of electrolyte (sodium hydrogen carbonate –  $\text{NaHCO}_3$  vs. potassium iodide –  $\text{KI}$ ), the applied voltage and current, and the duration of the process.

Our experiments showed that potassium iodide ( $\text{KI}$ ) is a more effective electrolyte than sodium hydrogen carbonate, resulting in greater gas production. We also confirmed that higher voltage and current increase the amount of gas produced, and that gas formation is proportional to time, following a consistent linear trend.

As a practical application, we built a simple PEM (Proton Exchange Membrane) fuel cell using materials available in the school laboratory. The fuel cell successfully generated 0.14 V, demonstrating the basic

principle of converting hydrogen into electrical energy, although the output was limited due to the simplicity of the setup.

Overall, our project highlighted the potential of hydrogen as a sustainable and clean energy source for the future, though further research is needed to improve efficiency, reduce costs, and enable large-scale applications.



Scheme 1: Volume of products

## References:

1. Barbir, F. PEM Fuel Cells: Theory and Practice; Elsevier Academic Press: Burlington, 2005
2. Smrdu, A. Snov in spremembe 2; Založništvo Jutro: Ljubljana, 2007; pp 100–101.



# ***Antimicrobial and antibiofilm activity of natural substances against Escherichia Coli bacteria***

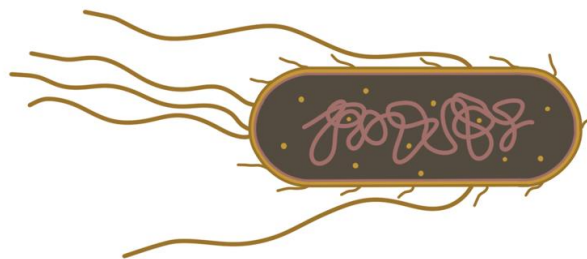
Jon Milič,<sup>1</sup> Mentors: dr. Marija Meznarič, prof. bio. in kem.<sup>1</sup>, izr. prof. dr. Martina Oder, dipl. san. inž.<sup>2</sup>

<sup>1</sup> Gimnazija Franca Miklošiča, Prešernova ulica 34, SI-9240 Ljutomer, Slovenia

<sup>2</sup> Zdravstvena fakulteta Univerze v Ljubljani, Zdravstvena pot 5, SI-1000 Ljubljana, Slovenia

Nowadays, people are increasingly exposed to microorganisms that have various effects on our health. Due to the increasing use of antibiotics, cleaning agents and other synthetic substances, pathogenic microorganisms are becoming resistant. This makes it difficult to remove them, which in turn can lead to more and more bacterial diseases. For this reason, we decided to study alternatives to modern cleaners in the research. Essential oils were used in the research. We determined the effectiveness of essential oils of lavender, ginger and spruce tops in removing *Escherichia coli* bacteria and the ability of lavender essential oil in removing biofilms. We used 100% concentration of all extracts, and for lavender essential oils we also used oils diluted to 50% and 25%. In the case of lavender essential oil, we also checked the effectiveness of these oils obtained from plants in 2022, 2023 and 2024. We first prepared an overnight culture of *E. coli* bacteria on a nutritious microbiological medium, which we later used in the experimental work. Discs soaked with essential oils were applied to the cultures and the antimicrobial effectiveness of each substance was determined based on the inhibition zones. In the second part of the experiments, we transferred the bacteria to microtiter plates, in which we grew a biofilm, which was treated with essential oils in the next steps. After exposing the biofilm to essential oils, we measured the optical density of the crystal violet dye, which was extracted from transiently colored cells, using a microtiter plate reader, and determined the effectiveness of the oils in removing biofilms. For the studied essential oils, we proved their effectiveness in destroying *E. coli* and removing biofilm. The amount of active substances in plants can also be

influenced by environmental factors, as we detected differences between individual ethereal charcoals, depending on the year the plants were harvested.



**Figure 1:** *Escherichia coli*

## **References:**

1. Nazzaro, F., Fratianni, F., De Martino, L., Coppola, R., De Feo, V., Effects of essential oils on pathogenic bacteria. *Pharmaceuticals* **2013**, *6*, 1451–1474
2. Nour, A. H., Modather, R. H., Yuns, R. M., Elnour, A. A. M., Ismail, N. A., Characterization of bioactive compounds in patchouli oil using microwave-assisted and traditional hydrodistillation methods. *Ind. Crops Prod.* **2024**, *208*, 117901
3. Oder, M., Piletić, K., Fink, R., Marijanović, Z., Krištof, R., Bićanić, L., Tomić Linšak, D., Gobin, I. A synergistic anti-bacterial and anti-adhesion activity of tea tree (*Melaleuca alternifolia*) and lemon eucalyptus tree (*Eucalyptus citriodora* Hook) essential oils on *Legionella pneumophila*. *Biofouling*, **2024**, *40*, 54–63.

**Keywords:** microorganisms, *Escherichia coli*, antibiogram, biofilms, essential oils

# Electrochemical determination of bisphenol S in thermal paper

Lara Marzidovšek,<sup>1</sup> Katarina Šela,<sup>1</sup> Mentors: Damijana Gregorič\*,<sup>1</sup> doc. Kristina Žagar Soderžnik\*,<sup>2</sup>

<sup>1</sup> Srednja šola Slovenska Bistrica, Ulica dr. Jožeta Pučnika 21, 2310 Slovenska Bistrica

<sup>2</sup> Faculty of Chemistry and Chemical Technology, University of Ljubljana, Večna pot 113, 1000 Ljubljana, Slovenia

Endocrine disruptors are substances that are foreign to the body but, due to their structural similarity to natural hormones, can mimic, enhance, or block their function. When their harmful effects are proven, they are referred to as endocrine-disrupting chemicals. Among them are bisphenols, a group of organic compounds that are widely used in industry, particularly in the production of plastics and epoxy resins. Due to their properties – such as strength, impact resistance, and transparency – bisphenols are essential for the manufacture of everyday products, such as plastic bottles, packaging, and children's toys.

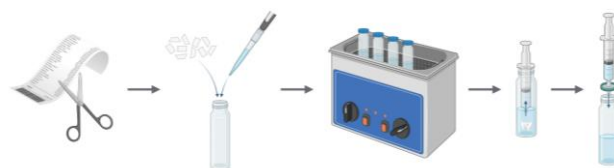
Bisphenols are also used as an organic acid in thermal paper, which is used to print invoices, labels, declarations, ATM receipts, airline tickets and parking tickets. In this form, they can be particularly problematic, as they can be more easily absorbed into food, our bodies and the environment as monomers.

The purpose of the present research work was to study the presence of bisphenol S (BPS) in thermal paper, which is often encountered in shops, restaurants, drugstores and other everyday environments. The aim was to determine whether BPS is present in most samples and to check the absence of bisphenol A, which is banned in the European Union.

Using cyclic voltammetry, we analysed 26 thermal paper samples and prepared BPS standard solutions of different concentrations, which enabled the calculation of BPS concentrations in real samples. During the analysis, we found that 62 % of the samples contained BPS, and these samples were mostly obtained from restaurants and grocery stores, indicating a wider presence of this compound in everyday life. The presence of bisphenol F (BPF) was observed in three samples, while seven samples did not contain either BPS or BPF.

We also estimated the daily intake of BPS in the body due to handling thermal paper. Estimates show that for the general population, the daily value of BPS is estimated to be 0,0000003 ng/day, while for occupationally exposed

people (OEP) such as shopkeepers and restaurant workers, the value is greater than 0.00002 ng/day. In the EU, the Tolerable Daily Intake (TDI) for BPS has not yet been determined. If the TDI limit were set the same as for BPA (0.2ng/kg body weight/day), occupationally exposed people could exceed this limit just from contact with thermal paper, bearing in mind that this does not include other possible sources of exposure.



**Scheme 1:** The process of preparing real samples

**Table 10:** Estimated TOTAL daily intake of BPS due to contact with thermal paper

All samples	EDI [ng/day]	EDI(OEP) [ng/day]	EDI [ng/day/kg bw]	EDI(OEP) [ng/day/kg bw]
Overall average	0,0000003	0,000022	0,004	0,31

## References:

1. Bisfenoli – ECHA <https://echa.europa.eu/sl/hot-topics/bisphenols> (accessed Oct 10, 2024).
2. Miller, G. Z.; Pitzzu, D. T.; Sargent, M. C.; Gearhart, J.; Bisphenols and Alternative Developers in Thermal Paper Receipts from the U.S. Market Assessed by Fourier Transform Infrared Spectroscopy. *Environ. Pollut.* **2023**, 335, 122232.
3. INTERNAL MARKET, INDUSTRY, ENTREPRENEURSHIP AND SMES – New safety requirements for toys. <https://ec.europa.eu/newsroom/growth/items/47671/en> (accessed Oct 10, 2024).

**Funding information:** /

# *Water never lies: Wastewater-Based Epidemiology as a Tool to Understand Psychoactive Substance Use Among Youth*

Lan Dular,<sup>1</sup> Aljaž Maraž,<sup>1</sup> Nejc Murn Blažič,<sup>2</sup> Mentors: dr. Ana Kroflič\*,<sup>3</sup> mag. Nika Cebin\*,<sup>1</sup> Stana Kovač Hace\*,<sup>2</sup> dr. Uroš Očepek\*,<sup>2</sup>

<sup>1</sup> Gimnazija Ledina, Resljeva cesta 12, 1000 Ljubljana

<sup>2</sup> Srednja tehniška in poklicna šola Trbovlje, Šuštarjeva kolonija 7a, 1420 Trbovlje,

<sup>3</sup> Kemijski inštitut Ljubljana, Hajdrihova ulica 19, 1000 Ljubljana

Understanding patterns of psychoactive substance (PAS) use among youth remains a public health and environmental challenge. In this interdisciplinary study, we employed wastewater-based epidemiology (WBE) to analyze wastewater samples from treatment plants in Ljubljana and Trbovlje, Slovenia, aiming to detect the presence of PAS and correlate them with survey-based data collected from high school students. Solid phase extraction was used to concentrate the wastewater samples before applying rapid immunoassay urine tests. We also conducted an anonymous online survey (N = 532) and analyzed the results using cluster analysis and AI-based data mining.

Our findings confirm the presence of cocaine, THC, and morphine in wastewater samples, particularly after sample concentration. Initial unprocessed samples yielded false negatives due to low analyte levels, confirming our hypothesis. The survey revealed significant peer influence and accessibility of PAS in urban areas. Data mining identified four distinct user groups differing in experience, attitudes, and risk perception.

This study highlights the complementary nature of chemical and social data in addressing PAS use. WBE offers an objective snapshot of substance use trends, while surveys provide insights into user behavior and context. Together, they represent a powerful toolset for schools, policymakers, and public health professionals aiming to combat youth substance abuse.



**Figure 1:** Solid-phase extraction cartridges (Oasis MCX) used for sample concentration from wastewater samples collected in Ljubljana and Trbovlje.

## **References:**

1. Castiglioni, S.; Zuccato, E.; Crisci, E.; Chiabrando, C.; Fanelli, R.; Bagnati, R. *Environ. Sci. Technol.* 2006, 40 (12), 357–363.
2. Castiglioni, S.; Bijlsma, L.; Covaci, A.; Emke, E.; Hernández, F. *Sci. Total Environ.* 2011, 409, 3564–3577.
3. European Monitoring Centre for Drugs and Drug Addiction (EMCDDA). *European Drug Report 2024*.
4. Barker, J. *Solid Phase Extraction Techniques*; Wiley: New York, 2000.
5. National Institute of Public Health (NIJZ). *Trends in Psychoactive Substance Use Among Adolescents in Slovenia*; 2024. <https://nijz.si/en/lifestyle/illicit-drugs/alarming-trends-in-the-use-of-psychoactive-substances-among-adolescents/> (accessed: Feb. 21. 2025)

# Analysis of awareness of “zero waste” and Maraton treh src

Petra Ouček<sup>1</sup>, Lara Širovnik<sup>\*1</sup>, Mentor: Mateja Godec<sup>1</sup>

<sup>1</sup> Gimnazija Franca Miklošiča Ljutomer, Prešernova ulica 34, SI-9240 Ljutomer, Slovenia

Recycling practices have been known for thousands of years. With the development of industry, we have become a community that exceeds 8 million tons of waste annually in Slovenia alone.<sup>1</sup> Despite the increasing amount of waste, attitudes towards it have begun to change – we have created a concept that tries to preserve resources through production, consumption, and reuse, without burning or otherwise endangering the health of the ecosystem and people. We started using the term “zero waste” for it.<sup>2</sup>

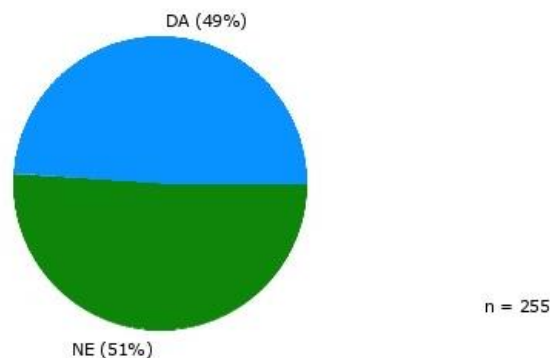
Most of the movement in Slovenia is promoted by the organization Ekologi brez meja, which aims to guide individuals and organizations in preventing waste generation through awareness and networking. And one such event where they help is the Maraton treh src.<sup>3</sup>

Maraton treh src is a sports event organized by Športno društvo Tri srca since 1981. At the same time, it is also the first running event in Slovenia with a “zero waste” vision and the “zero waste” event title it received in 2022. At the event itself, members of “zelena straža” are responsible for waste management, proper sorting, and educating visitors on proper waste sorting.<sup>4</sup>

The first research method was the observation of the “zelena straža” on how visitors handle waste. We noticed that a large number of visitors would have thrown away their trash incorrectly if it weren’t for the intervention of the “zelena straža”. Such waste was mainly plastic and paper packaging and cans. A big problem was also the used, i.e. dirty paper plates, which visitors wanted to throw into the paper bin, but they belong to the biological waste. Among the recorded observations, there were also records of littering outside of the trash cans. The latter was recorded several times in 2023, specifically near areas where large crowds of people were moving at the same time.

The second method of research was a survey. First, we were interested in the familiarity of the visitors with the term “zero waste”. Only 63% of the surveyed visitors knew this in 2022 and 2023. We then investigated the knowledge of Maraton treh src as a “zero waste” event, and it turned out that only half of the surveyed visitors knew about it, and they learned about it at the event itself the previous year or through social media. Visitors were

very supportive of the marathon's “zero waste” operation and encouraged more events like this.



**Scheme 1:** Percentage of participants that knew that Maraton treh src was and is a “zero waste” event

We also conducted two interviews. One was with Marko Pintarič, the main organizer of the marathon, where he told us that organizing such a big event as “zero waste” needs various adjustments and more financial resources, since environmentally friendly materials are often more expensive. The second interview was with Katja Sreš, a representative of the association Ekologi brez meja. She expressed the importance of “zelena straža” helpers at these events are of great meaning and that these big events, such as Maraton treh src, will always be needed. She said that when organizing such events, it is crucial to plan early enough for possible emerging problems such as poorly labeled modern materials, which still cause problems for organizers when sorting.

## References:

1. Portal Republike Slovenije, GOV.SI. – Odpadki: <https://www.gov.si/podrocja/okolje-in-prostor/okolje/ravnanje-z-odpadki/> (accessed: Jan. 24. 2025)
2. Janežič, L. (2015). ODPADKI - Gradivo za Ekokviz za srednje šole 2015/2016.
3. Zero Waste Slovenija. (2018) <https://ebm.si/zw/o/zero-waste-slovenija/> (accessed: Jan. 24. 2025)
4. Zero Waste Slovenija. (2016). Slovenske zero waste prireditve. <https://ebm.si/zw/turizem/prireditve/slovenske-prireditve/> (accessed: Jan. 24. 2025)



# *MR-Pingvini vs. Pasosaurs: A Mixed Reality Game for Raising Awareness about Psychoactive Substances*

Luka Tomažin,<sup>1</sup> Ajk Kalaba,<sup>1</sup> Aljaž Maraž,<sup>2</sup> Mentors: dr. Uroš Ocepek\*,<sup>1</sup> Stana Kovač Hace,<sup>1</sup> mag. Nika Cebin,<sup>2</sup>

<sup>1</sup> Srednja tehniška in poklicna šola Trbovlje, Šuštarjeva kolonija 7a, 1420 Trbovlje, Slovenia,

<sup>2</sup> Gimnazija Ledina, Resljeva cesta 12, 1001 Ljubljana, Slovenia

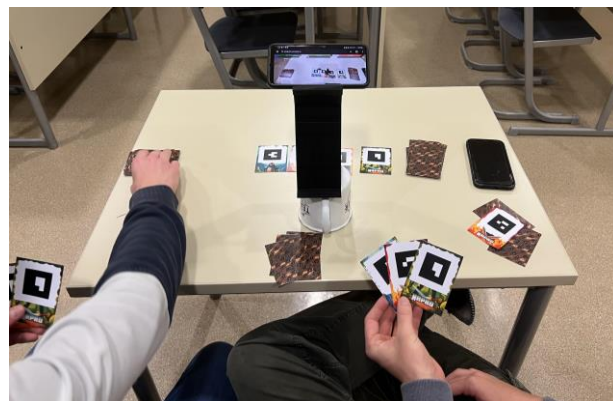
Rapid technological advancements, particularly in artificial intelligence (AI) and mixed reality (MR), offer new opportunities to create engaging educational tools. Our project aimed to develop an innovative card game enhanced by mixed reality to raise awareness among adolescents about the risks of psychoactive substances (PAS). Each card in the game represents a creature: penguins, symbolizing resistance strategies against PAS, and "pasosaurs", dinosaurs alike monsters, representing specific psychoactive substances—designed using generative AI to reflect the substance's characteristics and effects visually.

Considering the increasing popularity of tobacco and nicotine products among youth, we conducted a survey involving 532 students aged 14–19 from STPŠ Trbovlje and Gimnazija Ledina. Our results indicated that curiosity and peer influence are primary reasons behind adolescents' experimentation with new nicotine products such as vapes and nicotine pouches, surpassing traditional cigarette usage.

The developed game integrates digital MR elements via AR.js and p5.js libraries, enhancing interactivity and engagement. Through gameplay, participants confront realistic scenarios regarding substance effects, fostering critical thinking and informed decision-making. AI tools significantly expedited game development, enabling rapid prototyping, image generation, and the creation of interactive 3D models. Although the technology faced challenges, notably in marker recognition accuracy and AI licensing constraints, our findings demonstrate MR's substantial educational potential and AI's effectiveness in streamlining complex creative processes.

Our study underscores the value of merging AI and MR technologies in educational contexts, promoting innovative approaches to social awareness and preventive education. The project received the prestigious Gold Innovation Award at the Innovation Awards of the Zasavje Chamber of Commerce and was presented at numerous national and international conferences, including events in Kazakhstan, India, and prominent Slovenian international forums.

With this study, we demonstrated that young people can effectively engage their peers in understanding and embracing social values. As Peter Drucker famously said, "In times of turbulent change, the issue is not the turbulence, but rather acting with yesterday's logic."



**Figure 1:** Students playing the MR-enhanced card game, experiencing interactive learning through mixed reality technology.

## References:

1. Jannah, N. L.; Wasis, W.; Wiryanto, W.; Suryanti, S.; Widodo, W.; Murni, A. W.; Farokhah, L.; Penehafo, A. E. Design of Module Based Integrated Augmented Reality (AR) on Energy Transformation Material to Train Creative Thinking Skills of Elementary School Students. *J. Eng. Sci. Technol.* **2025**, *20*, 25–32.
2. Jelínková, E.; Nosková, M.; Pešík, J. In Business Trends 2024: 9th International Scientific Conference; Universe in West Bohemia: Plzen, Czech Republic, 2024; pp 80–89.
3. Nacionalni inštitut za javno zdravje. Nacionalno poročilo o drogah 2023. [https://nijz.si/wp-content/uploads/2024/03/Nacionalno-porocilo\\_2023-1.pdf](https://nijz.si/wp-content/uploads/2024/03/Nacionalno-porocilo_2023-1.pdf) (accessed Feb 20, 2025).
4. Nacionalni inštitut za javno zdravje. Zaskrbljujoči trendi v uporabi psihoaktivnih snovi med mladostniki. <https://nijz.si/zivljenjski-slog/prepovedane-> (accessed Feb 20, 2025).
5. Pellas, N.; Kazanidis, I.; Palaigeorgiou, G. A Systematic Literature Review of Mixed Reality Environments in K-12 Education. *Educ. Inf. Technol.* **2019**, *25*, 2481–2520.



# Microbiological analysis of concrete surfaces at Jože Plečnik Gymnasium Ljubljana

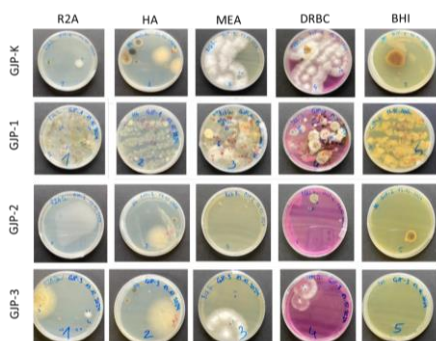
Mija Kapun,<sup>1</sup> Emilija Rojnik,<sup>1</sup> Mentors: mag. Darja Silan\*,<sup>1</sup> doc. dr. Polona Zalar,<sup>2</sup> doc. dr. Martina Turk,<sup>2</sup>

<sup>1</sup> High school Jože Plečnik Ljubljana, Šubičeva 1, SI-1000 Ljubljana, Slovenia, SI-1000 Ljubljana, Slovenia

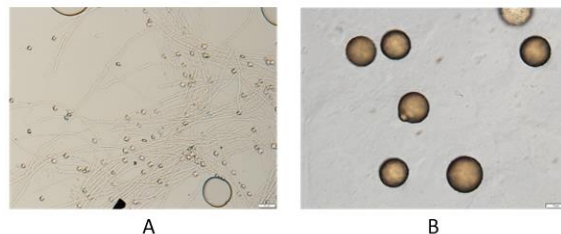
<sup>2</sup> Biotechnical Faculty, University of Ljubljana, Department of Biology, Večna pot 111, SI-1000 Ljubljana, Slovenia

In this study, we investigated the presence and potential impact of micro-organisms on concrete, focusing on their growth, metabolic properties and ability to dissolve and form minerals. We sampled different locations of the concrete fence on the terrace of the Jože Plečnik Gymnasium and also took concrete samples at selected sample points. When observing the growth of micro-organisms, we found that higher microbial diversity and abundance occur on wetter surfaces. By analysing the concrete samples under a scanning electron microscope (SEM), we detected biological debris and calcium carbonate ( $\text{CaCO}_3$ ) deposition, with the highest deposition detected on the sample with the higher moisture content, which also had the highest growth and biodiversity, indicating that the  $\text{CaCO}_3$  is formed due to microorganism activity.

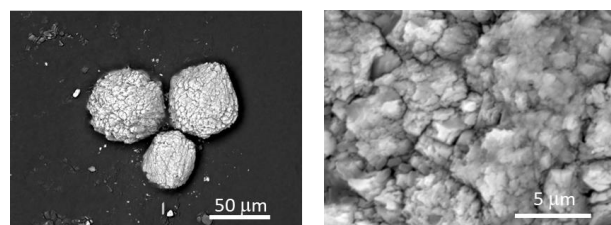
Further analysis showed that isolated micro-organisms can have both positive and negative effects on concrete. Some isolates form pigments that can cause undesirable aesthetic changes to concrete surfaces, while others are capable of dissolving  $\text{CaCO}_3$ , which can lead to material degradation. We have also identified micro-organisms that exhibit positive properties for concrete, such as the ability to biomineralise, which allows the concrete to self-harden. All fungi and two selected bacterial isolates are urease-positive, which means that they form minerals by the process of ureolysis. The results of our research also suggest ways to protect concrete heritage and support the development of the idea of biomineralisation and self-renewable materials for sustainable construction.



**Picture 1:** Comparison of pyramidal crystals – isolate G-3 (A) and round crystals – isolate G-1 (B), formed through the process of biomineralisation.



**Picture 2:** Overview of microbial growth on R2A, HA, MEA + Ch, DRBC and BHI media from all sampling sites after 144 hours of incubation.



**Picture 3:** Crystal formation by bacterial isolate B-2.

## References:

1. Agarwal, H.; Bajpai, S.; Mishra, A.; Kohli, I.; Varma, A.; Fouillaud, M.; Dufossé, L.; Joshi, N. C. Bacterial pigments and their multifaceted roles in contemporary biotechnology and pharmacological applications. *Microorganisms* **2023**, *11* (3), 614.
2. Boskey, A. L. Biomineralization: An overview. *Connect. Tissue Res.* **2003**, *44* (1), 5–9.
3. Buh, T. Samopopravljlivi betoni [Bachelor's thesis]. University of Ljubljana Repository, 2019.
4. Castro-Alonso, M. J.; Montañez-Hernandez, L. E.; Sanchez-Muñoz, M. A.; Macias Franco, M. R.; Narayanasamy, R.; Balagurusamy, N. Microbially induced calcium carbonate precipitation (MICP) and its potential in bioconcrete: Microbiological and molecular concepts. *Front. Mater.* **2019**, *6*, 126.

**Funding information:** The project was carried out as part of a high school research programme, supported by High School Jože Plečnik Ljubljana.

# Synthesis of silicon dioxide nanoparticles with incorporated fluorescent dyes

Petra Ouček\*,<sup>1</sup> Lani Habjanič,<sup>1</sup> Mentors: Mateja Godec,<sup>1</sup> Sebastjan Nemec<sup>2,3</sup>

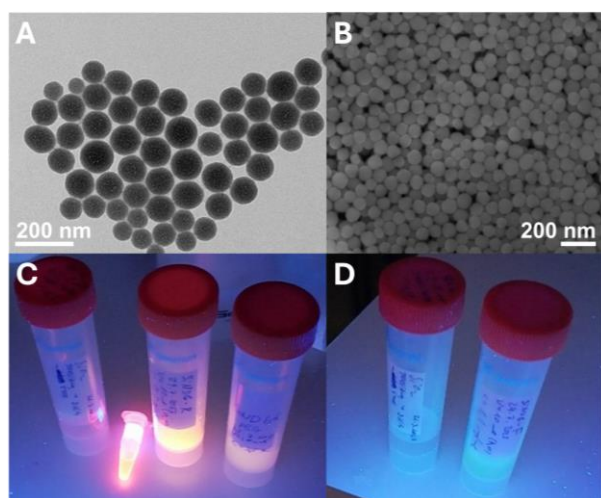
<sup>1</sup> Gimnazija Franca Miklošiča Ljutomer, Prešernova ulica 34, SI-9240 Ljutomer, Slovenia

<sup>2</sup> Materials Research Laboratory, University of Nova Gorica, Vipavska cesta 11c, 5270 Ajdovščina, Slovenia

<sup>3</sup> Department for materials synthesis, Jožef Stefan Institute, Jamova cesta 39, 1000 Ljubljana, Slovenia

Nanotechnology is an interdisciplinary and fast developing field focused on the research and creation of materials, usually nanoparticles (NP), with distinctive properties in the nanometer scale. The high surface-to-volume ratio of such materials enables innovations beyond the possibilities of conventional materials of larger size.<sup>1</sup>

Silicon dioxide, referred to as silica, is a material widely present in nature and everyday life – as silica gel packets, used to adsorb moisture, and as quartz sand in construction and glassmaking. Moreover, silica has low toxicity and is biocompatible, which enables its use in pharmaceutical, cosmetic and food industries. Silica nanoparticles are widely researched for applications in biomedical, analytical, optical, and environmental fields.<sup>2</sup>



**Figure.** Transmission (A) and scanning (B) electron microscope micrographs of silica NP. Fluorescence emission of Eu-complex (C; middle), rhodamine (C; right), and fluoresceine-embedded silica NP (D; right). On the left of (C) and (D) are silica NP with no dye.

In our work, we synthesized three types of fluorescent silica NP by embedding a fluorescent dye in the silica structure. The used dyes were fluorescein, rhodamine, and a europium complex (Eu-complex). The fluorescent silica NP were synthesized from TEOS in a mixture of water, ethanol and ammonia with admixed

individual silane-functionalized fluorescent dyes.<sup>3</sup> Furthermore, the NP were colloiddally stabilized by attaching polyethylene (PEG) molecules on their surface.

The NP were characterized with several analytical methods. Their dimensions were determined by electron microscopy (**Figure A and B**) and their hydrodynamic diameter was measured by dynamic light scattering. We found that the fluorescein-embedded NP had the largest diameter (147 nm) and rhodamine-embedded ones had the smallest (118 nm). As expected, the attachment of PEG to the NP surface increased the hydrodynamic diameter (by ~10 nm). Moreover, the surface charge of the NP was determined with zeta potential measurements. The rhodamine-embedded NP had zeta potential of -45 mV, which was 14 mV lower than fluoresceine or Eu-complex embedded NP (zeta around -31 mV). By attaching PEG-molecules to the surface, the zeta potential value did not change significantly, since PEG is uncharged. Lastly, the NP suspensions were exposed to UV light at 254 and 366 nm, where we qualitatively confirmed the successful incorporation of dyes by observing the distinctive emission of colored light from dye-embedded silica NP samples (**Figure C and D**).

In our study we successfully synthesized silica NP with embedded three different fluorescent dyes. Such NP will be used for future studies in biomedical, optical and sensing fields.

## References:

1. Britannica. (b. d.). Overview of nanotechnology. <https://www.britannica.com/technology/nanotechnology/Overview-of-nanotechnology>
2. Nayl, A. A., Abd-Elhamid, A. I., Aly, A. A., Bräse, S. Recent Progress in the Applications of Silica-Based Nanoparticles. *RSC Advances* **2022**, 12 (22), 13706–13726. DOI: <https://doi.org/10.1039/d2ra01587k>
3. Potrč, T., Kralj, S., Nemec, S., Kocbek, P., Kreft, M. E. The Shape Anisotropy of Magnetic Nanoparticles: An Approach to Cell-Type Selective and Enhanced Internalization. *Nanoscale* **2023**, 15 (19), 8611–8618. DOI: <https://doi.org/10.1039/d2nr06965b>.

**Funding information:** the research was funded by ARIS P2-0089, J2-3043, J7-4420, and J3-3079.

# Dimerization of T7 lysozyme using antiparallel coiled coils from protein Sso10a

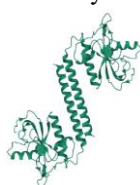
Tisa Lombar,<sup>2</sup> Urban Perko,<sup>2</sup> Mentors: Marko Novinec,<sup>\*,1</sup> Ana Obaha,<sup>1</sup> Alenka Mozer<sup>2</sup>

<sup>1</sup> Faculty of Chemistry and Chemical Technology, University of Ljubljana, Večna pot 113, SI-1000 Ljubljana, Slovenia

<sup>2</sup> Gimnazija Vič, Tržaška c. 72, SI-1000 Ljubljana, Slovenia

The objective of the study was to modify the tertiary structure of an enzyme in order to achieve greater stability and increased activity. More than 35% of the proteins in the cell are found in their oligomeric form, which has been shown to increase thermostability<sup>1,2</sup>. We investigated whether we could achieve an increase in stability and catalytic activity by dimerization of T7 lysozyme, an enzyme naturally found in bacteriophage T7, whose role is to break down peptidoglycans in the cell wall, causing cell lysis<sup>3</sup>.

After numerous attempts, we were able to create a self-assembling dimeric enzyme by fusing T7 lysozyme and the coiled-coil structure of protein Sso10a<sup>4</sup>. Coiled coils are naturally occurring protein structures composed of two or more  $\alpha$ -helices connected through hydrophobic and electrostatic interactions<sup>5</sup>. The antiparallel coiled coil found in protein Sso10a is recognized as one of the most stable two-stranded coiled coils known. By fusing it with T7 lysozyme, we obtain a dimer with two active sites, increasing the chance of a successful collision with the substrate. Using collision theory, we can therefore predict an increase in catalytic efficiency.

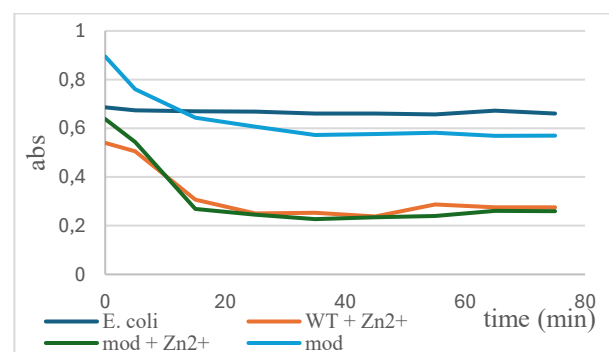


**Figure 1:** The schematic structure of the modified T7 lysozyme

We were able to confirm our predictions, as the modification resulted in a 58% increase in activity. T7 lysozyme's unique ability to lyse both Gram-positive and Gram-negative bacteria, which sets it apart from other enzymes, was maintained. Additionally, due to the fusion of  $\alpha$ -helices to the enzyme, T7 lysozyme's ability to inhibit T7 RNA polymerase was suppressed, which led to a substantial increase in expression levels. These improvements not only enhance the enzyme's performance but also make its large-scale production more efficient and cost-effective.

The modification of T7 lysozyme has enabled its production without the need for expensive filtration methods, allowing for more efficient and cost-effective manufacturing. This advancement opens new opportunities for addressing the escalating global threat of antibiotic-resistant bacterial infections. T7 lysozyme

exhibits broad-spectrum bacteriolytic activity against both Gram-positive and Gram-negative bacteria, making it a promising candidate in the development of novel antimicrobial strategies. Given the alarming rise in multidrug-resistant pathogens, particularly among Gram-negative species<sup>6</sup>, T7 lysozyme offers significant therapeutic potential. When used in combination with existing antibiotics or treatments, it can markedly enhance efficacy. Its unique lytic mechanism makes the development of bacterial resistance highly unlikely, positioning T7 lysozyme as a promising breakthrough in the fight against antibiotic-resistant infections.



**Figure 2:** The graph shows the activity of wild-type and mutant lysozyme with added Zn<sup>2+</sup> ions and the mutant lysozyme without Zn<sup>2+</sup> ions on *E. coli* using 5  $\mu$ M concentrations of the respective enzyme at 25°C.

## References:

1. Jones, S.; Thornton, J. M. Principles of protein-protein interactions. *Proc. Natl. Acad. Sci. U. S. A.* **1996**, *93* (1), 13–20.
2. Walden, H.; Bell, G. S.; Russell, R. J.; Siebers, B.; Hensel, R.; Taylor, G. L. Tiny TIM: a small, tetrameric, hyperthermostable triosephosphate isomerase. *J. Mol. Biol.* **2001**, *306* (4), 745–757.
3. Cheng, X.; Zhang, X.; Pflugrath, J. W.; Studier, F. W. The structure of bacteriophage T7 lysozyme, a zinc amidase and an inhibitor of T7 RNA polymerase. *Proc. Natl. Acad. Sci. U. S. A.* **1994**, *91* (9), 4034–4038.
4. Chen, L.; Chen, L. R.; Zhou, X. E.; Wang, Y.; Kahsai, M. A.; Clark, A. T.; Shriver, J. W. The Hyperthermophile Protein Sso10a is a Dimer of Winged Helix DNA-binding Domains Linked by an Antiparallel Coiled Coil Rod. *J. Mol. Biol.* **2004**, *341* (1), 73–91.
5. Truebestein, L.; Leonard, T. A. Coiled-coils: The long and short of it. *BioEssays* **2016**, *38* (9), 903–916.
6. Oliveira J., Reygaert W. C., Gram-Negative Bacteria. *StatPearls*, August 8, **2023**

# *A method of producing sodium metal on a laboratory scale*

Urban Ocvirk,<sup>1</sup> Mentor: Slavko Pečar\*,<sup>1</sup>

<sup>1</sup> Gimnazija in srednja šola Rudolfa Maistra, Novi trg 41a, 1241 Kamnik, Slovenia

This research article focuses on the production of sodium metal through high-temperature distillation from common and inexpensive reagents. Sodium is a very useful element that can be used on its own to dry certain organic solvents or to produce special sodium compounds such as sodium hydride and sodium amide. The synthesis begins with choosing the right reducing agents. The cheapest, most widely available, and most effective are aluminum and carbon, but for the reaction to proceed properly, both reducing agents must be used in a specific ratio. Unfortunately, it is not practical to use only one of the reducing agents without the other. My experiments have shown that aluminum behaves too aggressively at higher temperatures, producing a runaway thermite reaction that, despite yielding a decent amount of sodium, is very dangerous and places excessive demands on the apparatus. Carbon, on the other hand, is too mild. The reaction with carbon alone can be useful and has historically been used industrially to produce sodium, but it requires much higher temperatures to run smoothly, which would necessitate a different apparatus and heating system<sup>1</sup>. The solution to this problem is to use both reducing agents simultaneously in a 4:1 carbon-to-aluminum ratio. This achieves a reaction that has a manageable activation energy but does not turn into a runaway thermite reaction. When both reducing agents are used together, aluminum provides the energy for the reaction, while carbon moderates it, creating an ideal balance. The reaction also does not take very long to complete. In my case, it took only an hour and a half, and the reaction time could potentially be shortened further by optimizing the carbon-to-aluminum ratio. It is very important that completely dry reagents are used. Sodium carbonate must be in its anhydrous form, or it could lead to an explosion. The carbon must also be preheated—especially if charcoal is used—because it may still contain residual moisture from the pyrolysis of wood. Throughout the reaction, argon should be passed through the apparatus. Argon provides an inert atmosphere that prevents the freshly formed sodium from oxidizing or igniting. It also helps cool the reaction and condense the sodium vapors, although this cooling must be controlled—cooling the reaction too much will slow it down and lower the yield. Another benefit of argon is that it dilutes the carbon monoxide produced as a side product of the reaction. This minimizes the risk of sodium vapors reacting with the carbon monoxide. Because argon is denser than carbon monoxide, it also helps push the vapors through the cooling

tube. For the apparatus, a cylindrical design was chosen to fit the type of furnace used. The setup consisted of a reaction vessel with a cover plate screwed on top. A graphite gasket was placed between the reaction vessel and the cover plate to prevent the metal parts from fusing together while also ensuring a gas-tight seal. The cover plate featured two pipes: an argon feed pipe and a condenser pipe. At the end of the condenser pipe, a separate connected pipe served as an off-gas outlet to prevent pressure buildup. Beside the off-gas pipe, a receiving flask collected the distilled sodium. During the reaction, the heating was increased in stages. Initially, the temperature was raised to 400 °C to fully pyrolyze any remaining wood residues in the charcoal. It was then gradually increased to 1150 °C, the furnace's maximum limit. The first drops of sodium appeared at slightly below 1000 °C after 23 minutes. For the remainder of the reaction, the temperature was maintained at 1150 °C to maximize sodium recovery. Throughout the process, insulation covered the top of the reaction vessel, and temperature-monitoring equipment was used to track the reaction conditions. This apparatus is not limited to producing sodium alone. In a similar—or even identical—setup, other alkali metals (except lithium) could be prepared. Besides alkali metals, other elements and compounds such as mercury and phosphorus could also be produced with this apparatus. Mercury could be obtained by decomposing mercury sulfide in an oxygen atmosphere (argon would be replaced with oxygen), while phosphorus could be prepared from sodium hexametaphosphate, silica, and aluminum powder (in this reaction, argon is required).



**Figure 1:** Collected sodium in a flask

## References:

1. Lemke, C. H.; Markant, V. H. Sodium and Sodium Alloys. In Kirk-Othmer Encyclopedia of Chemical Technology; John Wiley & Sons, Inc.: Hoboken, NJ, 2007



# Effect of CnGL lectin from the Clouded Funnel Mushroom on the growth of *Escherichia coli* and *Listeria innocua*

Vid Kodrič,<sup>\*,1</sup> Matic Izak,<sup>1</sup> Anika Gregori Kmecl,<sup>1</sup> Mentors: Jerica Sabotič,<sup>2</sup> Nika Zaveršek<sup>2</sup>

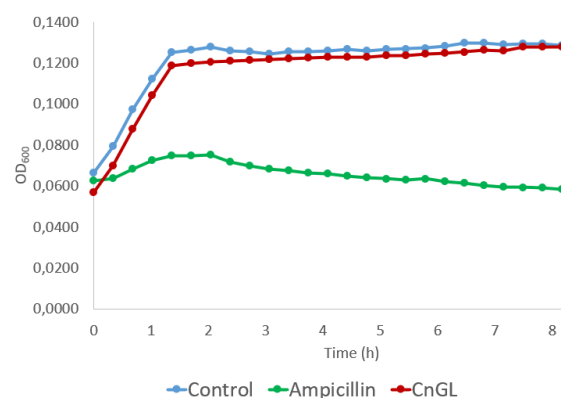
<sup>1</sup> Gimnazija Vič Grammar School, Tržaška cesta 72, SI-1000 Ljubljana, Slovenia, ([vidkodric9@gmail.com](mailto:vidkodric9@gmail.com))

<sup>2</sup> Department of Biotechnology, Jožef Stefan Institute, Jamova cesta 39, SI-1000 Ljubljana, Slovenia

Due to the overuse of antibiotics in the past, we are now facing one of the greatest threats to public health – antibiotic resistance in microorganisms. Therefore, it is crucial to find new antibacterial substances, and relatively unexplored fungi are an important source of such compounds. In our study, we focussed on lectins which are proteins that can reversibly bind to sugars. Various lectins with insecticidal activity and effects on cancer cells have already been isolated from the Clouded Funnel Mushroom (*Clitocybe nebularis*)<sup>1</sup>. One example is lactose-binding lectin CNL, which serves as a defence protein, as its nematotoxic and cytotoxic properties have been proven<sup>2,3</sup>. In our study, we isolated a lectin that binds to glucose (CnGL) from *C. nebularis* using affinity chromatography. The purity of the isolated lectin was verified by gel electrophoresis, which confirmed our assumption that the glucose-binding lectin would be present in our sample. We also found sepharose-binding lectin (CnSepLs), which was removed from our sample by further affinity chromatography.

In the second part of the study, we investigated how the isolated lectin affects the growth of the bacterial species *Listeria innocua* and *Escherichia coli*. We also investigated the effect of the *C. nebularis* extract on the bacteria and compared this effect with that of the antibiotic ampicillin. We monitored bacterial growth by measuring the optical density of the bacterial cultures using spectrophotometry. The results were presented as growth curves in various diagrams (Figure 1). The *C. nebularis* extract had a growth-promoting effect on both bacterial species, presumably due to the numerous nutrients it contained. We found that the CnGL lectin had a rather small inhibitory effect on *L. innocua* growth, especially when compared to the growth curve of the bacterial culture with the antibiotic ampicillin. However, the bacterial culture with added CnGL entered the lag phase later than the control group, so the lectin could affect bacterial interactions with the environment, which

would need to be investigated further. On the contrary, the lectin had a growth-promoting effect on *E. coli*. However, bacterial growth was lower at a higher lectin concentration than at a lower concentration, suggesting that further studies on the effects of higher CnGL lectin concentrations on bacteria would be worthwhile. *C. nebularis* proved to be an interesting source of substances that influence bacterial growth.



**Figure 1:** Growth curves of *Listeria innocua*: control sample (blue), sample with added antibiotic ampicillin (green) and sample with added CnGL lectin (red).

## References:

1. Pohleven, J.; Kos, J.; Sabotic, J. Medicinal Properties of the Genus *Clitocybe* and of Lectins from the Clouded Funnel Cap Mushroom, *C. nebularis* (Agaricomycetes): A Review. *Int. J. Med. Mushrooms* **2016**, *18* (11), 965–975
2. Sabotič, J.; Kos, J. CNL-*Clitocybe nebularis* Lectin-The Fungal GalNAc $\beta$ 1-4GlcNAc-Binding Lectin. *Molecules* **2019**, *24* (23), 4204
3. Perišić Nanut, M.; Žurga, S.; Konjar, Š.; Prunk, M.; Kos, J.; Sabotič, J.; The fungal *Clitocybe nebularis* lectin binds distinct cell surface glycoprotein receptors to induce cell death selectively in Jurkat cells. *FASEB J.* **2022**, *36* (4), 22215



# Sustainable Synthesis of Turbostratic Graphene from Waste Carbon Fiber Composites via Flash Joule Heating

Vinko Kosten,<sup>1</sup> Mentors: Nika Cebin\*,<sup>1</sup> Boštjan Genorio<sup>2</sup>

<sup>1</sup> Gimnazija Ledina, Resljeva cesta 12, 1000 Ljubljana, Slovenia

<sup>2</sup> Faculty of Chemistry and Chemical Technology, University of Ljubljana, Večna pot 113, SI-1000 Ljubljana, Slovenia

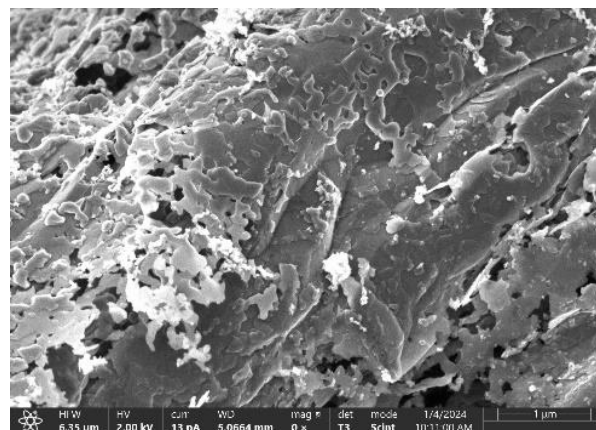
The growing environmental burden of carbon fiber composites, widely used in industries due to their excellent mechanical properties, highlights an urgent need for sustainable recycling solutions. This research explores the transformation of waste carbon fiber composites into turbostratic graphene using the Flash Joule Heating (FJH) method—a promising, cost-effective, and energy-efficient process. By exposing crushed carbon fiber composites to high-intensity electric discharges, the material rapidly heats to over 3000 K in milliseconds, resulting in the exfoliation of amorphous carbon into high-quality turbostratic graphene.

The study aimed to optimize the FJH process to achieve maximal conversion efficiency and minimal energy loss. Systematic experimentation was conducted to fine-tune critical parameters, including preheating intensity, sample resistance, voltage, and pulse duration. Optimal conditions were identified as a 200 ms electrical pulse at 150–175 V on preheated (10 A, 3×2 s) 40 mg samples with 120  $\Omega$  initial resistance. Characterization via Scanning Electron Microscopy (SEM) confirmed the formation of turbostratic graphene with characteristic layered morphology and significantly increased surface area.

The optimized process demonstrated near-complete energy utilization from the capacitor bank, validating the energy efficiency of the approach. Importantly, the obtained turbostratic graphene exhibited properties suitable for electrocatalysis, especially in the oxygen reduction reaction (ORR) for sustainable hydrogen peroxide ( $\text{H}_2\text{O}_2$ ) production. The material's high porosity, low oxygen content, and disordered stacking enhance its catalytic performance and position it as a viable alternative to costly platinum-based catalysts.

This research confirms the potential of FJH as a scalable and environmentally friendly method for recycling carbon fibre waste into high-value graphene-based materials. By bridging waste valorization with advanced nanomaterials, it contributes to circular economy principles and the development of sustainable electrochemical technologies. The findings pave the way

for future industrial applications in green energy, catalysis, and environmental protection.



**Figure 1:** SEM image of optimized turbostratic graphene showing layered and wrinkled morphology (magnification 20,000 $\times$ ).

## References:

1. Luong, D. X.; Bets, K.V.; Algozeeb, W. A.; Stanford, M. G.; Kittrell, C.; Chen, W.; Salvatierra, R. V.; Ren, M.; McHugh, E. A.; Advincula, P. A.; Wang, Z.; Bhatt, M.; Guo, H.; Mancevski, V.; Shahsavari, R.; Yakobson, B.I.; Tour, J. M. Gram-scale bottom-up flash graphene synthesis. *Nature* **2020**, *577*, 647–651.
2. Bardarov, I.; Yordanova Apostolova, D.; Martins, P.; Angelov, I.; Ruiz-Zepada, F.; Jerman, I.; Dular, M.; Strmčnik, D.; Genorio B. Flash Graphene from Carbon Fiber Composites: A Sustainable and High-Performance Electrocatalyst for Hydrogen Peroxide Production. *Electrochim. Acta* **2025**, *517*, 145754.
3. Kokmat, P.; Surinlert, P.; Ruammaitree, A. Growth of High-Purity and High-Quality Turbostratic Graphene with Different Interlayer Spacings. *ACS Omega* **2023**, *8*, 4010–4018.
4. Shi, X.; Back, S.; Gill, T. M.; Siahrostami, S.; Zheng, X. Electrochemical synthesis of  $\text{H}_2\text{O}_2$  by two-electron water oxidation reaction. *Chem.* **2021**, *7*, 38–63.
5. Jung, H.; Karmakar, A.; Adhikari, A.; Patel, R.; Kundu, S. Graphene-based materials as electrocatalysts for the oxygen evolution reaction: a review. *Sustainable Energy Fuels* **2022**, *6*, 640–667.

# *pH-Sensitive Fluorescent Probes for Detecting Urinary Tract Infections*

Živa Anderluh\*,<sup>1</sup> Jošt Dolinar,<sup>1</sup> Mentors: assoc. prof. Janez Mravljak, M. Pharm., Ph.D.<sup>2</sup>, Alenka Mozer\*,<sup>1</sup>

<sup>1</sup> Vič Grammar School, Tržaška cesta 72, SI-1000 Ljubljana, Slovenia, ([ziva.anderluh@gmail.com](mailto:ziva.anderluh@gmail.com))

<sup>2</sup> Faculty of Pharmacy, University of Ljubljana, Aškerčeva cesta 7, SI-1000 Ljubljana, Slovenia

Urinary tract infections are among the most common bacterial infections, with uropathogenic *Escherichia coli* being the most frequent causative agent.<sup>3</sup> Pathogens bind to glycoproteins on the surface of uroepithelial cells with their lectin FimH. This leads to the ability to oppose urinary flow, and thus prolong the infection time. FimH is a mannose-binding adhesin located at the tip of type 1 pili.<sup>3</sup>

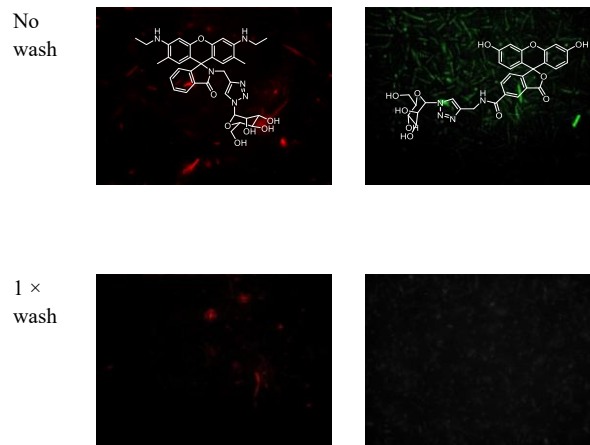
Current treatment approach is the usage of antibiotics. This method leads to development of strains resistant against most of the currently available antimicrobials.<sup>3</sup> New treatment strategies are already being developed, among which antiadhesive therapy represents an attractive alternative. New diagnostic therapies are also emerging.<sup>1,4</sup>

Within this research project, mannose-based FimH antagonists were synthesized. D-mannose's relatively weak affinity for FimH can be improved by incorporating various aglycones to the D-mannopyranose via  $\alpha$ -glycosidic bond. Therefore, fluorescent probes (rhodamine B, rhodamine 6G and 5-carboxyfluorescein) were attached to D-mannose. All the fluorescent dyes are pH-sensitive due to changing the shape of the molecule in a different environment.<sup>2</sup> Compound synthesized within the research project have an aglycon attached via N-glycosidic bond, which is known to be more stable in physiological environment.<sup>2</sup>

Absorbance and fluorescence of final fluorescently labeled compounds were measured at different pH values. Results were graphically displayed and evaluated. The pKa values were determined by analyzing titration curves. Two of the final products displayed maximum fluorescence in acidic environment, and one has a fluorescence maximum at cytosolic pH. All final compounds have a small Stokes shift (22-28 nm).

The final compounds synthesized from 5-carboxyfluorescein and rhodamine 6G were sent for testing on bacteria, while the compound from rhodamine B was eliminated due to its relatively low fluorescence. The two compounds are able to bind to the bacterial pili,

and even after washing, a portion of the compound remained bound to them.



**Figure 1:** Bacterial imaging of two final compounds, showing their presence in the sample before and after rinsing with buffer. The two final compounds are presented in the upper pictures.

## References:

1. Harris, M.; Fasolino, T. New and Emerging Technologies for the Diagnosis of Urinary Tract Infections. *J. Lab. Med.* **2022**, 46 (1), 3–15.
2. Janc, T. *Chemical Glycosylation of Rhodamine B and 6G with D-Mannose and D-Glucose*; Master's Thesis, University of Ljubljana, Faculty of Pharmacy, 2014. [http://www.ffa.uni-lj.si/fileadmin/datoteke/Knjiznica/magistrske/2014/Janc\\_Tadeja\\_mag\\_nal\\_2014.pdf](http://www.ffa.uni-lj.si/fileadmin/datoteke/Knjiznica/magistrske/2014/Janc_Tadeja_mag_nal_2014.pdf) (accessed Jan. 18. 2025)
3. Pelicon, V. *Synthesis of Alpha-D-Mannosyltriazoles as Antiadhesive Ligands for Bacterial Surface Lectin FimH*; Master's Thesis, University of Ljubljana, Faculty of Pharmacy, 2018. [http://www.ffa.uni-lj.si/docs/default-source/knjiznicadoc/magistrske/2018/pelicon\\_veronika\\_mag\\_nal\\_2018.pdf?sfvrsn=2](http://www.ffa.uni-lj.si/docs/default-source/knjiznicadoc/magistrske/2018/pelicon_veronika_mag_nal_2018.pdf?sfvrsn=2) (accessed Jan 18. 2025).
4. Xu, R.; Deebel, N.; Casals, R.; Dutta, R.; Mirzazadeh, M. A New Gold Rush: A Review of Current and Developing Diagnostic Tools for Urinary Tract Infections. *Diagnostics* **2021**, 11 (3), 479.

# We also thank:



SLOVENSKO  
MLADINSKO  
GLEDALIŠČE



MESTNI CITY  
MUZEJ MUSEUM  
LJUBLJANA OF LJUBLJANA

LEPA  
VIDA



TILIA  
WINES



Kinodvor.  
Mestni kino.  
[www.kinodvor.org](http://www.kinodvor.org)



TETA  
FRIDA®



GEOSS  
PUSTOLOVSKI PARK

DoNatural

Leone



PLASTIKATRČEK

Winery  
*Lisjak*



sekom  
grafika



PRUS  
*Bela krajina*

UTRIP PLESA





**CUTTING**  
EDGE